Single-Ended GaN Power Transistors Spawn New System-Level Capabilities **p29**

EM Modeling and Simulation Tools Offer a Means to Design Aircraft Antenna Systems **p41**

Over-the-Air Testing Will Be Needed for 5G — Here's Why **p78**

Microwaves & RF®

YOUR TRUSTED ENGINEERING RESOURCE FOR OVER 50 YEARS

JULY 2017 mwrf.com

BEYOND THE SCOPE

Real-time oscilloscopes bring more signals than ever into view **p58**

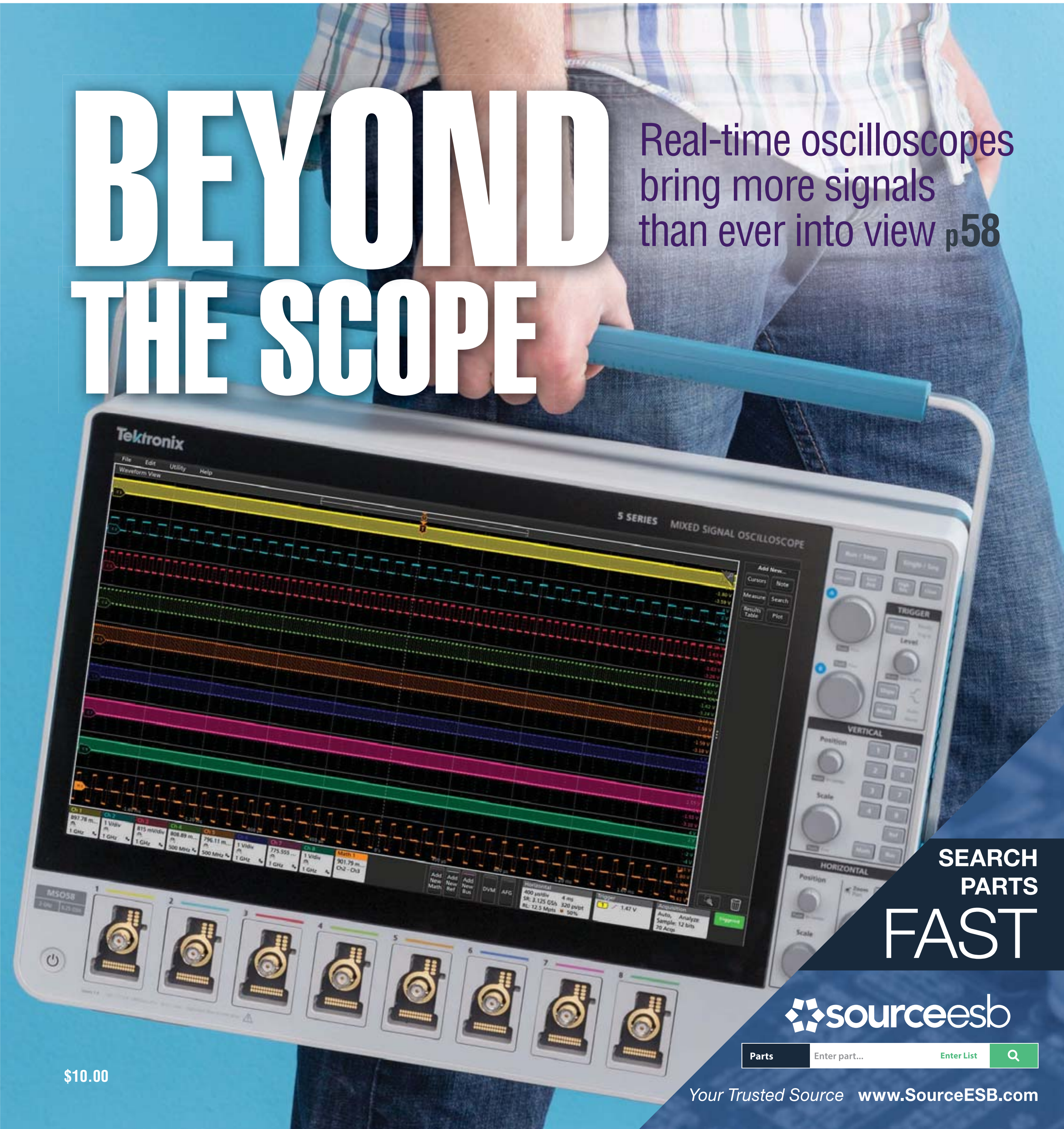

$10.00

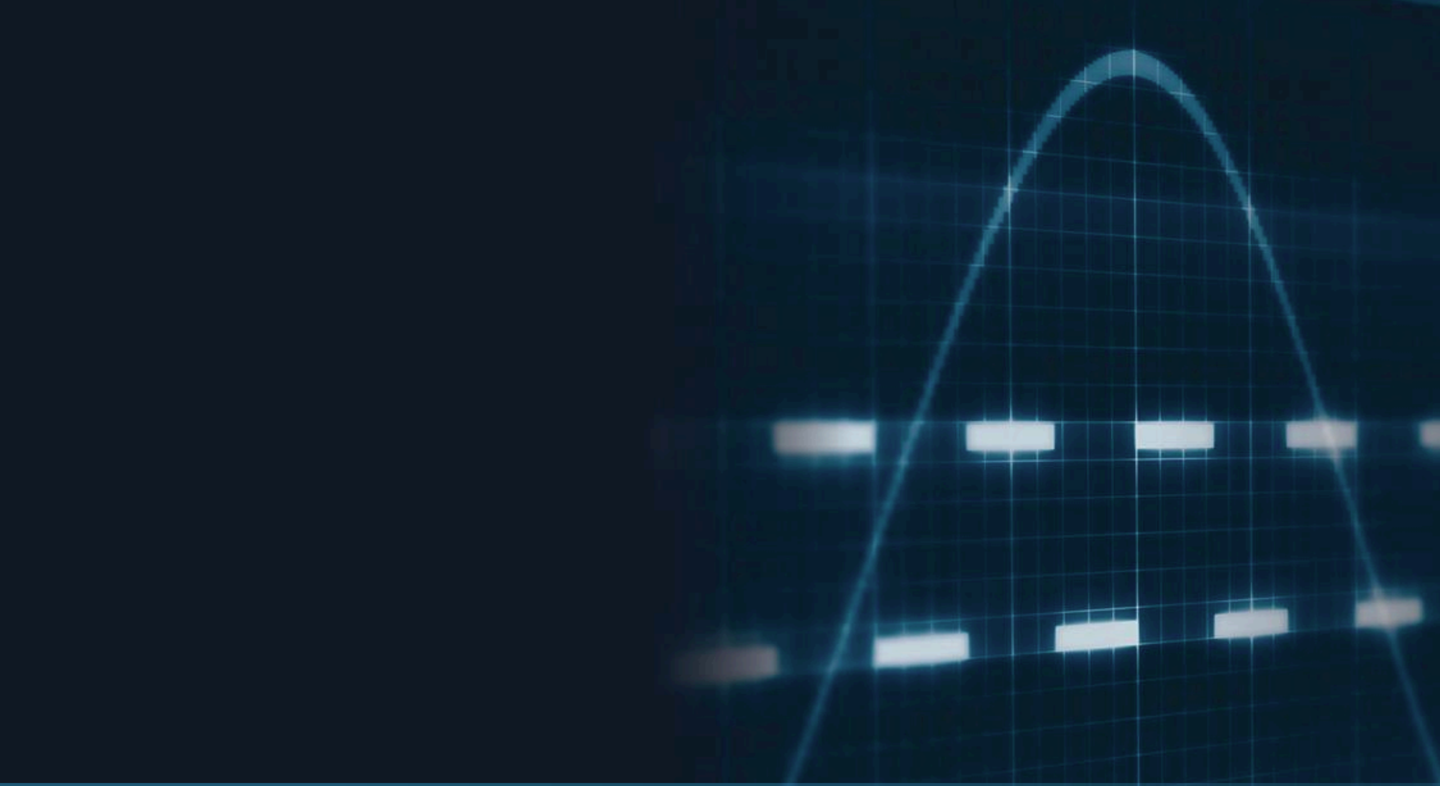

The Trusted Name in High

Industry's Largest Portfolio of Diodes

Test & Measurement

Public & Military Radios

Satellite Communication

Industrial, Scientific & Medical

Civil & Defense Radar

Diodes

Performance RF

MACOM is committed to delivering industry-leading diode design and application-specific solutions for our customers worldwide.

MACOM design and application engineers are continuing our 65-year legacy and commitment of leadership with next-gen wideband RF solutions for mission-critical applications. Our expert RF team leverages the latest semiconductor technologies and state-of-the-art foundry processes to reach new levels of performance in bandwidth, power, packaging and reliability.

Only MACOM delivers:

Diode Support Services

- Lot Approval offered: maintaining secured inventory at our factory
- Product extensions / variants, custom design & development
- Hi-Rel screening capabilities: space & JAN, JANTX, JANTXV, JANS-qualified RF & DC devices
- Applications support: world-class experienced team available to support your critical requirements

Expansive Diode Product Portfolio

- PINs, Schottkys, Varactors, Zeners, rectifiers, current regulators
- Chip capacitors, attenuator pads, thin film resistors, spiral inductors
- RF / Mw /mMW, DC general purpose solutions
- Integrated diode products: switch modules, limiter modules, comb generators, driver modules

Patented Technologies

- AlGaAs: high frequency switch portfolio up to 94 GHz
- HMIC: high power diode & switch portfolio (0.1-20 GHz, 6.5W CW incident power)

Featuring:
MSS Family of Silicon Schottky Mixer Diodes

MACOM™

Partners from RF to Light

Learn more at:
www.macom.com/diodes

IN THIS ISSUE

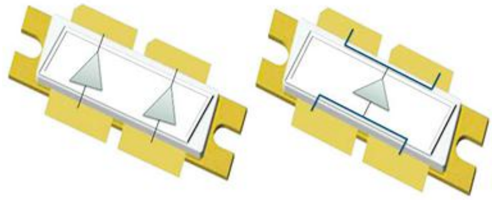

29

FEATURES

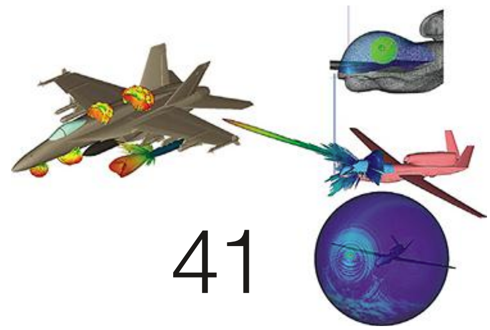

41

58

PRODUCT TECHNOLOGY

NEWS & COLUMNS

JOIN US ONLINE

follow us @MicrowavesRF

become a fan at facebook.com/microwavesRF

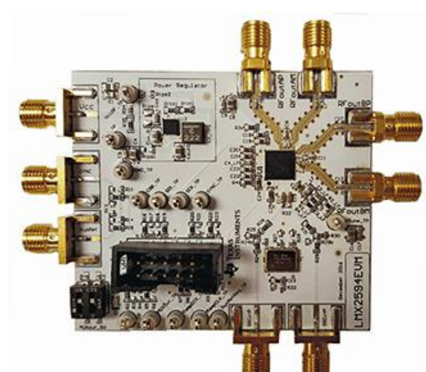

70

ON MICROWAVES&RF.COM

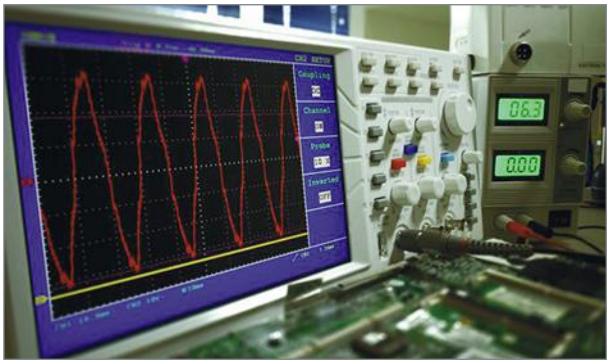

Measurements Help Minimize EMI and RFI

Electronic devices operate in a world of electromagnetic (EM) fields of various strengths. Each device is not only subject to interference from those EM fields, but may itself be a source of EM interference to other devices. EM interference can be conducted or radiated, either degrading or disrupting the performance of an electronic device.

http://www.mwrf.com/test-measurement/measurements-help-minimize-emi-and-rfi

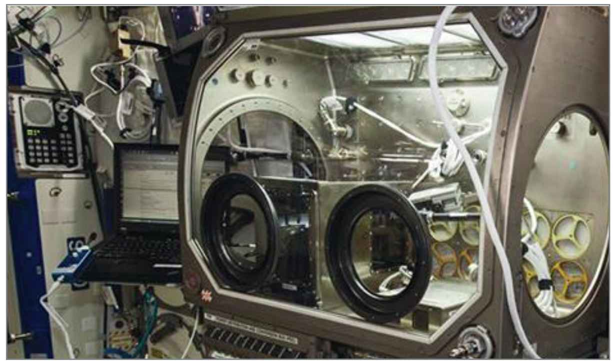

3D Printing Can Make Components for Space

3D printing enables the fabrication of objects through the deposition of material in order to obtain fit-for-purpose hardware. Like many new manufacturing processes, 3D printing arose from the merging of previously existing technologies: the coming together of computer-aided-design (CAD), inkjet nozzles, and automated machine systems.

http://www.mwrf.com/materials/additive-manufacturing-enables-microwave-components-space-applications

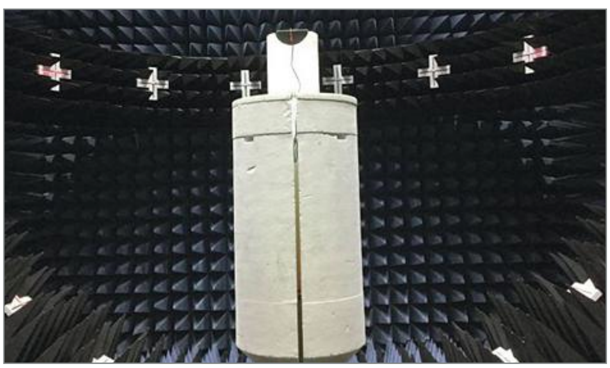

Antenna Testing Optimizes IoT Device Performance

Tight constraints on power, size, and cost make it challenging to design and manufacture IoT devices with good RF (wireless) performance, though. Particularly challenging is antenna performance, because its small size and close proximity to other components create problems in achieving good impedance matching and a good isotropic antenna radiation pattern.

http://www.mwrf.com/test-measurement/ble-antenna-testing-helps-optimize-iot-device-performance

Making the Case for Signal and Spectrum Analyzers

Spectrum measurements are invaluable in the laboratory to evaluate the signal characteristics of a new design, and in the field to monitor known signals and search for interference. To make such measurements, engineers have typically turned to the RF/microwave spectrum analyzer. It is widely available in benchtop and portable varieties, and even in compact-module form with a USB interface.

http://www.mwrf.com/test-measurement/making-case-signal-and-spectrum-analyzers

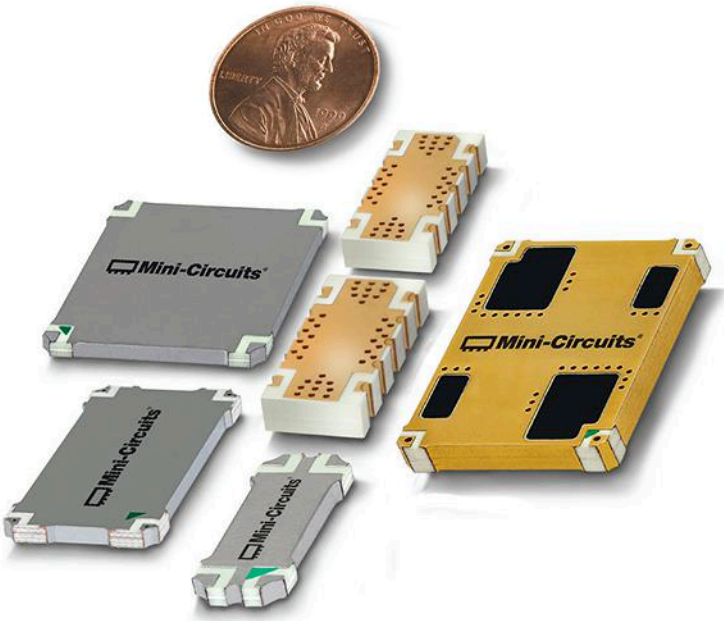

Editorial

CHRIS DeMARTINO | Technical Editor
chris.demartino@penton.com

Will Today's Microwave Oven Soon Be a Thing of the Past?

Odds are you currently have a microwave oven in your home. As you probably already know, those ovens, which can be found everywhere today, are based on magnetron technology. And while they have served households relatively well for many years, magnetron-based microwave ovens may likely disappear in the not-too-distant future. The reason why is solid-state RF energy.

Because the magnetron-based microwave oven has been used for so long and is so prevalent, it may be difficult to believe that it could simply go away. However, solid-state RF energy does offer several clear benefits that cannot be ignored. For one, it allows food to be cooked more precisely in comparison with the traditional magnetron ovens. Much healthier food can be cooked, too—surely an important aspect these days. In general, when you think of microwaveable food, "health" food is not exactly what comes to mind. But solid-state RF energy could revise our definition of the microwaved meal.

The RF Energy Alliance (RFEA; *www.rfenergy.org*) is a non-profit association that is determined to unlock the potential of solid-state RF energy (the March 2017 issue of *Microwaves & RF* featured an interview with Klaus Werner, executive director of the RF Energy Alliance). The RFEA believes that it offers a number of benefits, and could in turn have a major impact on a wide range of applications.

MACOM *(www.macom.com)*, one company at the forefront of RF energy, recently introduced its RF energy toolkit. This toolkit, demonstrated at IMS 2017, is intended for a number of applications, with cooking being one of them. The kit leverages MACOM's gallium-nitride-on-silicon (GaN-on-Si) technology.

While magnetron-based microwave ovens have been a staple in homes for many years, RF solid-state technology could rewrite that script, ushering in a dramatically new approach to cooking food. Perhaps it won't be too long before you head to the mall in search of your new wish list item: a cooking appliance based on solid-state RF energy. mw


MCL B 744
ADP-2-10
MCL B 744
ADP-2-10
MCL B 744
ADP-2-10
MCL BP2C
MCL BPNC
MCL BPNC
MCL BPNC
MCL QBA-12 071838
MCL QBA-12 071838
MCL QBA-12 071838
MCL SBA-2-20 071840
MCL SBA-2-20 071840
MCL SBA-2-20 071840

Microwaves&RF JULY 2017

EDITORIAL

CONTENT DIRECTOR: **NANCY K. FRIEDRICH** nancy.friedrich@penton.com
TECHNICAL CONTRIBUTOR: **JACK BROWNE** jack.browne@penton.com
TECHNICAL ENGINEERING EDITOR: **CHRIS DeMARTINO** chris.demartino@penton.com
CONTENT PRODUCTION DIRECTOR: **MICHAEL BROWNE** michael.browne@penton.com
PRODUCTION EDITOR: **JEREMY COHEN** jeremy.cohen@penton.com
CONTENT PRODUCTION SPECIALIST: **ROGER ENGELKE** roger.engelke@penton.com
CONTENT OPTIMIZATION SPECIALIST: **WES SHOCKLEY** wes.shockley@penton.com
ASSOCIATE CONTENT PRODUCER: **LEAH SCULLY** leah.scully@penton.com
ASSOCIATE CONTENT PRODUCER: **JAMES MORRA** james.morra@penton.com

ART DEPARTMENT

GROUP DESIGN DIRECTOR: **ANTHONY VITOLO** tony.vitolo@penton.com
SENIOR ARTIST: **JIM MILLER** jim.miller@penton.com
CONTENT DESIGN SPECIALIST: **JOCELYN HARTZOG** jocelyn.hartzog@penton.com
CONTENT DESIGN SPECIALIST: **TIM DRIVER** tim.driver@penton.com
CONTENT & DESIGN PRODUCTION MANAGER: **JULIE JANTZER-WARD** julie.jantzer-ward@penton.com

PRODUCTION

GROUP PRODUCTION MANAGER: **CAREY SWEETEN** carey.sweeten@penton.com
PRODUCTION MANAGER: **VICKI MCCARTY** vicki.mccarty@penton.com
CLASSIFIED PRODUCTION COORDINATOR: **LINDA SARGENT** linda.sargent@penton.com

AUDIENCE MARKETING

USER MARKETING DIRECTOR: **BRENDA ROODE** brenda.roode@penton.com
USER MARKETING MANAGER: **DEBBIE BRADY** debbie.brady@penton.com
FREE SUBSCRIPTION/STATUS OF SUBSCRIPTION/ADDRESS CHANGE/MISSING BACK ISSUES
OMEDA **T** | 847.513.6022 **TOLL FREE** | 866.505.7173

SALES & MARKETING

MANAGING DIRECTOR: **TRACY SMITH** **T** | 913.967.1324 **F** | 913.514.6881 tracy.smith@penton.com

REGIONAL SALES REPRESENTATIVES
AZ, NM, TX: **GREGORY MONTGOMERY** **T** | 480.254.5540 gregory.montgomery@penton.com

AK, NORTHERN CA, OR, WA, WESTERN CANADA: **STUART BOWEN** **T** | 425.681.4395 stuart.bowen@penton.com

AL, AR, SOUTHERN CA, CO, FL, GA, HI, IA, ID, IL, IN, KS, KY, LA, MI, MN, MO, MS, MT, NC, ND, NE, NV, OH, OK, SC, SD, TN, UT, VA, WI, WV, WY, CENTRAL CANADA: **JAMIE ALLEN** **T** | 415.608.1959 **F** | 913.514.3667 jamie.allen@penton.com

CT, DE, MA, MD, ME, NH, NJ, NY, PA, RI, VT, EASTERN CANADA:
SHANNON ALO-MENDOSA **T** | 978.501.9116 shannon.alo-mendosa@penton.com

INTERNATIONAL SALES
GERMANY, AUSTRIA, SWITZERLAND: **CHRISTIAN HOELSCHER** **T** | 011.49.89.95002778
christian.hoelscher@husonmedia.com

BELGIUM, NETHERLANDS, LUXEMBURG, UNITED KINGDOM, SCANDINAVIA, FRANCE, SPAIN, PORTUGAL:
JAMES RHOADES-BROWN **T** | +011 44 1932 564999 **M** | +011 44 1932 564998 james.rhoadesbrown@husonmedia.com

ITALY: **DIEGO CASIRAGHI** **T** | +011 390 31 261407 diego@casiraghi-adv.com
PAN-ASIA: **HELEN LAI** **T** | 886 2 2727 7799 helen@twoway-com.com
PAN-ASIA: **CHARLES LIU** **T** | 886 2 2727 7799 liu@twoway-com.com

PLEASE SEND INSERTION ORDERS TO: orders@penton.com
PENTON REPRINTS: **WRIGHT'S MEDIA** **T** | 877.652.5295 penton@wrightsmedia.com
LIST RENTALS:
SMARTREACH CLIENT SERVICES MANAGER: **JAMES ADDISON** **T** | 212.204.4318 james.addison@penton.com

ONLINE

PRODUCT DEVELOPMENT DIRECTOR: **RYAN MALEC** ryan.malec@penton.com

DESIGN ENGINEERING & SOURCING GROUP

EXECUTIVE DIRECTOR OF CONTENT AND USER ENGAGEMENT: **NANCY K. FRIEDRICH**
GROUP DIRECTOR OF OPERATIONS: **CHRISTINA CAVANO**
GROUP DIRECTOR OF MARKETING: **JANE COOPER**

PENTON

1166 AVENUE OF THE AMERICAS, 10TH FLOOR, NEW YORK, NY 10036 **T** | 212.204.4200

Electronic Design | Machine Design | Microwaves & RF | Source ESB | Hydraulics & Pneumatics |
Global Purchasing | Distribution Resource | Power Electronics | Defense Electronics

JACK BROWNE | Technical Contributor

Test & Measurement Techniques: High Frequency and Wireless Test Methods

MEASUREMENTS CAN MAKE or break a high-frequency design. When properly performed, they can be very revealing, uncovering both good and bad performance aspects of an electronic design. Of course, high-frequency measurements can also be very complex, and knowing which measurements to perform on which device under test (DUT) can be an adventure in itself.

Fortunately, *Test & Measurement Techniques: High Frequency and Wireless Test Methods*, edited by *Microwaves & RF* Contributing Editor Lou Frenzel, helps to take some of the guesswork out of which measurements are needed in different situations, and how to best perform those measurements. Written by Frenzel and other contributors, the e-book's 10 chapters provide insights into key electronic performance parameters.

Many of the chapters focus on measurements that are synonymous with the microwave industry, such as vector network analysis, and the high-performance instruments—vector network analyzers (VNAs)—that have been refined through the years to keep pace with always-changing test requirements.

Measurement professionals may find the e-book somewhat tutorial, since it attempts to cover a surprisingly broad range of measurements and test instruments. But for those who may be knowledgeable about measurements for one particular type of DUT, the e-book provides a refreshing introduction into measurements pertinent to DUTs at many levels.

The e-book also provides basic guidance on measurements that can be applied to digital and photonics components, such as jitter measurements. The measurement advice is practical rather than theoretical, and includes instruction on how to adjust controls on the test equipment, how to read different types of test display screens, and even the basics of measuring different signal power levels. A handy reference, it is well worth a download. mw

News

DARPA Looks to BAE Systems FOR IMPROVED UAS TECHNOLOGY

Unmanned aerial systems (UAS) are being designed for a wide range of missions, including surveillance and intelligence gathering. Unfortunately, the size weight, and power (SWaP) restrictions on these systems typically limit their designs to one type of payload, meaning that they lack the flexibility for conducting multiple missions. However, fueled by two recent contracts from DARPA worth a combined $5.4 million, BAE Systems is developing technology that will equip single UAS payloads with the flexibility to perform multiple missions and adapt quickly to changing battlefield conditions.

"This agility is particularly important in denied environments, where multiple mission functions are typically needed to penetrate defenses and remain operational," said Randall Lapierre, technology development manager at BAE Systems. "By enabling small platform systems to share core components, we're helping them become more agile and stay on station longer."

The DARPA program for enhanced UAS technology, CONverged Collaborative Elements for RF Task Operations (CONCERTO), is seeking the functionality of communications, radar, and electronic-warfare (EW) systems from UAS drones (see photo). The goal of the program is to create an electronic architecture that can effectively switch among multiple functions electronically—such as intelligence, surveillance, command and control, networking, and combat operations—ideally under remote control and without need of physical payload changes (such as swapping radar antennas for communications antennas). ■

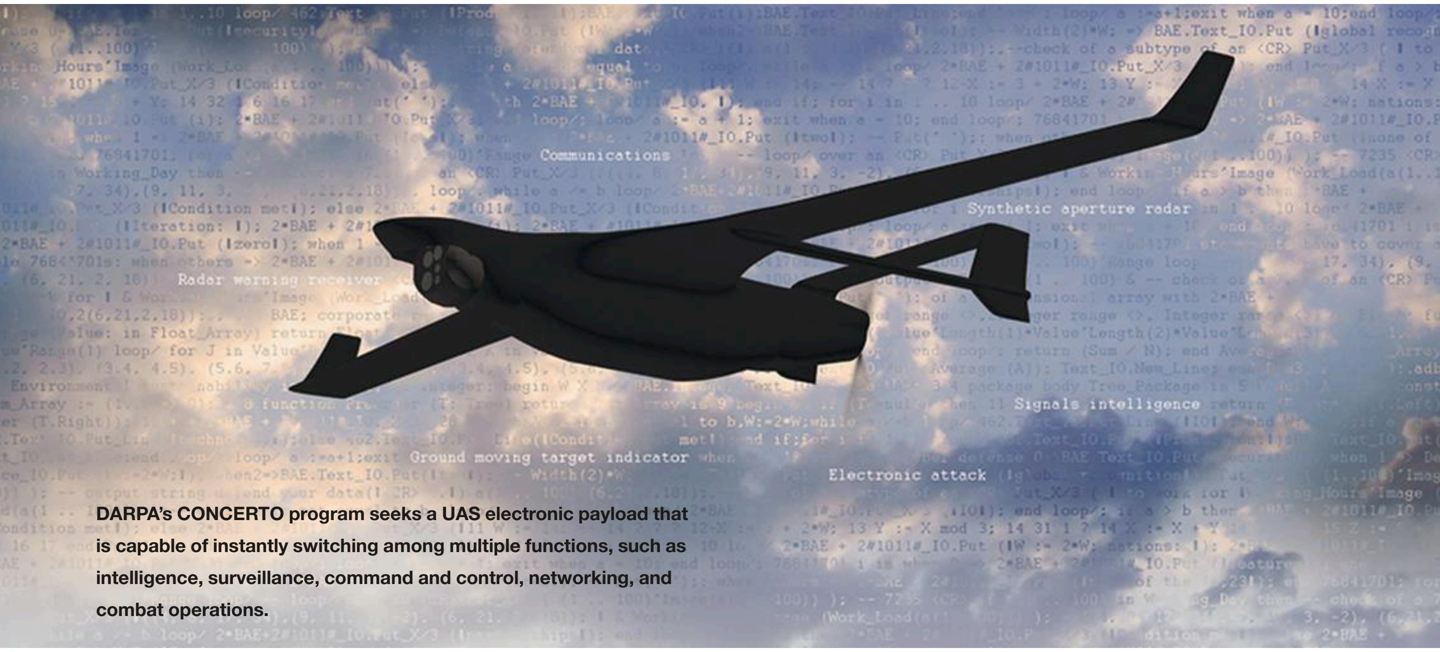

DARPA's CONCERTO program seeks a UAS electronic payload that is capable of instantly switching among multiple functions, such as intelligence, surveillance, command and control, networking, and combat operations.

TRANSISTORS BEAM RADIO ENERGY to Cure Ceramics, Relieve Pain, and Cook Food

USING THE SAME TECHNOLOGY that powers cellular infrastructure, a new RF transistor hits the high power levels to enable applications from drying industrial ceramics or warming organs in hospital treatments..

NXP Semiconductors has begun sampling the new component, the latest in the slowly growing market for alternatives to the vacuum tubes widely used in bulky magnetrons for industrial heating systems. The MRF13750H can be controlled over its full dynamic range up to 750 watts and enables frequency shifting to conserve the radio energy.

"The reliability and enhanced control features of solid-state have long been understood, but industrial system designers had difficulties combining many transistors to match the power level of magnetrons," said Pierre Piel, the general manager of NXP's RF Power business, in a statement.

The radio waves emitted from the transistors act like a volumetric heat source injecting energy into large loads and blocking large temperature gradients. The transistors are capable of changing frequencies rapidly, allowing power to be spread more efficiently when processing chemicals or manufacturing ceramics or glass fibers.

The new transistor operates in the 700 to 1300 MHz spectrum, which is reserved for industrial, scientific, and medical applications. It is based on laterally diffused metal oxide semiconductor or LDMOS transistors, whose lower maximum power gain frequency than gallium arsenide chips also make them suitable for aerospace and radar applications.

NXP has kept alive the solid state RF business that started inside Freescale Semiconductor, which it acquired in 2014 for almost $12 billion. For that deal to pass through regulators, the Dutch supplier sold off its own RF business that became Ampleon, the other major vendor of LDMOS transistors for radio frequency power.

For the last two years, NXP has been demonstrating other transistors in a concept ovens that can precisely control the amount of heat directed into food and that has a longer lifespan that the magnetrons inside traditional microwaves. The MRF13750H will enter production in this December, the company said in a statement. ■

MICROSEMI ENTERS FILTERS for Radar and Satellites with Phonon Deal

LAST YEAR, MICROSEMI sold its custom electronics and RF businesses for $300 million to Mercury Systems, which sells parts for satellites and missile guidance systems. Now it is restocking its defense business with parts that sort signals by frequency..

In late June, the Aliso Viejo, Calif.-based company said that it had acquired Photon Corp., which designs custom surface acoustic wave filters—more commonly known as SAW filters—for applications like military radar and jam-resistant satellite communications.

These parts complement Microsemi's existing business in diodes, transistors, and power amplifiers for the aerospace and defense markets. Microsemi also sells mixed-signal and programmable chips hardened against radiation for satellite applications to many of the same contractors that buy from Photon, which is named after a unit of vibration energy.

Rick Goerner, Microsemi's executive vice president of worldwide marketing and sales, announced the deal in an email to customers viewed by Microwaves & RF. Phonon, which is based in Simsbury, Conn., also builds modules using own delay lines, correlators, and oscillators.

Among the company's products are band pass filters, which sell for up to a dollar in cell phones, a hundred in wireless infrastructure, and a thousand in military applications like those of Phonon's customers. Phonon estimates that space and defense customers account for 3% of all SAW filter sales, which total around $2 billion per year.

It also sells so-called dispersive filters, which change the delay uniformly across the pass band. That effect can be used to increase the range of military radars, for instance, or improve the resolution of military surveillance receivers. These parts typically cost up to ten thousand dollars.

Around 85% of Phonon's sales are custom modules that contain at least one of its components. To design and fabricate these parts used in waveform generators for radar and demodulators for military communications, costs up to a hundred thousand dollars, Phonon says on its website.

Founded in 1982, Phonon is privately held. But the company reported that its revenue was around $15 million in 2009, the same year that it started a major expansion of its manufacturing plant. Thomas Martin, Phonon's president and founder, said at the time that the company aimed to double its revenues by 2014.

Microsemi did not say how much it paid in the deal. ■

SAKOR SUPPORTS LOCKHEED'S Advanced Aerospace Projects

LOCKHEED MARTIN SPACE Systems Company has again looked to SAKOR Technologies, Inc. for a pair of dynamometers, intended for use in advanced research projects. The dynamometers will be used in Lockheed's Materials Technology Laboratory for R&D, quality control, and design validation of a variety of technologies for advanced aerospace projects.

SAKOR previously supplied two AccuDyne AC motoring dynamometers to Lockheed Martin in 2012 for help in testing the National Oceanic and Atmospheric Administration's (NOAA) Geostationary Operational Environmental Satellite–R-Series (GOES-R). The newer models (see photo) feature increased efficiency, with the capabilities to characterize a wider range of motors and drives operating with or without the MIL-STD-1553 bus.

The dynamometers can be used as independent test systems or with as many as four dynamometers networked together. They typically are located outside a vacuum chamber, with a device under test (DUT) within the chamber for simulated deep-space conditions. ■

GROUND-PENETRATING Radar Looks for Deep Tunnels

SURPRISE ATTACKS BY enemy troops hiding in tunnels are difficult to predict, although radar technology can help by finding the tunnels. The Rapid Reaction Tunnel Detection (R2TD) system can detect the underground void created by a tunnel, as well as electrical cables or devices within the tunnels, using ground-penetrating-radar (GPR) technology.

The system was developed by engineers several years ago at the Geotechnical and Structural Laboratory of the U.S. Army Engineer Research and Development Center (Vicksburg, Miss.) It employs sensors to detect acoustic and seismic energy. The R2TD system can be mounted in a vehicle or carried by a soldier to an area of interest, and is capable of transmitting data to a remote post for data analysis.

The system has been in use since 2014 and typically requires only one day of training by combat engineers for fully effective operation and results. Because adversaries are continually adapting—using different tunnel depths and more complex maze configurations—the analysis software for the R2TD system must be continually refined, with increased transmit power for greater ground penetration. ■

NEW HEAT-SPREADING DIAMOND for Radio Frequency Applications

A LESSER-KNOWN CHARACTERISTIC of diamond is that it absorbs heat more readily than any other material at room temperature. A subsidiary of the diamond giant De Beers aims to exploit that ability for whisking away heat from electronics.

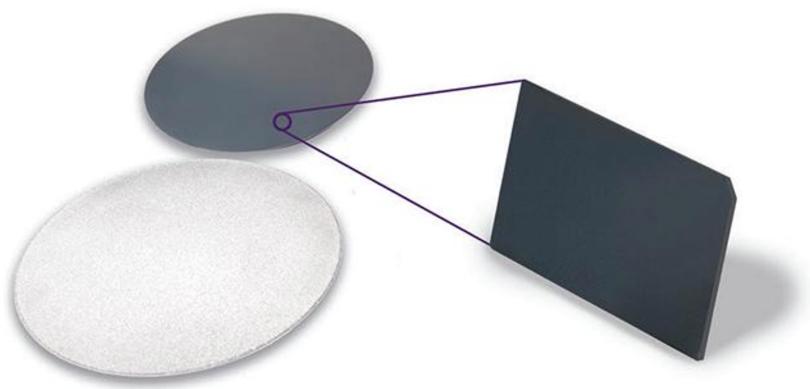

The company, Element Six, released its latest grade of synthetic diamond for thermal management applications. The new product exhibits a thermal conductivity up to 700 W/mK, three times more effective at spreading heat equally from hot spots in RF power amplifiers and other electronics than alternative ceramic products.

Thomas Obeloer, business development manager at Element Six, said in a statement that Diafilm ETC700 delivered high thermal conductivity "far surpassing the performance of competing materials such as copper or ceramics." It is the lowest of six grades in the company's Diafilm product line, which range up to 2000 W/mK.

Element Six, which also sells artificial diamonds for laser optics and industrial drills, has touted its heat spreading materials for over a decade. But recreating diamond, which is formed naturally through billions of years of heat and pressure, is not cheap. The high manufacturing costs have kept it in a few high-performance markets.

In telecommunications and other wireless products, a thin slab of synthetic diamond is soldered between the chip and the substrate. The thermal resistance increases as the separation between the layers goes down. Like other heat spreaders, the diamond is typically coated with metal to improve the interface between the diamond and the chip.

But the Diafilm ETC700 is capable of conducting electricity without the metal coating – usually a combination of titanium, platinum, and gold – resulting in reduced frequency-dependent conductive losses.

Element Six's diamonds are made through chemical vapor deposition, a process normally used in manufacturing semiconductors in thin films. The diamonds usually paired with RF and microwave products are polycrystalline, Bruce Bollinger, the company's head of marketing, told Microwaves & RF in 2015. The single-crystal diamond used in laser optics has better thermal conductivity but its higher cost makes it the wrong choice for RF, Bollinger said.

The market for diamond heat spreaders has a few bright spots. Raytheon has tested it as a substrate material in electronic warfare systems, with tests showing a three-fold increase in power density from gallium nitride chips. At least one company, Akash Systems, is using diamond as a substrate for its wireless amplifiers – to be used in communications satellites.

The new Diafilm product exhibits a large "conduction cross-section" that enables better RF performance by improving the ground-plane isolation. Its high bulk thermal conductivity "reduces capacitive coupling between ground planes at low frequencies, and reduces conductive losses at higher frequencies," Element Six said in a statement. ■

PUTTING A LOCK ON Crystal Oscillator Phase Noise

FREQUENCY GENERATION USUALLY comes at a cost: a certain amount of phase noise. Even for the crystal oscillators typically used as time and frequency references in RF/microwave systems, some phase noise must be accepted and overcome as part of the system design. However, as part of the work that won the 2016 International Microwave Symposium (IMS) Student Design Competition in the category focused on a 100-MHz crystal oscillator, Anisha Apte and Matthias Rudolph of Germany's Bradenburg University explored the various noise limitations of quartz-crystal-resonator-based signal sources. They designed a circuit to optimize the phase-noise performance of a 100-MHz source.

The winners were aided by several co-authors knowledgeable in the design of oscillators, and frequency synthesizers, including Ulrich Rohde (chairman of Synergy Microwave Corp.) and Ajay Poddar (Synergy's chief scientist). The student researchers compared the design and performance of 100-MHz crystal oscillators based on different thicknesses of AT-cut quartz crystal material. They then developed several equivalent-circuit diagrams for the crystal oscillators based on various well-accepted circuit models, such as the Van Dyke model. By modeling variations of Colpitts oscillator circuits, the researchers accounted for fundamental and harmonic operating modes and mode-coupling effects.

Using commercial computer simulation software, they predicted the phase noise for a 100-MHz fifth-overtone crystal oscillator circuit with small size and excellent spectral purity. They were able to enhance the dynamic loaded quality factor (Q) and minimize phase noise through the use of dynamic phase-injection and mode-coupling techniques. Their design approach optimizes the noise factor, startup characteristics, and resonator frequency-drive sensitivity for voltage-controlled crystal oscillators (VCXOs) and was put to the test by fabricating a prototype 100-MHz VCXO.

To verify the design approach, measurements were made on the 100-MHz oscillator using a test system capable of a -193 dBm/Hz noise floor. Initial measurements revealed phase noise of −141 dBc/Hz offset 100 Hz from the carrier. Following optimization using phase-injection, mode-coupling, and noise-filtering techniques, the measured phase noise improved to −144 dBc/Hz offset 100 Hz from the carrier, compared to computer simulations of −142 dBc/Hz at the same offset frequency. As the researchers noted, these phase-injection and mode-locking techniques can be applied to other variations of oscillator circuits.

See "Optimizing Phase-Noise Performance," *IEEE Microwave Magazine*, Vol. 18, No. 4, June 2017, p. 108.

CALIBRATING THE TEST NEEDS of 5G Networks

THE ALMOST ADDICTIVE reliance on wireless communications devices such as smartphones has spurred the planning and development of Fifth-Generation (5G) wireless networks, so as to support the constantly increasing need for additional wireless data. Part of building those networks will be testing and characterizing them, and this will mean the evaluation of components and systems with many new technologies.

Led by Kate Remley, Dylan Williams, and associates, the National Institute of Standards and Technology (NIST) at Boulder, Colo., has launched a new Communications Technology Laboratory with a mission of identifying new measurement requirements and solutions related to the expected operational needs of 5G wireless communications networks. Since 5G networks and equipment are still in their formative stages, NIST faces a wide open challenge of preparing for high-frequency systems and technologies that may or may not be applied in the future.

What appears to be an inevitable extension of the technology in current 4G and 4G LTE networks will be the use of signal frequencies at millimeter-wave bands. NIST is developing a traceability path to millimeter-wave modulated communications signals through at least 70 GHz in frequency, with the need for test solutions capable of fully characterizing such signals in terms of amplitude, phase, and frequency using S-parameters. NIST strives to develop such measurements with the highest levels of accuracy possible, correcting or calibrating out measurement errors. Current research is evaluating calibrating methods for sampling oscilloscopes and vector network analyzers (VNAs) at 50 GHz and beyond.

The NIST traceability plan applies not only to the test equipment, but also to the measurement techniques and types of measurements—including for S-parameter measurements and error-vector-magnitude (EVM) measurements. For example, based on an arbitrary waveform generator (AWG), NIST has developed low-EVM source for calibrating vector receivers. By using predistortion, the EVM of the AWG can be minimized, with levels of 0.5% EVM already having been recorded at 44 GHz.

Robots are helping with these new levels of measurement precision for 5G systems. NIST has developed a robotic antenna range called the Configurable Robotic Millimeter-Wave Antenna (CROMMA) facility that combined robotic control with optical spatial metrology for antenna positioning accuracy of better than ±25 μm for alignment and tracking within a 1.5-m radius spherical volume.

See "Measurement Challenges for 5G and Beyond," *IEEE Microwave Magazine*, Vol. 18, No. 5, July/August 2017, p. 41.

DAMIAN McCANN | Director of Engineering, Discrete Products Group, Microsemi
CANG NGUYEN | Design Engineer, Discrete Products Group, Microsemi

Single-Ended GAN Power Transistors Spawn New System-Level Capabilities

Engineers tasked with building next-gen L-band systems can now take advantage of new single-ended transistors based on gallium-nitride (GaN), which offer better performance across the board.

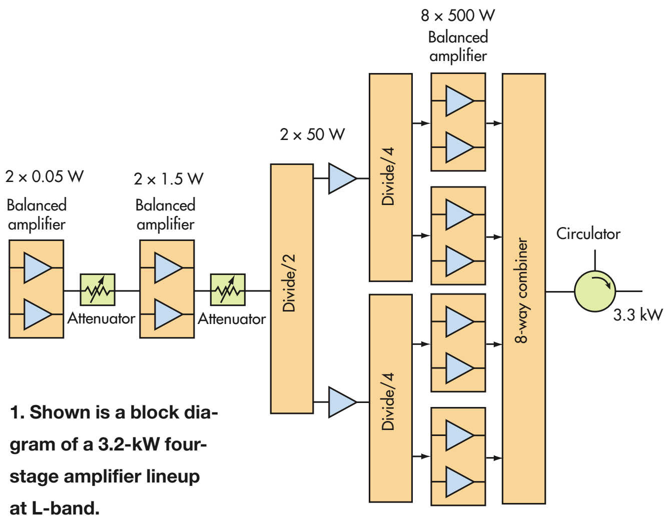

1. Shown is a block diagram of a 3.2-kW four-stage amplifier lineup at L-band.

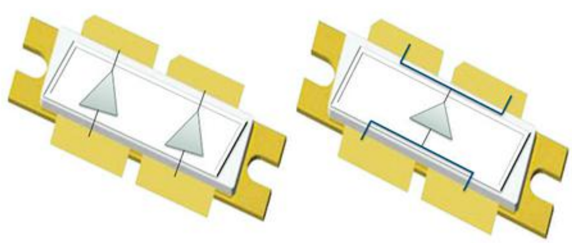

2. This image compares a high-power transistor in a Gemini package (left) with a single-ended 1600-W transistor (right).

Equipment designers often face power-level requirements that far exceed what is achievable from a single solid-state device. While laterally diffused metal-oxide semiconductor (LDMOS) devices offer ever-higher power levels, gallium-nitride (GaN) technology takes it one step further: GaN brings higher power densities and efficiencies to the designer's toolbox, making it possible to achieve even more power in smaller packages while reducing the overall size of the final solution.

Paralleling two or more RF power devices to increase power levels is still routinely done in the industry. However, a better way to scale power when combining multiple devices is to push the output power of single-ended transistors to significantly higher levels. This simplifies the bias needs and distribution, reduces size and weight, and enables additional system benefits previously contained in two rack-and-stack amplifier boxes. This article reports on the attributes and benefits of using these very-high-power transistors in the design and application of next-generation L-band systems.

INVIGORATING L-BAND WITH GAN

As manufacturers address re-engineering existing L-band systems, GaN offers key benefits that lead to new capabilities. Bipolar transistors used in traditional avionics and radar capabilities have already been replaced by both LDMOS and GaN transistors to more than double power while maintaining power-supply dissipation levels. The new transistors' greater levels of gain and efficiency are the main reasons behind the surge in power. Numerous suppliers already offer 500-, 600-, and 700-W transistors to make such a cascade possible. *Figure 1* shows a conceptual block diagram of a typical 3.2-kW amplifier.

A key driver of a high-reliability system design is redundancy. Thus, it is common to have parallel paths throughout the cascade chain, preventing soft failure. However, additional challenges arise in terms of bias distribution and the pulsing electrolytic cap placement.

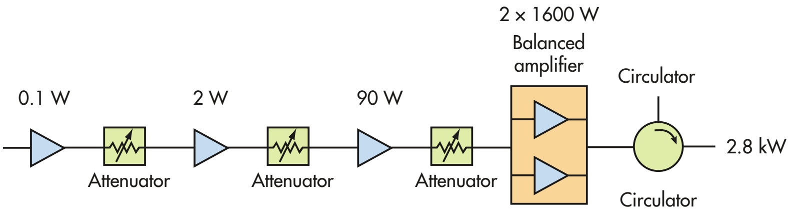

3. As seen in this block diagram, a 2.8-kW L-band amplifier utilizes a 1600-W single-ended transistor in a pallet configuration.

5. The package size of this transistor is a mere 0.385-in × 1.34-in.

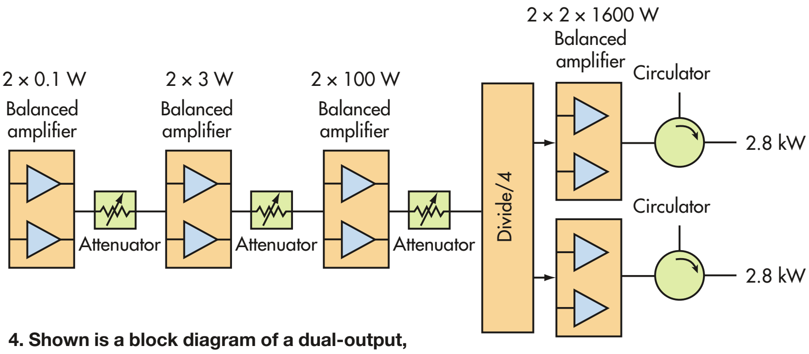

4. Shown is a block diagram of a dual-output, 2.8-kW L-band amplifier that incorporates four 1600-W transistors.

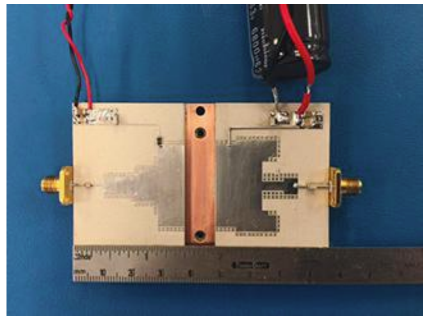

6. This photo shows the application circuit of the 1600-W transistor.

GaN presents the additional challenge of introducing a negative supply voltage that also requires routing. To date, manufacturers have come to the system engineer's aid by offering a wide array of balanced pallets with ever higher levels of integration. This has often been accomplished with what is called a "Gemini package"—two transistors and two leads at the input and output to allow for external combining *(Fig. 2a)*.

Alternatively, a single-ended transistor can deliver the required higher power levels. One example is Microsemi's 1011GN-1600VG 1600-W transistor, which is designed to combine higher RF output power with improved efficiency and ease-of-use in a smaller footprint.

The latest single-ended transistors combine multiple, large transistor cell arrays with high levels of efficiency while meeting all requirements for thermal performance and robust and reliable operation inside existing rack boxes. *Figure 3* shows how combining two GaN-based, 1.6-kW, single-ended transistors can create upwards of 3 kW of power, simplifying dc and RF distribution and reducing the complexity, size, and weight of the final solution.

Size diminishes because the system engineer can use the two single-ended transistors to make two separate outputs available in an existing rack amplifier outline, eliminating one rack-and-stack amplifier *(Fig. 4)*. That alone is a key step toward reducing overall system size and weight.

However, system size and weight shrink even more due to the small size of the single-ended transistor package—in the case of the Microsemi solution, just 0.385 × 1.340 in. *(Fig. 5)*.

Within today's small packages, the single-ended transistor application solution can include input and output matching circuitry as well as bias feeds. Special design techniques are used to minimize the size of the heat sink and metal pallet. This involves ensuring that output impedances have the ability to be set higher, so that the matching circuitry can be resized consistent with the transistor's width.

At the same time, the use of impedance transformation techniques ensures the transistor can be shortened. In the case of the Microsemi devices, the application circuitry is created on 20-mil RO6010 material and measures less than 3.5 in. long by 2 in. wide *(Fig. 6)*. This configuration also simplifies the bias scheme, which leads to fewer components and higher power gain and efficiency—even under Mode S-ELM signals.

GAN VS. LDMOS AND GAN-ON-SILICON

In addition to reductions in size, weight, and power, GaN-enabled transistors in a small, single-ended package outperform less-capable technologies such as LDMOS and GaN-on-silicon (both of which lack the necessary power densities, thermal performance, and efficiencies to address the next generation of avionics equipment).

Tables 1 and 2 summarize the performance and efficiencies of designs using single-ended transistors. Drain efficiencies exceeding 70% make it possible to reduce device heating and allow the transistor to operate reliably under typical system

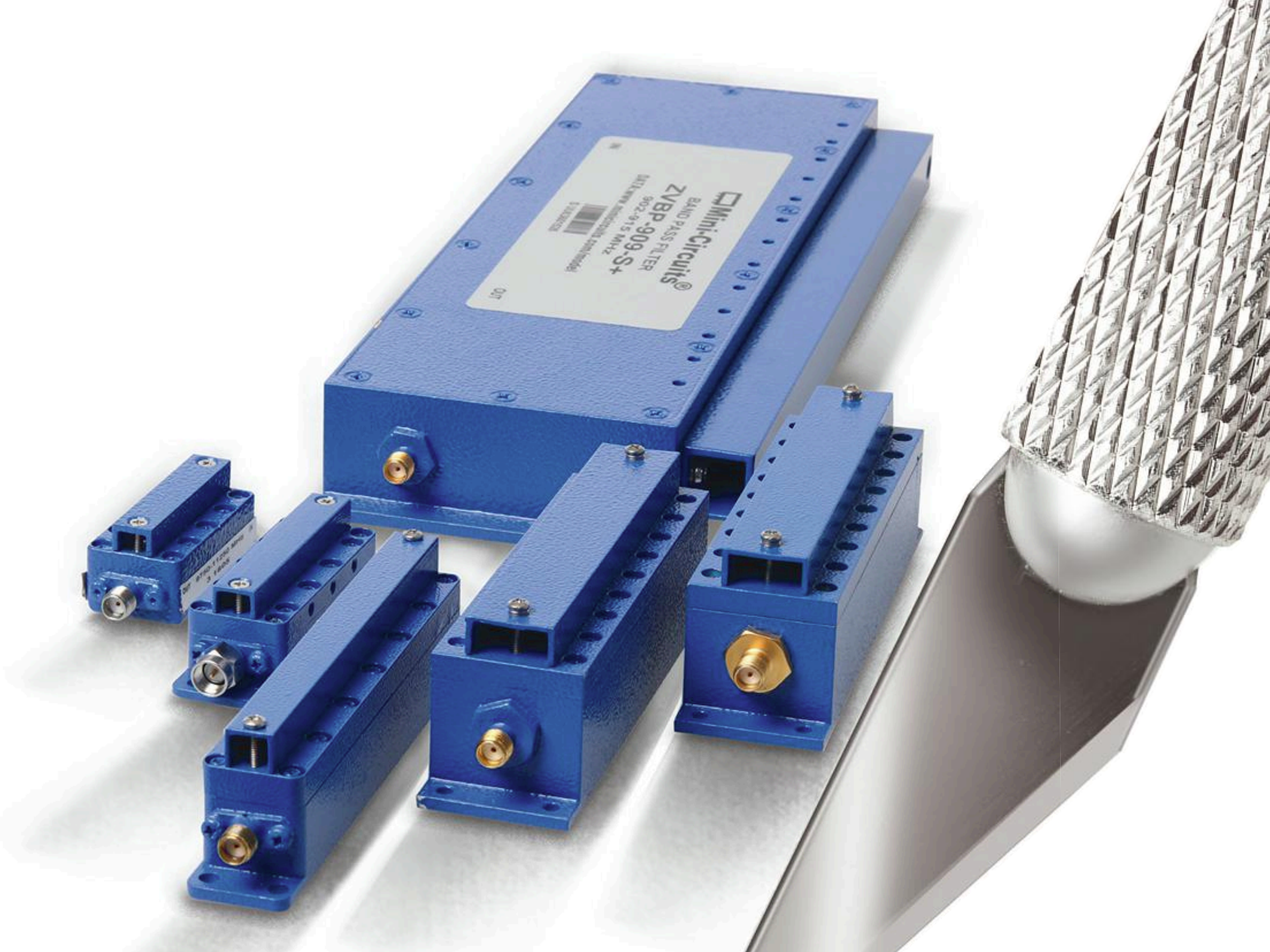
Mini-Circuits®
BAND PASS FILTER
ZVBP-909-S+

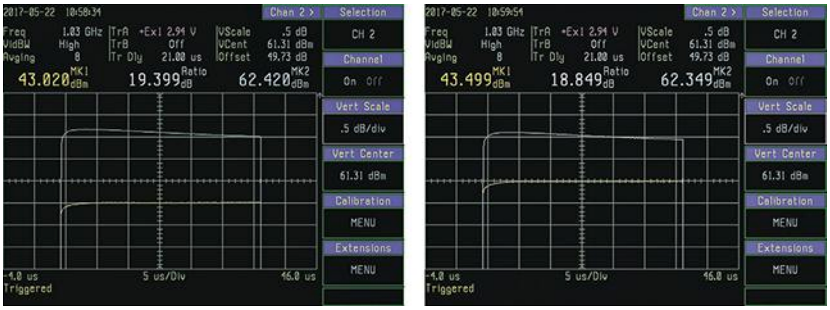

7. These screen captures depict performance at 1.03 GHz.

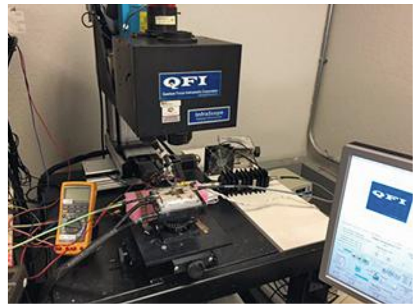

8. This test setup was configured to perform thermal measurements.

TABLE 1: TYPICAL RF MEASUREMENTS OF 1011GN-1600VG PACKAGED TRANSISTOR

	Output pulse 1 of 48								
Freq (MHz)	P_{in} (dBm)	P_{in} (W)	P_{out} (dBm)	P_{out} (W)	G_P (dB)	IRL (dB)	Max G_P (dB)	I_D (A)	Efficiency (%)
1030	43.5	22.4	62.19	1655.8	18.69	–18.0	20.16	2.92	72.6%
	43	20.0	62.1	1621.8	19.1			2.89	71.8%
	42	15.8	61.54	1425.6	19.54			2.7	67.6%
	41	12.6	60.83	1210.6	19.83			2.35	65.9%
	40	10.0	59.92	981.7	19.92			2.31	54.4%

V_{DD} = 50 V; I_{DQ} = 1 A; Pulse: Mode-S ELM 32-µs on, 18-µs off; Duty factor = 6.4%

TABLE 2: TYPICAL RF MEASUREMENTS OF 1011GN-1600VG PACKAGED TRANSISTOR

Output pulse 48 of 48						
Freq (MHz)	P_{in} (dBm)	P_{in} (W)	G_P (dB)	P_{out} (dBm)	P_{out} (W)	Droop (dB)
1030	43.5	22.4	18.16	61.66	1465.5	0.53

V_{DD} = 50 V; I_{DQ} = 1 A; Pulse: Mode-S ELM 32-µs on, 18-µs off; Duty factor = 6.4%

TABLE 3: TABULATED TRANSIENT THERMAL DATA

V_{GS} = -3.51 V	Freq	P_{in} (dBm)	P_{in} (W)	P_{out} (dBm)	P_{out} (W)	Gain	I_C/Avg (A)	Transient	Delta T	Thermal resistance
SN#1	MHz	(dBm)	W	dBm	W	dB	Actual	°C	°C	°C/W
Based temp: 70°C	1030	43	20.0	61.89	1545.3	18.89	1.031	104.6	34.6	0.57
	TOP									
		43.5	22.4	61.91	1552.4	18.41	1.028	112.8	42.8	0.58
	Freq	P_{in} (dBm)	P_{in} (W)	P_{out} (dBm)	P_{out} (W)	Gain	I_C/Avg (A)	Transient	Delta T	Thermal resistance
	MHz	(dBm)					Actual	°C		°C/W
	1030	43	20.0	61.89	1545.3	18.89	1.031	104.82	34.82	0.57
	BOTTOM									
		43.5	22.4	61.91	1552.4	18.41	1.028	104.68	34.68	0.58

V_{DD} = 52 V; I_{DQ}= 1 A; Pulse width = 32 µs; Pulse period = 1.6 ms

environmental requirements. Tangible benefits go beyond higher power levels to include lower pulse droop—even in Mode-S applications.

This performance data is illustrated in *Figure 7*. The transistor demonstrates high levels of pulse-to-pulse stability, linearity, and droop.

To maximize power performance, it is essential to maintain the highest efficiency. Thus, it becomes possible to maintain the lower operating channel temperatures essential for robust application reliability and satisfy the general lifetime requirements of high-reliability systems. Performance measurements consist of both average and transient thermal measurements using QFI (www.quantumfocus.com) thermal-imaging equipment, backed by thermal modeling and extraction of the true channel temperature *(Fig. 8)*.

Single-ended transistors must demonstrate excellent balance on both the top and bottom transistor arrays inside the package *(Figs. 9 and 10, and Table 3)*. In this example, the temperature difference is less than 5 degrees, demonstrating that each cell is being driven in amplitude and phase. As a result, high levels of combined efficiency and performance are achieved.

The benefits of GaN are well known, but only with the recent advent of single-ended GaN transistors has the technology emerged as a promising alternative to

(Continued on page 80)

JACK BROWNE | Technical Contributor

Packaging Provides Microwave Protection

Whether a device is made to fit a package or the package designed for the device, the best packages are those that are least noticed under all operating conditions.

1. HTCC QFN packages such as these are capable of excellent high-frequency performance, at frequencies to 40 GHz and beyond. *(Courtesy of Barry Industries; www.barryind.com)*

PACKAGING MEANS DIFFERENT things to different people. For a device designer, it is an enclosure of almost microscopic size. For a systems-level engineer, it may be a series of racks that must fight on a battleship. No matter the size, electronic packaging is meant to provide mechanical protection while remaining electrically invisible.

When factors such as high production volumes come into play, then packaging goals must also be met with cost constraints. At the other extreme, electronic packaging for devices heading into outer space, such as on satellites, must endure temperature extremes and vacuum environments. Packaging is often taken for granted as part of an integrated-circuit (IC) design process, but the reliability and successful operation of that IC usually hinge on the quality of its package.

Higher-frequency packages must be considered as part of the circuits they enclose. For example, semiconductor die are typically either fully encapsulated in some form of epoxy-based compound, or else they are mounted in some form of cavity package formed of different materials (including metals, ceramic, and plastic).

In addition to an IC, the package may also contain passive impedance-matching components, bias circuitry, components for suppression of EMI, etc. The first method, of over-molding a device or IC in a polymeric material, is the most cost-effective packaging approach, but it requires significant tooling costs and is susceptible to high moisture absorption and high dielectric loss at RF/microwave frequencies.

Package complexity and materials contribute a great deal to its cost, and the RF/microwave industry has traditionally been faced with relatively mild demands in terms of volume for device packages compared to broader electronic industries, such as for power and computer applications. Packages for RF/microwave applications must also support wide bandwidths and high frequency ranges, and this has traditionally required costly package substrate materials, such as ceramic.

Higher-volume device packaging has turned to enclosing conductive metal leadframes with lower-cost plastic materials, and many of these plastic packages are finding application for RF/microwave devices. One challenge facing all high-frequency device package developers is the production of lower-cost package solutions capable of working well into the millimeter-wave frequency range, but also with the durability to survive long-term use in hostile operating environments, such as in automotive electronic safety systems.

Within lower microwave frequency ranges, one of the more popular device packages at present is the quad, flat, no-leads (QFN) package *(Fig. 1)*. It is small in size and relatively low in cost. A QFN package allows for attachment and connection of an IC to a PCB without through-hole connections, using surface-mount technology (SMT) for compatibility with PCBs using microstrip and coplanar-waveguide (CPW) transmission-line technologies.

Such a package consists of a leadframe, wire bonds, and a molding compound as a cover. The lead frame is formed of a conductive copper alloy for low-loss electrical connections. A thermally conductive adhesive attaches the device to be packaged to the leadframe thermal bead. Gold bond wires are used for electrical connections from the device's leads to the package leadframe.

QFN packages are available in two formats: plastic molded QFNs and air-cavity QFNs. A plastic-molded QFN is basically a copper leadframe with a plastic cover and is typically usable to about 3 GHz. An air-cavity QFN package, which consists of a copper leadframe, plastic molded body (open and not sealed), and either a ceramic or a plastic lid, is usable to about 20 GHz.

Air-cavity packages have been developed in many configurations, including for optical and photonic devices—as well as

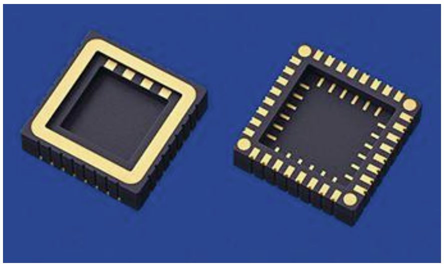

2. Newer package configurations are often required to accommodate the contact connections and mechanical requirements of a relatively unconventional electronic device, such as a MEMS switch. *(Courtesy of Kyocera; www.kyocera.com)*

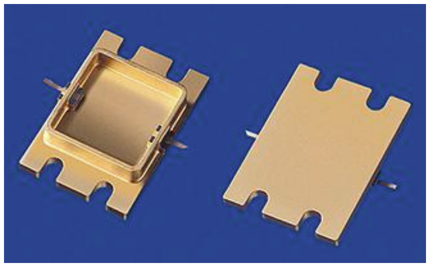

3. High-power device packages require large metallized mounting areas with high thermal conductivity to facilitate the flow of heat away from the active device. *(Courtesy of Kyocera)*

4. The LL series high-power millimeter-wave packages operate at frequencies from DC to 63 GHz. *(Courtesy of StratEdge Corp.)*

for relatively new device technologies such as microelectromechanical-systems (MEMS) devices, in which mechanical and electrical functions must be supported.

These packages are usually based upon ceramic materials and may be a simple as "can-like" structures to hold a device, such as leadless chip carriers (LCCs). More often, custom packaging is required for MEMS devices, which has encouraged the use of package designs with premolded thermoplastic leadframes that preserve both cost and performance while providing the flexibility of rapid design modifications to meet the needs of a multiple-contact MEMS device *(Fig. 2)*. One of the thermoplastic materials used in high-frequency device packages is liquid crystal polymer (LCP), which is favored for its low moisture absorption and low dissipation factor (low loss).

Manufacturing process temperatures will play a part in the selection of package materials, such as the elevated temperatures required for lead-free (RoHS-compliant) soldering processes. Ceramic materials such as alumina, for example, have very high firing temperatures (about +1,600°C) which will limit the choice of metallization (to tungsten) for package leads since most metals can't survive such a high firing temperature.

By blending ceramic materials with other materials, such as glass as used in low-temperature-cofired-ceramic (LTCC) packages, the firing temperature of the ceramic composite can be reduced to about +700 to +800°C, in contrast to the much higher firing temperatures of high-temperature-cofired-ceramic (HTCC).

As the power of the packaged circuit or device increases, the thermal capacity of the package must follow. In higher-power RF/microwave device packages, thermal design is given as much attention as electrical design. Device packaging for RF/microwave discrete power transistors must provide low-loss electrical connections that are stable at high power levels. This usually means also dissipating large amounts of heat. High-power transistor packages are usually identified by large mounting areas to a PCB, such as flange-mount attachments, to allow maximum flow of heat away from the transistor or other active device *(Fig. 3)*.

MM-WAVE PACKAGES

Package developers are often challenged by emerging technologies and trends. With so much attention being paid to the next, Fifth Generation (5G) of wireless communications, and its uses of new and different frequency bands than past generations of wireless systems, there is concern about how to cost-effectively package active devices operating at millimeter-wave frequencies for use in those 5G systems.

One company that has been instrumental in driving performance levels for millimeter-wave packages is StratEdge (www.stratedge.com). The firm has been a pioneer in addressing the high-power-density requirements of RF/microwave GaN devices, using high-power laminate copper-moly-copper (CMC) base packages to promote consistent heat flow away from GaN devices, whether as discrete or monolithic-microwave-integrated-circuit (MMIC) devices. The packages are also suitable for other high-frequency semiconductor processes, such as gallium arsenide (GaAs) and silicon carbide (SiC) capable of producing high-frequency devices with high-power output levels.

At the recent 2017 IMS, StratEdge announced additions to its LL family of high-frequency packages, which combine the thermal requirements of high-power packaging with the extended-frequency performance needed for millimeter-wave devices *(Fig. 4)*. The packages support discrete and MMIC device applications from DC to 63 GHz in applications requiring high-power millimeter-wave signals, including commercial and military radar systems.

The LL packages are available in leaded and leadless versions. They are either flangeless, with a hermetic seal and ceramic lid, or with flanges for mounting on a PCB for effective thermal transfer. The company also offers complete automated assembly and test services for the high-power, high-frequency packages. mw

ULTRA-REL™
CERAMIC MMIC AMPLIFIERS

10 MHz to 7 GHz

Low NF from 0.5 dB   *High IP3 up to +42 dBm*   *Low DC current 65 mA*   from $7.45 ea. (qty 20)

When failure is not an option! Our CMA family of ceramic MMIC amplifiers is expanding to meet your needs for more critical applications. Designed into a nitrogen-filled, hermetic LTCC package just 0.045" high, these rugged models have been qualified and are capable of meeting MIL standards for a whole battery of harsh environmental conditions:

Qualified for: *(see website for complete list and details)*

Gross and Fine Leak	*HTOL (1700 hours @ +105°C)*
Mechanical Shock	*Steam Aging*
Vibration	*Solder Heat Resistance*
Acceleration	*Autoclave*
PIND	*And More!*

**Gross leak only*

Robust performance across wide bandwidths makes them ideal for military and defense applications, hi-rel instrumentation, and anywhere long-term reliability adds bottom-line value. Go to minicircuits.com for all the details today, and have them in your hands as soon as tomorrow!

Electrical Specifications *(-55 to +105°C)*

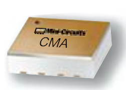

3 x 3 x 1.14 mm

Model	Freq. (GHz)	Gain (dB)	P_{OUT} (dBm)	IP3 (dBm)	NF (dB)	DC (V)	Price $ ea. (qty 20)
CMA-81+	DC-6	10	19.5	38	7.5	5	8.95
CMA-82+	DC-7	15	20	42	6.8	5	8.95
CMA-84+	DC-7	24	21	38	5.5	5	8.95
CMA-62+	0.01-6	15	19	33	5	5	7.45
CMA-63+	0.01-6	20	18	32	4	5	7.45
CMA-545+	0.05-6	15	20	37	1	3	7.45
CMA-5043+	0.05-4	18	20	33	0.8	5	7.45
CMA-545G1+	0.4-2.2	32	23	36	0.9	5	7.95
CMA-162LN+	0.7-1.6	23	19	30	0.5	4	7.45
CMA-252LN+	1.5-2.5	17	18	30	1	4	7.45

RoHS compliant

Mini-Circuits®

www.minicircuits.com   P.O. Box 350166, Brooklyn, NY 11235-0003   (718) 934-4500   sales@minicircuits.com

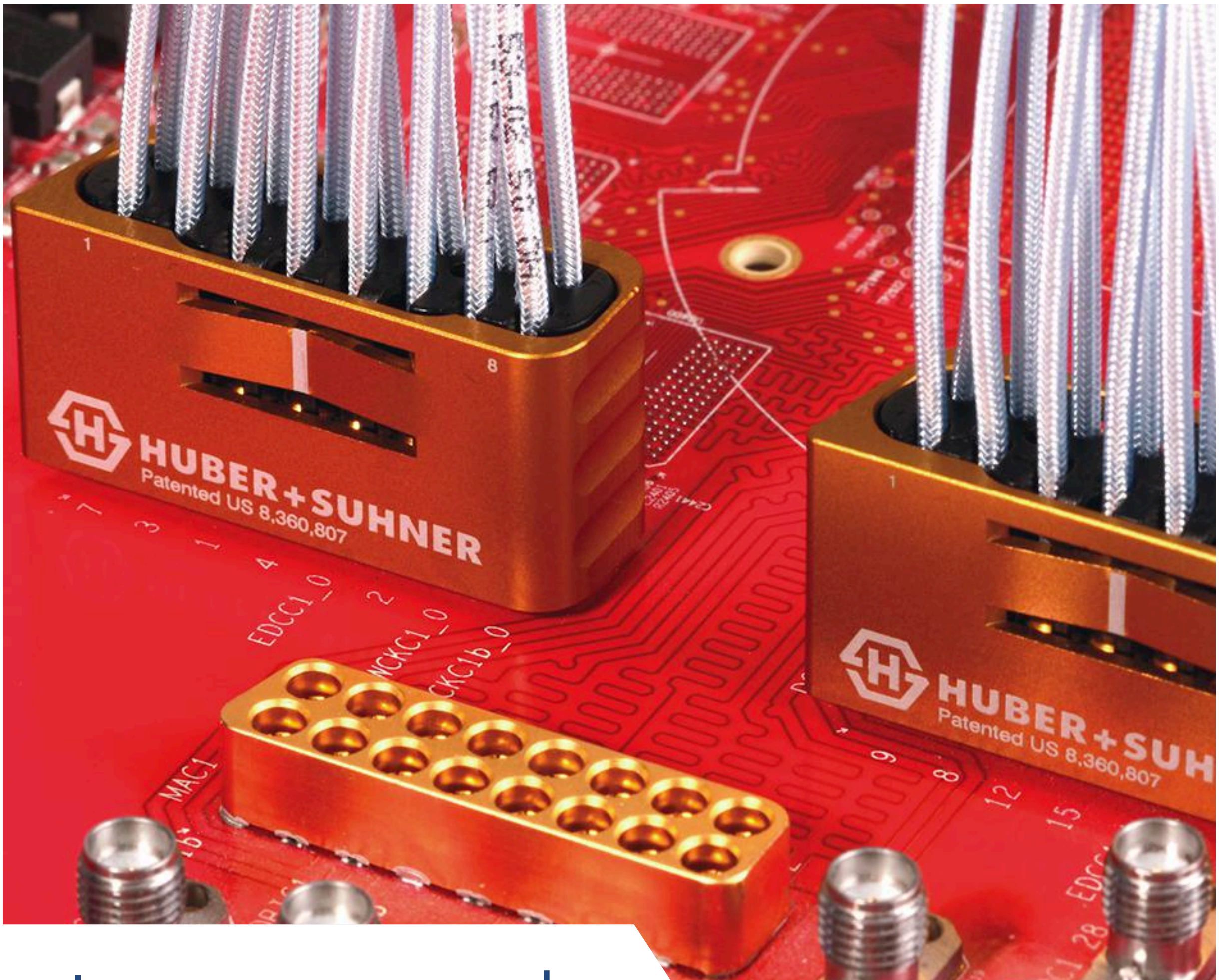

In one easy push – up to 16 high speed connections

The small form factor and outstanding electrical characteristics combined with reliable mating and ease of use make our MXP – ganged multicoax interconnect - an excellent solution for bench-top and system testing. The HUBER+SUHNER MXP product line offers a large selection of bandwidths: MXP 50 (50GHz), MXP 40(40GHz) and MXP 18 (18GHz) that covers the current data rates requirements. All of the MXP family comes standard with the highly flexible and ultra-stable Multiflex cable (MF53-02).

MANNY RAJU, SHAWN CARPENTER, and MATTHEW COMMENS | Ph.D., ANSYS
www.ansys.com

Simulate Installed Antenna and RF Co-Site Issues with EM Tools

Current electromagnetic (EM) modeling and simulation tools offer a means to effectively design aircraft antenna systems.

MODERN AIRCRAFT CONTAIN many sophisticated electronic systems for communications, telemetry, navigation, guidance, radar detection, tracking, and more. Onboard radar systems typically help to maintain safety along the flight path by detecting thunderstorms, identifying regions of potential turbulences, and avoiding collisions. Other antenna-enabled systems for command and control, such as Identification Friend or Foe (IFF), also exist on commercial and military aircraft. In all of these avionic systems, antennas are key internal components. Their performance is critical to ensure these systems function properly.

For a long time, aircraft antenna designers have grappled with the challenges associated with designing antennas, integrating antennas into airborne avionic systems, and determining the best locations to install these systems on an aircraft. The build-and-test approach can address some of these challenges. However, for a vehicle as complex, large, and advanced as an aircraft, organizations are bound to incur huge expenses when they follow this approach.

To understand the difficulty involved, this method requires test chambers (which are sometimes very large), scheduling vehicle assets and their equipment, and significant manpower, as well as considerations in terms of infrastructure and facilities. Each of these requirements can be prohibitively expensive, potentially limiting the scope of testing available within a given project.

THE MODELING AND SIMULATION SOLUTION

In contrast, modeling and simulation offers an economical, smart, and efficient means of rapidly addressing these design and engineering challenges *(Fig. 1)*. The end result is usually improved system performance and compressed design cycles.

Many electromagnetic (EM) simulators are available for designing antennas. Key factors that influence the choice of EM simulation tool include accuracy, speed, usability, and efficiency.

With ANSYS EM tools, one only needs to import the design's geometry and specify materials and the excitations. ANSYS HFSS automatically generates accurate solutions for EM problems, thereby alleviating the user from knowing how the device works in order to know how to mesh the design. Moreover, ANSYS EM tools are equipped with many solver technologies.

Furthermore, HFSS SBR+ and ANSYS EMIT can be used in conjunction with HFSS. Users can then follow a smooth and integrated workflow for simulating installed antenna and RF system performance on airborne platforms. In addition, it's possible to achieve RF co-site interference between RF systems.

SIMULATION WORKFLOW

A simulation workflow can be followed to solve diverse sets of EM problems concerning antenna integration on an aircraft. This workflow involves only a few steps from initiation to completion. Generally, an antenna is initially designed under the

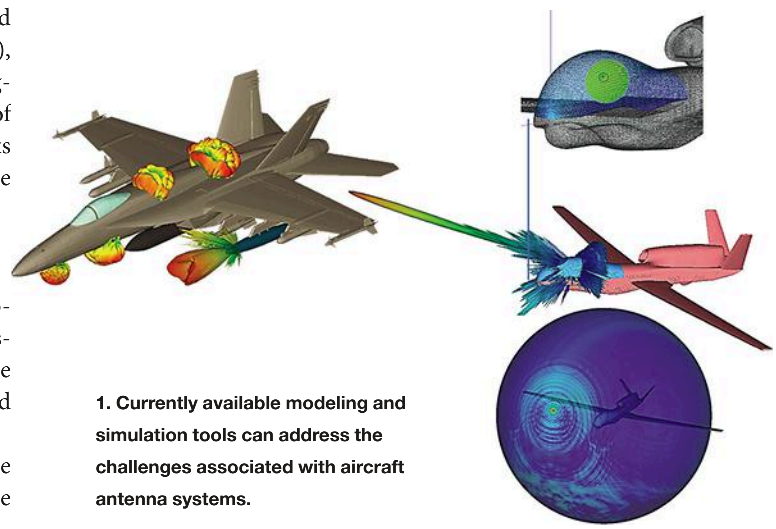

1. Currently available modeling and simulation tools can address the challenges associated with aircraft antenna systems.

assumption that it exists in free space by itself or on a ground plane. In the first step, one can select a standalone antenna element from a known set of antenna topologies already available in an antenna design toolkit. These antennas are preconfigured—users only need to enter the desired frequency. HFSS then automatically creates the antenna.

Additionally, users have the flexibility to modify antenna properties, such as dimensions and materials. Any antenna from the toolkit comes in a ready-to-solve state. Reports are automatically generated for return loss, 2D and 3D radiation patterns for antenna gain, and animations of electric fields, etc. Since antennas couple to their local environment, the next step of the workflow involves adding the antenna to its housing. A simulation can then be run to understand the antenna's performance within the system.

Next, the user can create an HFSS 3D component of this final model to facilitate sharing the design with vendors, customers, and collaborators. A noteworthy feature of the HFSS antenna toolkit is its ability to generate parameterized antennas. This capability allows users to vary antenna sizes and other properties as needed to fit them within their respective systems. Moreover, a parameterized design makes it much easier to tune the antenna.

HFSS offers several features like optimization, automated parametrics, tuning, and analytic derivatives that aid with antenna tuning and integration. With these features, one can generate a 3D component model (of the antenna in its system) to eventually add to a large assembly, i.e., the aircraft. Furthermore, 3D components facilitate the creation of wireless communication systems by enabling easy drag-and-drop assembly of complex systems from a set of predefined components.

An HFSS 3D component is extremely useful, especially as these avionic systems become increasingly complex and users need to leverage pieces of a system's design from other sources. Think of an HFSS 3D component as a self-contained model comprising the antenna feed-point and EM characteristics wrapped up in a plug-and-play module. It is immediately ready for use once connected to a large assembly, such as an aircraft.

HFSS 3D components can be encrypted and password-protected. Users are able to hide internal details of the structure, materials, and other properties that comprise the antenna design. Antenna vendors can use these features to protect their intellectual property and easily share the 3D components with system integrators, while allowing the same system integrators to simulate, design, and integrate with the deep rigorous simulation approach of HFSS. Since 3D components are simulation-ready, users can execute the next workflow step of performing installed antenna analysis with minimal additional user input.

SOLUTIONS FOR PROBLEMS OF ALL SIZES

ANSYS HFSS has many solvers suited for different kinds of EM problems. Finite element solvers in HFSS can be used to simulate and design the antenna elements in detail. Users can then extend the simulation scale and perform installed antenna analysis with the integrated 3D method-of-moments (MoM) solver that now comes with HFSS (as of ANSYS 18).

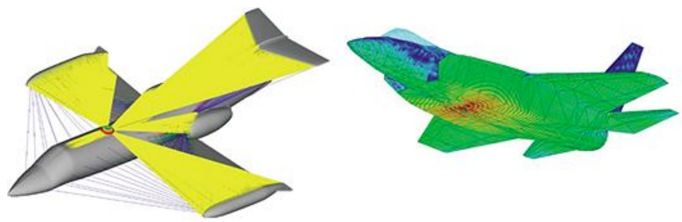

2. Software tools allow for EM analysis of very large platforms, such as aircraft.

HFSS SBR+ can be employed for very electrically large problems. It uses a high-frequency asymptotic shooting and bouncing ray technique to track the scattering of EM energy across hundreds or even thousands of wavelengths *(Fig. 2)*. Full-wave results from HFSS can be employed as initial excitations for SBR+ when solving scattering problems in electrically large structures.

For instance, an antenna or array integrated into an aircraft body is sensitive to the shape of the aircraft. The antenna's radiation pattern is affected by the surface currents on the aircraft. The pattern also experiences blockage by wings and engines, as well as multi-path reflections between structures like stabilizers and wings. Analysis in HFSS and HFSS SBR+ provides critical insights into an antenna's behavior when integrated on its platform. HFSS and HFSS SBR+ can also be used to model antenna-radome interactions to assess the antenna's complete installed performance.

Finally, it's important to consider antenna-to-antenna coupling issues when designing antenna systems. Since there are multiple antennas on an aircraft, the coupling—including out of band—can lead to interference between the associated radios and RF systems.

In the final step of the workflow, ANSYS EMIT can be used to predict and mitigate these interference issues, known as co-site RFI. ANSYS EMIT, with its built-in radio and component models, can solve the full aircraft system and predict the performance of the entire wireless system on the aircraft. Easy to use and interpret "RF threat matrices" can help an engineer determine and test mitigation strategies with the system simulations available in EMIT.

In the end, the combination of HFSS, HFSS SBR+, and EMIT help engineers devise a system frequency plan for ensuring smooth and interference-free operation of wireless systems. By following this integrated simulation workflow, ANSYS EM tools can predict the performance and improve the reliability of wireless systems on an aircraft. This approach helps reduce design cycles, and in turn saves on costly empirical testing and shrinks development time.

For more information about the workflow, visit *ansys.com*. mw

CHIN-LEONG LIM | Engineer, chin-leong.lim@avagotech.com
Avago Technologies, Penang, Malaysia

Low-Noise Amplifier Aids TDD Small Cells

This MMIC LNA design includes bias, ESD, and power-down circuitry for reduced cost and parts count in support of 3G and 4G wireless small cell stations.

Large capacity is essential to the success of present and future cellular wireless networks, and a well-designed low-noise amplifier (LNA) can help increase the capacity of a small cell. A typical small cell has a range of about 10 m to 1 km compared to a traditional macrocell at a few tens of kilometers.[1] As a result, a small cell can improve frequency reuse by as much as 1600×.[2]

On the flip side, hundreds of small cells are needed to provide the same coverage as one macrocell. Hence, it is necessary to make small cell equipment significantly less expensive than its macrocell counterpart. One way to save cost is by using one broadband radio module instead of multiple narrowband radio modules in support of different air interfaces. The LNA is an essential component for the receiver portion of a small cell's radio module.

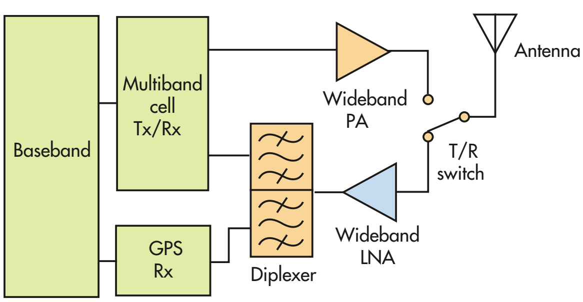

1. A wideband LNA enables a small cellular base station to operate on different air interfaces and frequencies.

An LNA is the first stage of a radio module's receiving section (*Fig. 1*). It is usually impedance matched for low noise at one frequency although, in a small wireless cell, an LNA must cover a wide range of frequencies. Resistive shunt feedback can widen an LNA's impedance-matched bandwidth[3, 4] but results in tradeoffs of noise, gain, and output-power performance[5]; hence, it can only be used sparingly. Fortunately, small cells have less demanding noise requirements than macrocells since they cover smaller areas.

The output-power requirements of small cells are also lower because a small cell's low height (about 10 m) makes it less susceptible to interference.[6] To compensate for the increased noise of a feedback amplifier's configuration, a low-noise semiconductor process, such as a GaAs enhancement-mode pseudomorphic high-electron-mobility-transistor process (GaAs E-pHEMT),[7, 8] can be used. Although low-noise feedback amplifiers have been realized with discrete ePHEMTs,[9, 10] the use of monolithic microwave integrated circuit (MMIC) technology can significantly reduce component count by integrating amplifier, feedback network, and biasing circuits.

Such integration has been used in an SOT-363-packaged amplifier with sub-1-dB noise figure (NF) over two octaves of bandwidth.[11, 12] The device's small size and good performance have led to its adoption in many small-cell LNAs, although it is not as popular lately. While its NF performance was considered state-of-the-art when it was introduced in 2003, it has since been surpassed by competitors (*Table 1*).

Small cells serve a number of time-division-duplex (TDD) networks, including time-division synchronous code-division-multiple-access (TD-SCDMA) technology for Third-Generation (3G) cellular networks and time-division Long Term Evolution (TD-LTE) for Fourth-Generation (4G) cellular networks. Due to the use of a common frequency for transmit and receive functions, the LNA must be powered down during transmission to prevent overdrive. Traditionally, the power-down function is implemented off-chip by wiring a transistor switch in series with the LNA's supply voltage. However, a competitor's recent design integrates an LNA and power-down switch into a silicon germanium (SiGe) MMIC.[13] Since this approach saves components in TDD implementations, it has been well received by carriers for use in small cells.

To improve upon this approach, it is necessary to develop a lower-cost MMIC LNA with smaller size that still provides a two-octave bandwidth. The choice of MMIC semiconductor process is critical for achieving the necessary NF performance at low cost. A 0.25-μm GaAs E-pHEMT process was selected for its excellent balance of cost and performance. Performance-wise, E-pHEMT and SiGe processes are roughly equivalent, but mask sets for E-pHEMT technology are fewer and less expensive.[14, 15]

TABLE 1: COMPARING COMMERCIALLY AVAILABLE WIDEBAND LNA MMICS.									
Reference	Technology	Size (mm)	Part count	DC power (mW)	Power down	Noise figure (dB)	Gain (dB)	OIP3 (dBm)	P1dB (dBm)
11	GaAs pHEMT	2.1 × 2.0 × 1.0	10	180	-	0.9	20.0	+34.0	+17.6
13	SiGe	2.0 × 2.0 × 0.8	9	240	Y	0.4	18.3	+39.0	+19.4
23	GaAs pHEMT	1.5 × 1.5 × 0.5	10	350	Y	0.8	21.0	+34.0	+20.0
This work	GaAs pHEMT	2.0 × 2.0 × 0.8	9	260	Y	0.6	19.0	+36.6	+20.4

Note: Noise figure, gain, OIP3, and P1dB are shown at 900 MHz.

Setup costs are important because of the relatively small volume requirements for small-cell LNAs compared to devices used in mass-market wireless handsets. Another factor in favor of E-pHEMT technology is the capability to integrate a switch with the amplifier.

A traditional design approach uses feedback to tune the input and output impedances to approximately the target characteristic impedance. However, at VHF and lower microwave frequencies, a large amount of feedback is required, which will significantly degrade NF and output power. Relying on feedback alone to match a GaAs E-pHEMT device resulted in a modest NF of 0.8 dB at 900 MHz.[10]

One way to reduce the feedback requirement is to tailor the gate dimensions for a good impedance match at midband frequencies. However, once the gate width has been set for a good midband match, the impedances may still vary too much over the full frequency range for realistic wideband operation. As a result, only a small amount of feedback was used to reduce the impedance spread over frequency (*Fig. 2*). This alternative design approach also results in less NF degradation.

Since gain and NF are key parameters in an LNA, the E-pHEMT was configured as a common-source amplifier. Aside from the LNA, the MMIC chip also contains circuits for the power-down function, active bias, and electrostatic-discharge (ESD) protection (*Fig. 3*). The active bias is designed to draw a nominal 65 mA from a single +4-V dc supply.

The power-down function is performed by a switch that disconnects the E-pHEMT's gate from the active bias. Since the function is designed to activate the LNA if its control terminal (V power-down, pin 6) is either grounded or open, the control terminal can be conveniently left unconnected in non-TDD applications.

The chip is epoxy encapsulated in an eight-lead quad-flat-no-lead (QFN) package measuring 2 × 2 × 0.75 mm^3. This package was chosen for two reasons: It is 25% lower in height than the legacy device, and the absence of leads eliminates the lead-forming process.

Due to the MMIC's high level of integration, only eight external components are needed. (*Fig. 3*). It is impractical to integrate these components, which perform choking and DC

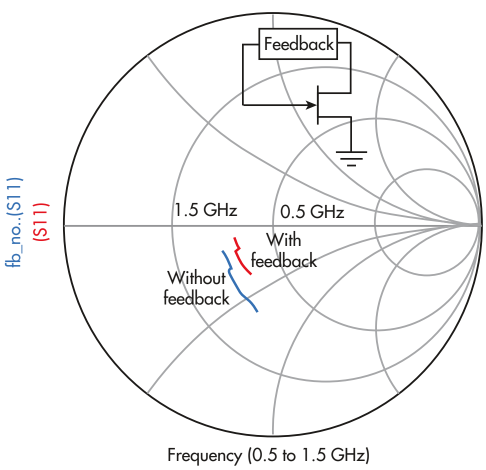

2. Feedback can beneficially reduce the frequency dispersion of S11, and thereby increase the impedance matched bandwidth (red trace). A 1600-µm E-pHEMT model was chosen for this simulation because it already has relatively low S11 over the 0.5-to-1.5-GHz frequency range (blue trace).

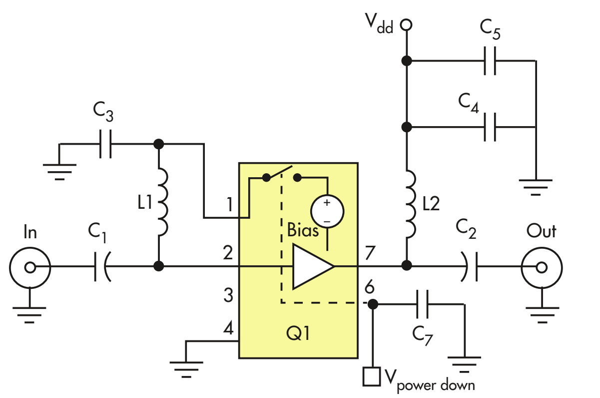

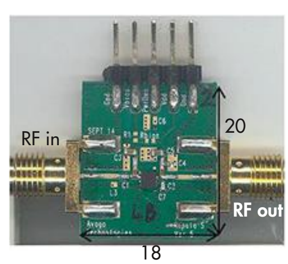

3. This circuit diagram and photograph show the prototype LNA design for 0.3 to 1.6 GHz.

blocking roles, because of their large values. To create an LNA module, all of the components and connectors were assembled on a 10-mil-thick RO4350 printed-circuit board (PCB) from Rogers Corp. (*www.rogerscorp.com*).[16] All signal and power traces are on one side of the PCB, with the ground plane on the other side. An FR-4 circuit-board backing layer was attached to the ground plane for strength and to increase the stack height of the circuit module to the standard 1.6 mm.

Advanced Design System 2009 (ADS 2009) simulation software from Keysight Technologies (*www.keysight.com*) was used to simulate the LNA's linear performance levels. The MMIC was modeled using manufacturer-supplied Touchstone-formatted file containing both S-parameters and noise parameters (*Fig. 4*). Inductors were modeled using manufacturer-supplied compact models.[18]

Other passive components (resistors and capacitors) were modeled using lumped equivalent circuit models, which only account for first-order parasitic effects. The values of the parasitic elements were estimated. Although the models were not exact, they made it possible to perform a rapid simulation of the LNA design without the need (and required resources) for performing model extractions.

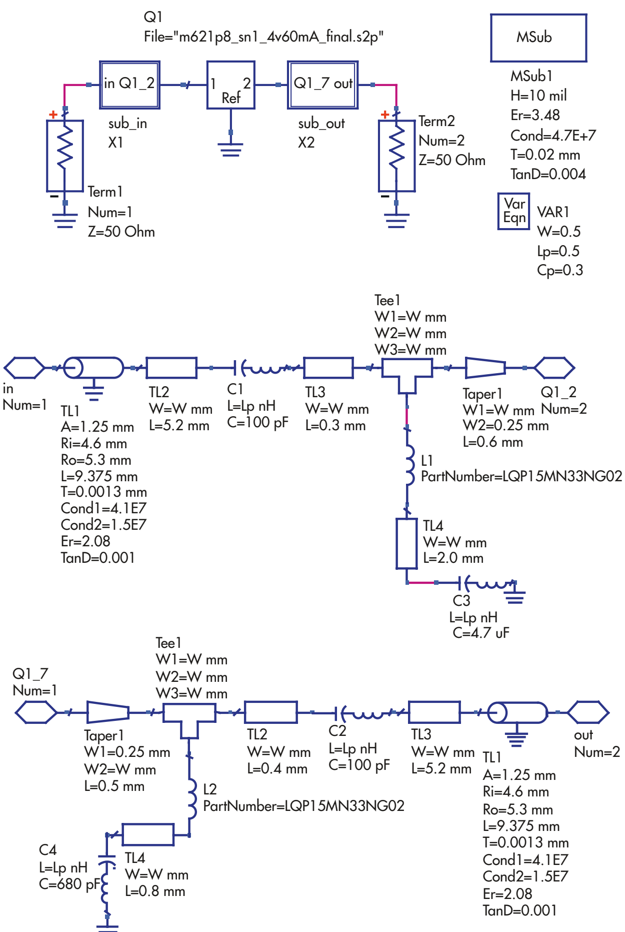

4. This is an equivalent-circuit model of the amplifier application circuit.

TABLE 2: COMPONENTS USED IN THE PROTOTYPES.			
Component	**Part number**	**Supplier**	**Value**
C1, C2, C3	GRM1555C1H101JA01D	Murata	100 pF
C5	GRM188R60J475KE19D	Murata	4.7 µF
C4	GRM155R71H681KA01D	Murata	680 pF
C7	GRM1555C1H100JA01D	Murata	10 pF
L1, L2	LQP15MN33NG02	Murata	33 nH
Q1	MGA-621P8	Avago	

To validate the design, three experimental units were built and tested; the units were based on MMICs randomly selected from the same wafer. Other components required for the experimental units are listed in *Table 2*. The experimental performance shows the LNA to cover a frequency range of 0.3 to 1.6 GHz, or better than two octaves, or about a 188% fractional bandwidth. The unit is characterized by increasing noise at the lower bandedge and decreasing gain at the upper bandedge.

The design is capable of sub-0.8-dB NF within in its target frequency range. Variations between device samples were less than 0.05 dB. The NF of these experimental units was lowest at about 1.2 GHz, rising abruptly as frequency decreases (*Fig. 5*). With an NF specification set at 0.8 dB, the lowest usable frequency for the LNA is 0.3 GHz, enabling it to support T-GSM-380 (380 MHz). The simulated NF shows the same trend as the experimental results and has a maximum error of 0.1 dB over the evaluated frequency range.

The upper end of the frequency range is 1.6 GHz due to the gain decreasing with frequency. The gain levels of the samples are highly uniform (*Fig. 6*). The experimental gain reaches a peak of 23 dB at about 0.3 GHz. Assuming a min-

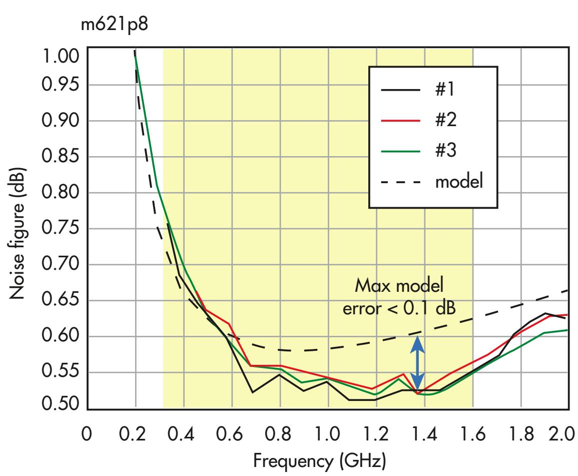

5. The experimental NF is better than 0.8 dB (n = 3) from 0.3 to 1.6 GHz.

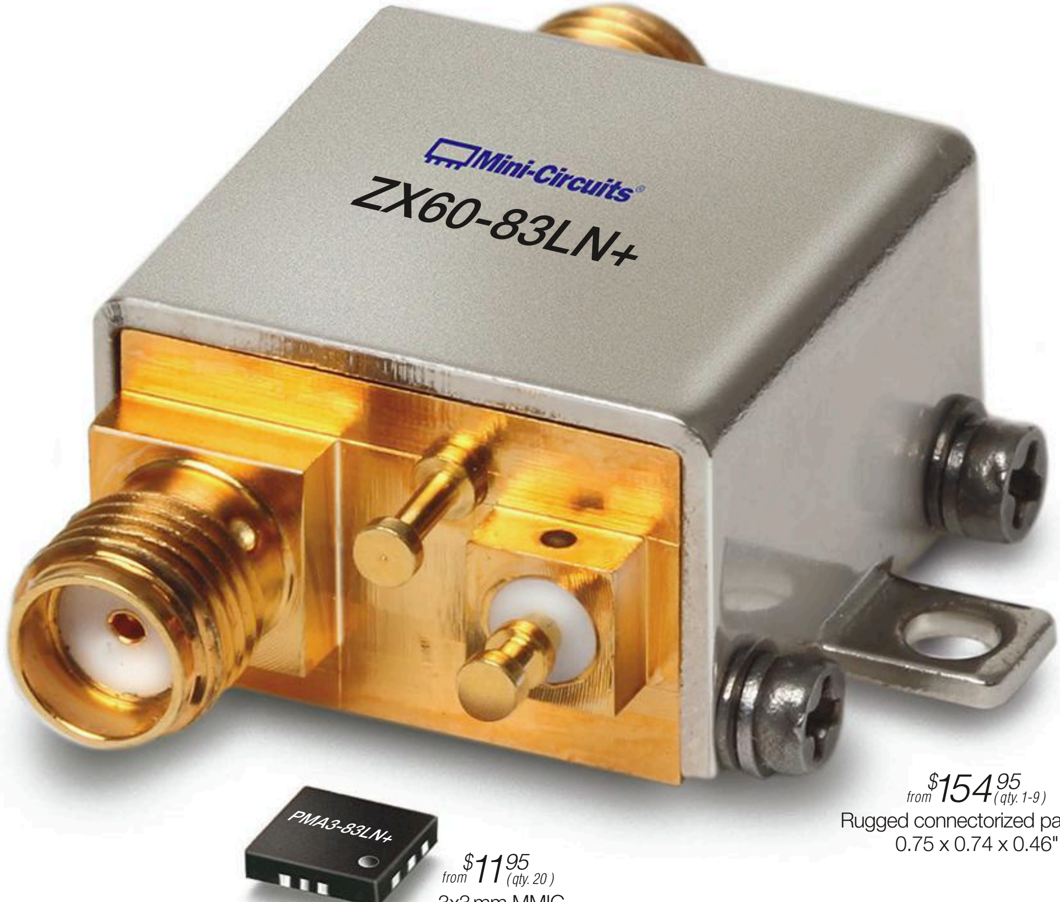

from 154^{95} (qty. 1-9)
Rugged connectorized package
0.75 x 0.74 x 0.46"

from 11^{95} (qty. 20)
3x3 mm MMIC

0.5 to 8 GHz

LOW NOISE AMPLIFIERS

IN/OUT Termination Matched!

Low noise, high dynamic range, high output power, and flat gain from 0.5 to 8 GHz, all in a single amplifier! Mini-Circuits' popular ultra-wideband LNAs are now available in both a 3x3mm QFN for your PCB and a rugged connectorized package to facilitate your cable assemblies. Both models are matched over the 0.5 to 8 GHz range*, making them a snap to use for sensitive, high-dynamic-range receivers, instrumentation, defense systems, LTE, WiFi, S-Band and C-Band radar, SatCom and more! They're available off the shelf for a great value, so visit minicircuits.com and place your order today for delivery as soon as tomorrow!

FEATURES:

- *Low Noise Figure, 1.3 dB*
- *High Gain, 21 dB*
- *Excellent Gain Flatness, ±0.7dB†*
- *High IP3, +35 dBm*
- *High POUT, +23.2 dBm*

*See datasheet for suggested application circuit for PMA3-83LN+
†Flatness specified over 0.5 to 7 GHz

Mini-Circuits®

www.minicircuits.com P.O. Box 350166, Brooklyn, NY 11235-0003 (718) 934-4500 sales@minicircuits.com

553 revA

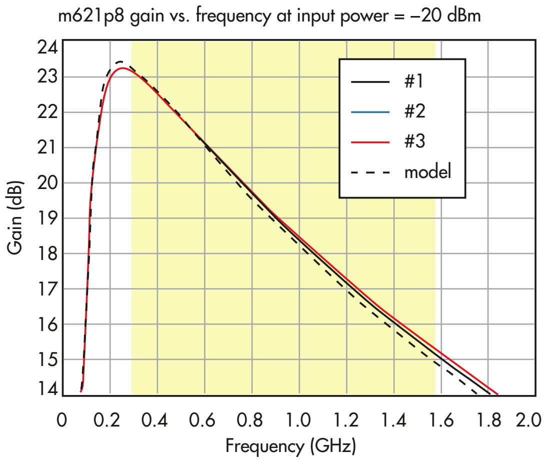

6. The modeled and experimental gain values exceed 15 dB over the 0.3-to-1.6-GHz range (n = 3).

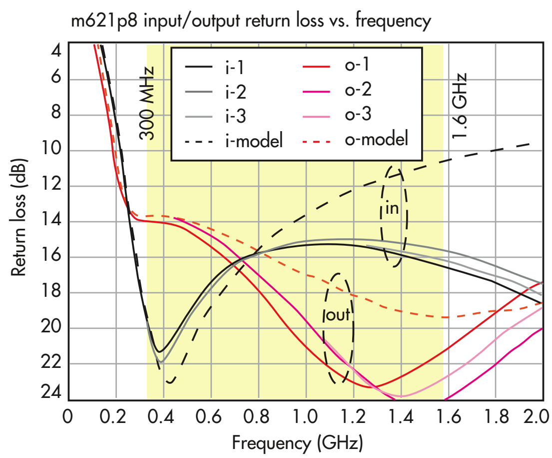

7. The experimental input and output return losses are better than −15 and −14 dB, respectively (n = 3), within the 0.3-to-1.6-GHz passband.

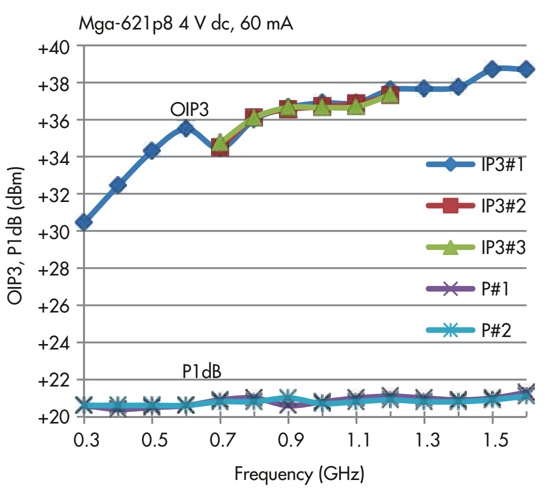

8. The experimental third-order intercept point (OIP3) and the output power at 1 dB gain compression (P1dB) exceed +30 and +20.4 dBm, respectively.

imum required gain of 15 dB, then this design has an upper frequency limit of 1.6 GHz. Therefore, the highest cellular band that can be supported is LTE/WCDMA band 21 (1448 to 1463 MHz).

This frequency range also allows concurrent reception of GPS signals for base-station timing and location (*Fig. 1*). Within the target frequency range, the gain varies 8 dB. The simulated gain agrees with the experimental gain within a fraction of a decibel.

Neither input nor output matching limits the bandwidth of this design. The experimental input return loss (IRL) is better than −15 dB in the 0.3-to-1.6-GHz range. The experimental IRL varies less than 7 dB within the target frequency range (*Fig. 7*). Both experimental and simulated IRL minima converge at about 0.4 GHz. The simulation is relatively accurate at low frequencies but the simulation error increases at higher frequencies. Within the target frequency range, the error is less than 6 dB, probably due to the lack of precision for the models.

The experimental output return loss (ORL) is better than −14 dB in the target frequency range. The best output impedance matching occurs at about 1.4 GHz (*Fig. 8*). The experimental ORL variation is less than 11 dB within the target frequency range. The simulation is accurate at low frequencies, but deviates from the experimental measured results at higher frequencies—although the simulation error is less than 5 dB.

The experimental output third order intercept point (OIP3) exceeds +30 dBm within the target frequency range of 0.3 to 1.6 GHz. The OIP3 rises rapidly at low frequencies and then plateaus at higher frequencies (*Fig. 8*). At midband (900 MHz), the OIP3 is +36.6 dBm, which corresponds to an input IP3 of +19.6 dBm. Compared to similar devices without feedback, this OIP3 is a fraction of a decibel lower. The in-band variation in OIP3 is approximately 9 dB.

The experimental power output at 1-dB gain compression (P1dB) exceeds +20.4 dBm within the target frequency range. The P1dB is relatively flat over frequency, with an inband variation of about 0.9 dB. The corresponding input P1dB at midband (900 MHz) is +1.6 dBm. The LNA showed above-average linearity behavior. Using midband OIP3 and P1dB values, the linearity figure of merit (LFOM) was determined as equal to OIP3 – P1dB[19] and equals 15.8 dB for the LNA at midband.

To minimize dead time in TDD applications, the integrated power-down function should ideally be capable of fast switching times. For measuring the switching speed of the integrated power-down function, the turn-on time (t_{ON}) and turn-off time (t_{OFF}) are defined from the time at 50% of the control signal to the time at 90% of the final RF output amplitude.[20]

(Continued on page 82)

Design Feature

BECHAREF KADA | Ph.D. Candidate
NOURI KELTOUMA | Associate Professor
BOUAZZA BOUBAKAR SEDDIK | Associate Professor
DAMOU MEHDI | Ph.D. Candidate
BOUAZZA TAYEB HABIB CHAWKI | Ph.D. Candidate
LTC Laboratory, Department of Electronics, Faculty of Technology, University Dr. Moulay Tahar of Saida, Saida, Algeria;
e-mail: BECHAREF_KADA@yahoo.fr.

Balance Microwave LPF Responses with CSRRs

Adding complementary-split-ring-resonators to the ground planes of microstrip filters can result in sharper cutoff-frequency responses with low loss and flat amplitude across the passband.

Resonant structures capable of metamaterial behavior can be quite beneficial when it comes to microwave filter designs. In particular, split-ring resonators (SRRs) and complementary SRRs (CSRRs) were found to enhance the performance of a conventional stepped-impedance microstrip lowpass filter (LPF) when etched into the filter's ground plane. The metamaterial-like properties of CSRRs include the capabilities to achieve negative relative permeability and permittivity within the rejection band of the LPF while providing low insertion loss in the filter passband.

To explore the potential of SRRs and CSRRs in filter design, a conventional microstrip-based LPF was designed and simulated with the aid of a commercial electromagnetic (EM) simulator. Then variations were made with the addition of the CSRRs to understand their effects on performance. Filters were fabricated on commercial printed-circuit-board (PCB) material to validate the results of the simulation.

For electromagnetic (EM) applications, metamaterials refer to composite materials with EM properties that are not naturally occurring. Metamaterials typically feature periodic dielectric or metallic structures that act as homogeneous materials. These types of materials were first discovered by Veselago in 1968.[1] Thirty years later, the properties were verified experimentally by Pendry.[2,3] One year later, Smith and associates demonstrated a split ring resonator (SRR) using a left-handed metamaterial obtained by combining two periodic and homogeneous materials.[4,5] It was capable of producing negative values of effective permeability and effective permittivity for metamaterials with negative refractive index.[6,7]

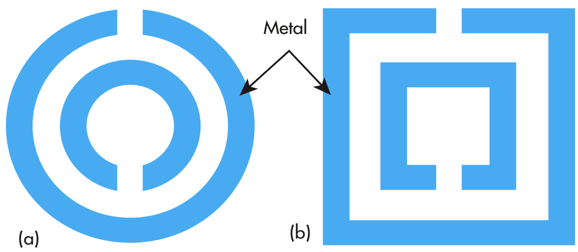

1. These sketches show (a) circular and (b) square layouts for split-ring resonators (SRRs).

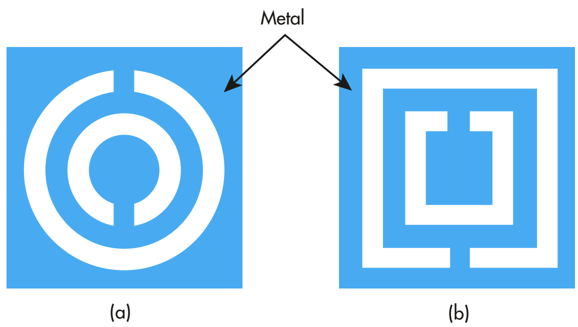

2. These layouts represent two different kinds of complementary SRRs (CSRRs): (a) circular CSRRs and (b) square CSRRs.

Some years later, Caloz and Itoh proposed another method to produce left-handed metamaterials by using a transmission-line format based on microstrip technology.[8,9] Of the many EM metamaterial-type structures currently available, most are based on the SRR concept. These are resonators with magnetic responses well suited for microwave applications, including waveguide transmission lines, filters, and antennas.[10,11]

EXPLORING THE SRR EFFECT ON HF FILTERS

To understand the impact of different types of SRRs on high-frequency filter circuits, a stepped-impedance LPF was designed in microstrip with a cutoff frequency of 5.5 GHz. CSRRs were etched into the ground planes of the LPF to explore their metamaterial properties. The CSRRs contributed to low passband insertion loss and flat passband amplitude response, with improved filter rolloff characteristics. The effects were studied by means of computer simulations, using the HFSS finite-element EM simulation software from ANSYS *(www.ansys.com)*.

SRRs were among the first resonant structures proposed for metamaterial construction purposes. Metallic metamaterials formed of double SRRs achieve magnetic responses at microwave frequencies. For example, the SRR structures shown in *Figure 1* have been used to obtain a negative value of effective permeability over a desired frequency range. Negative permeability can prevent wave propagation at a resonant frequency.[12]

A CSRR structure is achieved by doubling the number of SRRs in the ground plane in different shapes, to create double split rings and structures having apertures in metal surfaces (such as a microstrip ground plane).[13] Some examples of CSRRs with different shapes are shown in *Figure 2*.

Extracting the effective parameters of the SRRs and CSRRs needed to achieve a particular filter response known as the Nicolson-Ross-Weir (NRW) method.[14] The values of the required EM parameters are determined according to a homogenization theory and extracted from reflection and transmission coefficients, such as scattering (S) parameters.

The purpose of the homogenization theory is to describe in a simple way, but with microscopic detail, the response of a structure such as a CSRR to incident EM radiation. The basic idea involved modeling a metamaterial structure as a homogeneous, isotropic slab, calculating the effective parameters ε and μ of the homogeneous slab from the transmission and reflection coefficients obtained by simulations using MATLAB mathematics-based software from MathWorks *(www.mathworks.com)*.

For an isotropic homogeneous slab in a vacuum, transmission (t) and reflection (r) have the following relationships with the refractive index (n) and the impedance (z) of the slab[15]:

$$t^{-1} = \{\cos(nkd) - (i/2)[z + (1/z)] \sin(nkd)\} \qquad (1)$$

$$r/t = \{-(i/2)[z - (1/z)]\sin(nkd)\} \qquad (2)$$

where k and d are the wave vector and thickness of the slab, respectively. By inverting Eqs. 1 and 2, n and z can be calculated from t and r. Performing the inversions results in (Eqs. 3 and 4):

$$z = \pm\{ [(1 + r)^2 - t^2]/[(1 - r)^2 - t^2]\}^{0.5} \qquad (3)$$

$$\cos(nkd) = (1/2t)(1 + t^2 - r^2) \qquad (4)$$

By using the S_{ij} scattering parameters, the effective material parameters can be extracted[16]:

$$z = \pm\{[(1 + S11)^2 - S_{21}{}^2]/[(1 - S_{11})^2 - S_{21}{}^2]\}^{0.5} \qquad (5)$$

$$Re(n) = \pm Re(\{\cos^{-1}[1/2S_{21}(1 - S_{11}{}^2 + S_{21}{}^2)]\}/kd) \qquad (6)$$

$$Im(n) = \pm Im(\{\cos^{-1}[1/2S_{21}(1 - S_{11}{}^2 + S_{21}{}^2)]\}/kd) \qquad (7)$$

The ambiguity of the signs (±) for Eqs. 5, 6, and 7 can be avoided by noting that the real part of the impedance is positive if it is for a passive medium, while the imaginary part of the refractive index is positive to ensure that the amplitude of the incident wave decreases inside the structure. The effective permittivity and permeability can be computed by using Eqs. 8 and 9:

$$\varepsilon = n/z \qquad (8)$$

$$\mu = nz \qquad (9)$$

MICROSTRIP LPF DESIGN

Figure 3a shows the general structure of a conventional stepped-impedance microstrip LPF. It employs a cascaded structure of alternating high- and low-impedance transmission lines. The high-impedance lines act as series inductors and the low-impedance lines behave as shunt capacitors in the filter circuit. *Figure 3b* shows the equivalent-circuit representation of the LPF structure.[17]

For the stepped-impedance design prototype, a third-order (n = 3) Chebyshev response was chosen, with prototype circuit-element values given by:

$g_0 = 1$
$g_1 = 1.0316$
$g_2 = 1.1474$
$g_3 = 1.0316$
$g_4 = 1$

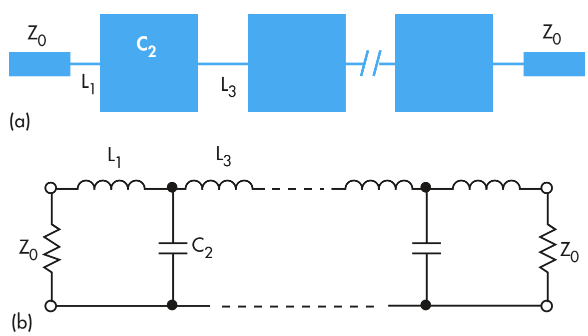

3. The (a) basic structure and (b) equivalent-circuit representation of a stepped-impedance microstrip LPF are shown here.

KEY PARAMETERS FOR THE STEPPED-IMPEDANCE LPF			
Model	**Frequency range (MHz)**	**Peak RF output power (dBm)**	**Efficiency (%)**
Characteristic impedance (Ω)	$Z_{0C} = 26$	$Z_0 = 50$	$Z_{0L} = 95$
Guided wavelengths (mm)	$\lambda_{gC} = 18.52$	$\lambda_{g0} = 19.96$	$\lambda_{gL} = 21.41$
Microstrip line widths (mm)	$W_C = 3.57$	$W_0 = 1.12$	$W_L = 0.15$

For the normalized cutoff impedance, $\Omega_c = 1$, the element transformations in ref. 17 were used to find the values of inductors and capacitors for the filter by applying Eqs. 10 and 11:

$$L_1 = L_3 = (Z_0/g_0)(\Omega_c/2\pi f_c)g_1 = 1.492 \times 10^{-9}\ \text{H} \qquad (10)$$

$$C_2 = (g_0/Z_0)(\Omega_c/2\pi f_c)g_2 = 0.664 \times 10^{-12}\ \text{F} \qquad (11)$$

The filters were implemented on circuit-board material with relative dielectric constant (ε_r) of 10.2 and a substrate height (h) of 1.27 mm. The characteristic impedances (Z_0) of the high- and low-impedance lines, L and C, respectively, were chosen as 95 and 26 Ω, respectively, by controlling the widths (W) of the microstrip transmission lines for the target frequency range. The relevant design parameters of microstrip lines, which were determined using the formulas in ref. 17, are listed in the *table*.

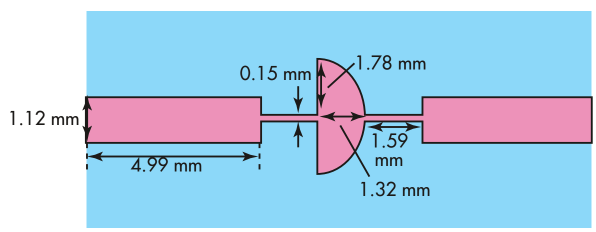

4. This is the layout of the microstrip LPF configured according to the design equations for a high-dielectric-constant (10.2) circuit substrate.

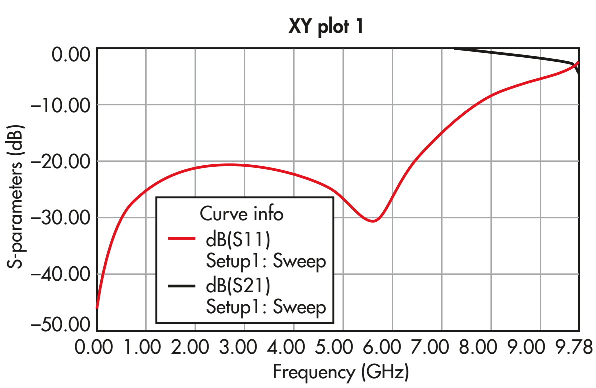

5. The simulated S_{21} and S_{11} responses for the microstrip LPF are plotted in this illustration.

The physical lengths of the high- and low-impedance lines may be found by using Eqs. 12 and 13:

$$l_L = (\lambda_{gL}/2\pi)\sin^{-1}(\omega_C L/Z_{0L}) \qquad (12)$$

$$l_C = (\lambda_{gC}/2\pi)\sin^{-1}(\omega_C C Z_{0C}) \qquad (13)$$

where L and C represent the circuit-element values for the lumped inductors and capacitors, respectively. The equations result in l_L of 1.95 mm and l_C of 1.88 mm. The results do not take into account the series reactance of the low-impedance line and shunt susceptance of the high-impedance lines. To include these effects, the lengths of the high- and low-impedance lines should be adjusted to satisfy the following relationships:

$$\omega_C L = Z_{0L}\sin(2\pi l_L/\lambda_{gL}) + Z_{0C}\tan(\pi l_C/\lambda_{gC})$$

$$\omega_C C = (1/Z_{0L})\sin(2\pi l_C/\lambda_{gC}) + 2(1/Z_{0L})\tan(\pi l_L/\lambda_{gL})$$

By solving this set of equations for l_L and l_C, the results are 1.59 mm and 1.32 mm, respectively. *Figure 4* shows a layout of the microstrip filter designed with these circuit-element values. *Figure 5* shows the simulated transmission (S_{21}) and reflection (S_{11}) coefficients as determined by HFSS.

A CSRR is a dual counterpart of an SRR, with dual EM behavior expected according to the duality theorem. The incident electric field must be polarized in the axial direction of the resonator. In this way, CSRRs are etched on center line of a microstrip transmission line layout.[18] This ensures that the CSRRs are properly excited by the electric field applied parallel to the ring axis. Since CSRRs are excited by the electric field, they produce negative effective permittivity, or $\text{Re}(\varepsilon_{eff}) < 0$. *Figure 6* shows the CSRR topology and equivalent-circuit model.

The CSRR unit cell was designed to operate around 7 GHz. The geometry of the cell is as follows: c = d = 0.3 mm; g = 0.3 mm; and m = 3 mm. It was fabricated on RO3210C circuit material from Rogers Corp. *(www.rogerscorp.com)* with relative permittivity (ε_r) of 10.8, loss tangent (tan δ) of 0.0019,

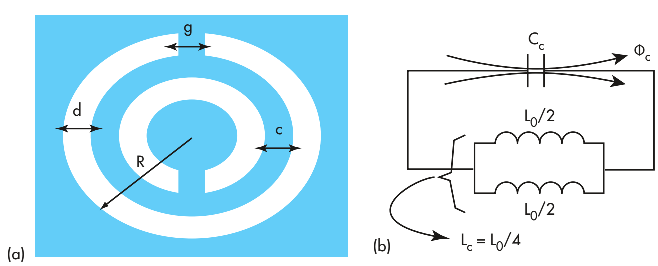

6. The layout (a) depicts a CSRR with its relevant dimensions, with (b) an equivalent circuit for a CSRR-loaded microstrip line.

and thickness (h) of 1.27 mm. The CSRR was simulated by HFSS.

The CSRR can be described as an LC resonant circuit. The resonant frequency, f, is described by the following expression[18]:

$$f = 1/[2\pi(L_C C_C)^{0.5}] \qquad (14)$$

Figure 7 shows the S_{ij} parameters for the simulated results. The frequency-rejection band occurs around the design frequency, at 7.1 GHz, with transmission loss of about 26 dB. *Figure 8* shows that the real part of the permittivity exhibits Lorenzian response behavior, with negative value in the frequency range between 5.5 and 6.13 GHz.

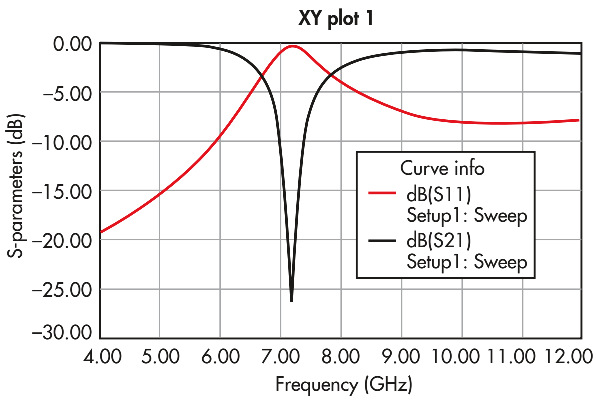

7. The S_{ij} parameters for the CSRR were simulated with HFSS finite-element EM simulation software.

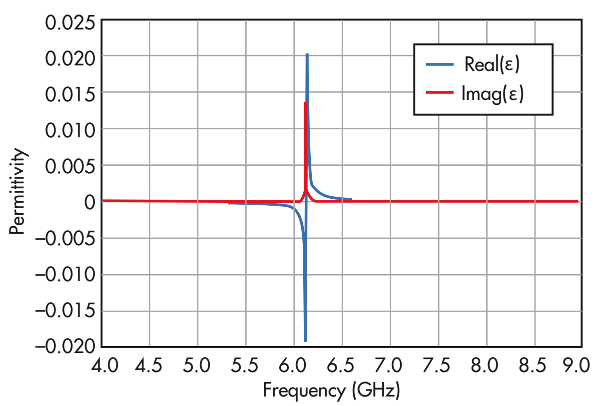

8. These plots show the real and imaginary parts of the permittivity.

To achieve good electrical performance for the filters, the design parameters were tuned and optimized using HFSS. *Figure 9* shows the two cells of circular CSRRs etched into the microstrip ground plane. The geometric parameters a = b as well as c are 3 mm and 0.3 mm, respectively. The gap between the inner and outer etched forms is 0.3 mm, and each of the splits in the inner and outer rings has the same width of 0.3 mm. *Figure 10* shows simulation results for the microstrip LPF using Ansoft Design from ANSYS. As can be seen, the response is on the order of -20 dB for the frequency range below 6.25 GHz.

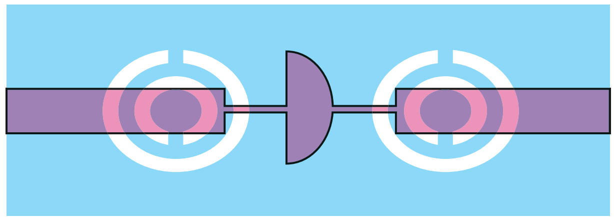

9. This layout depicts a microstrip LPF loaded with two CSRRs.

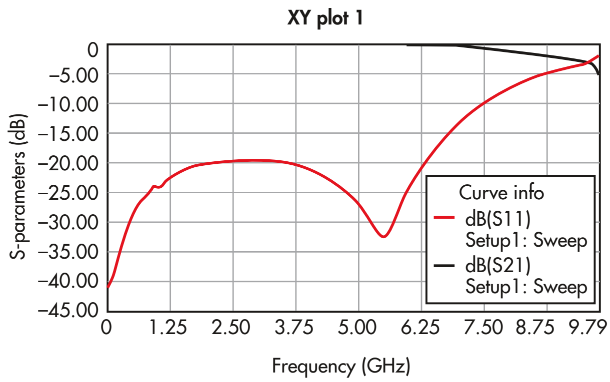

10. The S_{21} and S_{11} responses for the two-CSRR-loaded filter were simulated with HFSS.

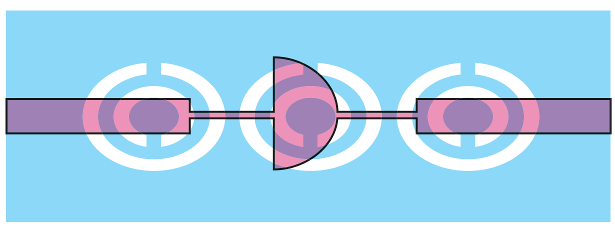

11. This layout represents a microstrip LPF loaded with three CSRRs.

Figure 11 depicts the microstrip filter with three circular CSRRs etched into the ground plane. The resonators, which are etched into the high-impedance transmission lines, have 0.2-mm spacing between them. *Figure 12* shows the effects of the CSRRs on the filter's performance, with a frequency response of about −15 dB below 6.25 GHz. The frequency band for the negative refractive index lies approximately between 2.4 and 5.31 GHz. This is the frequency range in which the permittivity and the permeability are simultaneously negative *(Fig. 13)*.

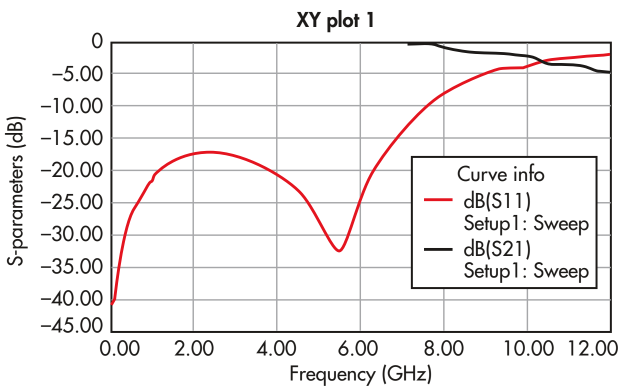

12. These are the simulated S_{21} and S_{11} responses for the three-CSRR-loaded filter.

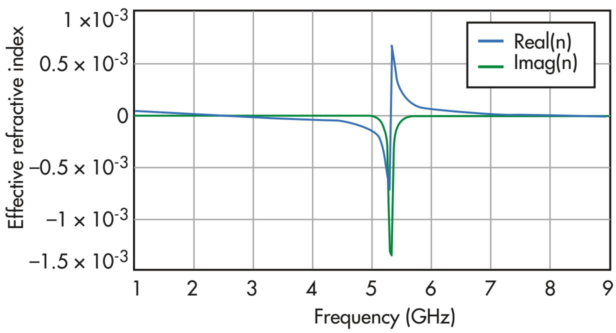

13. The plots show the real and imaginary values for the effective refractive index as impacted by the CSRRs.

In summary, the design efforts started with a conventional stepped-impedance LPF with cutoff frequency of 5.5 GHz. By loading it with CSRRs, a negative refractive index was achieved. Loading can be accomplished by etching circular CSRRs in the ground plane of microstrip LPF circuits. The result is a CSRR-loaded LPF with low passband insertion loss and good cutoff response. Adding resonators can increase the frequency band, with some degradation in passband response. mw

REFERENCES

1. V. G. Veselago, "Electrodynamics of substances with simultaneously negative electrical and magnetic properties," *Soviet Physics*, Vol. 10, 1968, pp 509-517.
2. J. B. Pendry, A. J. Holden, W. J. Stewart, and I. Youngs, "Extremely low frequency plasmons in metallic mesostructures," *Physical Review Letters*, Vol. 76, 1996, pp. 4773-4776.
3. J. B. Pendry, A. J. Holden, D. J. Ribbins, and W.J. Stewart, "Magnetism from conductors and enhanced nonlinear phenomena," *IEEE Transactions on Microwave Theory & Techniques*, Vol. 47, November 1999, pp. 2075-2084.
4. D. R. Smith et al., "Composite Medium with Simultaneously Negative Permeability and Permittivity," *Physical Review Letters*, Vol, 84, May 2000, p. 4184.
5. R. A. Shelby, D. R. Smith, and S. Shultz, "Experimental verification of a negative index of refraction," *Science*, Vol. 292, April 2001, pp. 77-79.
6. D. R. Smith, "The reality of negative refraction," *Physics World*, Vol. 16, 2003, pp. 23–24.
7. D. R. Smith, J. B. Pendry, and M. C. K. Wiltshire, "Metamaterials and negative refractive index," *Science*, Vol. 305, 2004, pp. 788–792.
8. S. Atsushi; C. Caloz, and T. Itoh, "Characteristics of the Composite Right/Left-Handed Transmission lines," *IEEE Microwave and Wireless Components Letters*, Vol. 14, No. 2, February 2004, pp. 68-70.
9. C. Caloz and T. Itoh, *Electromagnetic Metamaterials: Transmission Line Theory and Microwave Applications*, Wiley, New York, 2006.
10. M. Gupta, J. Saxena, "Microstrip Filter Design by SRR Metamaterial," *Wireless Personal Communications,* Vol. 71, No. 4, August 2013, pp 3011-3022.
11. S. Naoui, L. Latrach, and A. Gharsallah, "Metamaterials dipole antenna by using split ring resonators for RFID technology," *Microwave & Optical Technology Letters*, Vol. 56, 2014, pp. 2899-2903.
12. Ho Lim, Jong-Hyuk Lee, Sang-Ho Lim, Dong-Wook Seo, Dong-Hoon Shin, and Noh-Hoon Myung, "A Novel Compact Coplanar Waveguide Bandstop Filter Based on Split ring Resonators," Proceedings of ISAP2007, Niigata, Japan, 2007.
13. W. H. Hayt and J. A. Buck, *Engineering Electromagnetics*, 6th ed., McGraw-Hill, New York, 2001.
14. A. M. Nicolson and G. F. Ross, "Measurement of the intrinsic properties of materials by Time-Domain techniques," *IEEE Transactions on Instrumentation and Measurement,* Vol. 19,
No. 4, 1970, pp. 377–382.
15. D. R. Smith, S. Schultz , P.Markos, and C.M.Soukoulis, "Determination of effective permittivity and permeability of metamaterials from reflection and transmission coefficients," *Physical Review*, Vol. 65, 2002, p. 195.
16. C. Sabah, "Tunable metamaterial design composed of triangular split ring resonator and wire strip for S and C microwave bands," *Progress in Electromagnetics Research B*, Vol. 22, 2010.
17. Jia-Sheng and M. J. Lancaster, *Microstrip Filters for RF/Microwave Applications*, Wiley, New York, 2001.
18. F. Falcone, T. Lopetegi, J. D. Baena, R. Marqués, F. Martín, and M. Sorolla, "Effective Negative Epsilon Stop-Band Microstrip Lines Based on Complementary Split Ring Resonators," *IEEE Microwave and Wireless Components Letters,* Vol. 14, June 2004, pp. 280-282.

IMPLEMENT THE CORRECT WIRE-BONDING PROCESS

SMALLER MESA DEVICES, as well as today's demand for faster processes, have resulted in greater challenges in terms of wire bonding. Overcoming the challenges associated with successfully applying wire bonds to small mesa chips requires the latest wire-bonding equipment, specially designed tools, and right expertise. In the tech brief, "Tips for Increasing Yields when Wire Bonding Small MESA Chips," SemiGen discusses some of the issues that concern the wire bonding of small mesa chips, as well as how to solve these problems.

The tech brief gives a basic definition of wire bonding before explaining how it is performed in more than 40 million integrated circuits (ICs) each year. Wire bonding is essentially the predominant form of electrical die-to-package bonding. Wires with diameters ranging from one to three mils have traditionally been used, but to reduce parasitics, sub-1-mil diameter wires are now being applied more frequently. Nonetheless, wire-bond failures can be attributed to a number of semiconductor device issues.

SemiGen,
920 Candia Rd.
Manchester, NH 03109
(603) 624-8311
www.semigen.net

Three types of wire bonding are mentioned in the note. High-temperature thermocompression is largely used to bond aluminum (Al) wires to Al or gold (Au) pads. Another method is ultrasonic welding at room temperature. Lastly, but certainly not least, there is thermosonic bonding, which accounts for more than 90% of wire bonding, according to the document.

To illustrate the challenges in terms of working with small mesa devices, the tech brief describes five common forms of wire-bond failures. They include cratering and peeling; over-stretching and over-twisting; untamed tails; poor adhesion; and missed targets.

An application may require specific evaluation methods and testing procedures. Various forms of testing include internal visual testing, ball-bond shear tests, constant acceleration tests, random vibration, mechanical shock tests, and stabilization bake. Moreover, the app note points out that customized wire-bond tools are often necessary to meet stringent application-specific evaluation parameters and standards. It concludes by presenting a table that contains a range of wire-bonding process variables.

SPEED UP YOUR NEXT TEST SYSTEM

A TEST SYSTEM optimized for speed is likely to result in reduced overall device production costs. Speed can be augmented by different factors in various stages of a test system. In the application note, "Accelerate Your PXI Test Development and Test System Speed," Keysight Technologies recommends how to optimize the speed of a PXI test system before presenting specific application examples.

The application note explains how PXI test system speed can be optimized in any of five different test system stages: instrument selection, measurement setup, data acquisition, data processing, and measurement return results. In terms of instrument selection, PXI system development begins with selecting a chassis, interface cards, and a CPU/controller that are capable of high-speed data transfers. The fastest speeds can be achieved with Gen 3 PXI. Moreover, the document points out that data-transfer rates are limited by the slowest component contained in a link.

Keysight Technologies
1400 Fountaingrove Pkwy.
Santa Rosa, CA, CA 95403
(800) 829-4444
www.keysight.com

Many PXI test systems include advanced features that enable their quick configuration. These features are intended to expedite measurement setup and more quickly acquire data. One such feature is list mode, which allows signal analyzers and signal generators to execute a list of specific commands in a predetermined order. The other features mentioned are digital downconversion and fast Fourier transform (FFT) mode. Digital downconversion involves converting an RF signal to a lower-frequency signal to remove unwanted signal components. The FFT mode of a digital oscilloscope saves time by acquiring wide bands of data with fewer measurements.

The application note then describes peer-to-peer data transfers and on-board processing. These features make it possible for modules to communicate with one another and perform other functions without using the system controller.

Peer-to-peer communications enables direct point-to-point transfers between multiple modules within an instrument, avoiding sending data through the PC or system controller. On-board signal processing allows a module to manage specific data processing itself without having to transfer data to the controller. The application note concludes by presenting application examples for power-amplifier (PA) and wireless component testing.

JACK BROWNE | Technical Contributor

Oscilloscopes Bring More Signals than Ever into View

When four channels aren't enough, these real-time oscilloscopes capture as many as eight analog and 64 digital signals with up to 2-GHz bandwidth and sampling rates to 6.25 Gsamples/s.

AN OSCILLOSCOPE MAY be the closest thing to a "universal" test instrument for most engineers. One is usually found on every testbench and design station, for checking both high-frequency analog and high-speed digital designs. But with electronic designs growing denser and more complex, traditional two- or four-channel oscilloscopes lack the firepower needed to test multiple-channel circuits and systems.

Fortunately, the designers at Tektronix *(www.tek.com)* have spent time looking and listening to what modern mixed-signal engineers need in terms of oscilloscope capability. The end result is an instrument family for today and tomorrow: the 5 Series mixed-signal oscilloscope (MSO) family, with as many as eight simultaneous measurement channels. Of course, having all of hose channels without top-level performance would be meaningless, and the 5 Series MSO instruments deliver with bandwidths as wide as 2 GHz, 12-b vertical resolution, and real-time sampling rates to 6.25 Gsamples/s.

The 5 Series MSO oscilloscopes are the culmination of some serious industrial as well as electronic design efforts. They are attention-grabbing and game-changing in both appearance and performance. In terms of appearance, perhaps the most noticeable features are the eight input ports and the large display screen. The eight input ports provide plenty of measurement flexibility—they can each be used for any variety of signals, including analog, digital, and power signals. The large screen is in strong contrast to a typical oscilloscope, where a screen might be about one-half of the front face, while all of the controls fill the rest of the instrument's front face.

1. The 5 Series MSO oscilloscopes offer sampling rates to 6.25 Gsamples/s and bandwidths to 2 GHz with as much as 12-b vertical resolution (and 16-b vertical resolution with a high-definition function).

LOOK AND FEEL

The 5 Series MSO oscilloscopes show results on a large, 15.6-in. capacitive touchscreen with 1920- × 1080-pixel resolution *(Fig. 1)*. It dominates the front face area of the instrument (about 85% of the total area), part of the clever industrial design of the oscilloscopes in which the majority of the control surface is on the touchscreen. The scopes incorporate an advanced graphical user interface (GUI); operators access controls by touching objects on the display screen rather than navigating through multiple layers of menus to try to find a desired control function. A user can reach control functions by touching icons on the screen or by connecting a computer mouse to click on the same icons.

For simplicity, a streamlined control panel, found to the right of the screen, contains the most essential controls, including trigger, vertical and horizontal scale and position, run/stop, and cursor functions. Also, the front panel includes LED rings that highlight selected waveforms and trigger sources for easy identification.

While the 5 Series MSO oscilloscopes are not meant to be portable, they are transportable *(Fig. 2)*, designed with a slim (less than 8 in. deep) profile and constructed with a solid housing and strong metal carrying handle. In addition, they have fixed front feet and adjustable rear feet to set viewing angles to a personal preference. With the growing trend of working at home, these scopes can readily become part of that equation.

2. The intelligent industrial design of the 5 Series MSO oscilloscopes makes for easy transportability.

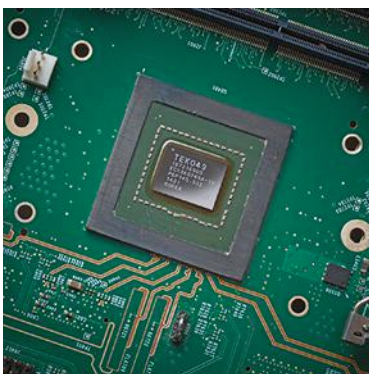

3. A custom ASIC was developed with many of the front-end mixed-signal circuit functions, including a 12-b ADC.

To achieve the compact design while, at the same time, achieving the equivalent of about a half-dozen different test functions, a new application-specific integrated circuit (ASIC) was developed as part of the multiple-year program to design and develop the oscilloscopes *(Fig. 3)*. The ASIC combines an analog-to-digital converter (ADC), demultiplexer, trigger, and digital-acquisition components within a single IC. In addition, a new low-noise amplifier (LNA) helps improve the capture of extremely low-level signals.

The ADC provides as much as 12-b resolution for detailed waveform information. The vertical resolution is actually 8 b at 6.25 Gsamples/s and 12 b at 3.125 Gsamples/s. In addition, the 5 Series MSOs offer a high-resolution mode, in which 16-b vertical resolution is possible. This is achieved by using a digital-signal-processing (DSP) filter with finite-impulse-response (FIR) function at each sampling rate to limit bandwidth and noise and improve resolution.

4. The 5 Series MSO oscilloscopes are available as three models with four, six, or eight channels, and with different bandwidths.

Appearance is just part of the appeal of these oscilloscopes, which provide enough performance for most applications: their real-time sampling rate of 6.25 Gsamples/s can reach as high as 500 Gsamples/s through interpolation. They can capture more than 500,000 waveforms/s, and store data by means of standard record length of 62.5 Mpoints, and 125-Mpoints record length as an option. For truly critical timing measurements, the time base system can lock to a high-stability, external 10-MHz reference clock oscillator.

The 5 Series scopes come in three basic models—the MSO54, MSO56, and MSO58—with four, six, and eight channels, respectively *(Fig. 4)*. Once the number of channels is selected, the choice of bandwidth is among 350 MHz, 500 MHz, 1 GHz, and 2 GHz. A choice of bandwidth need not be permanent, since the bandwidth can be upgraded to as much as 1 GHz in the field; upgrades to 2 GHz must be performed at a Tektronix service center.

PROBING THE DIFFERENCE

Unlike conventional oscilloscopes with fixed input connectors that essentially determine the functionality for each input port, the 5 Series MSOs employ innovative FlexChannel technology on their input ports. These are basically flexible interfaces that allow an operator to choose a desired input channel configuration, using each input port as one analog channel or eight digital channels. Therefore, an eight-channel oscilloscope can handle as many as eight analog channels and as many as 64 digital channels. The channels can be configured for any mixture of analog and digital signals to support probing of the most complex mixed-signal circuit architectures.

The FlexChannel inputs on the oscilloscopes work with the firm's TekVPI probe interface to enable connections to both analog and digital probes. All FlexChannel ports accept all TekVPI analog probes. When a TLP058 logic probe is connected, however, its single TekVPI connector is terminated in eight digital logic probe points. These eight logic channels run at the same maximum sampling rate (6.25 Gsamples/s) and bandwidth as the single analog channels. And there are no performance compromises for the additional signal channels, simplifying comparisons between different types of signals.

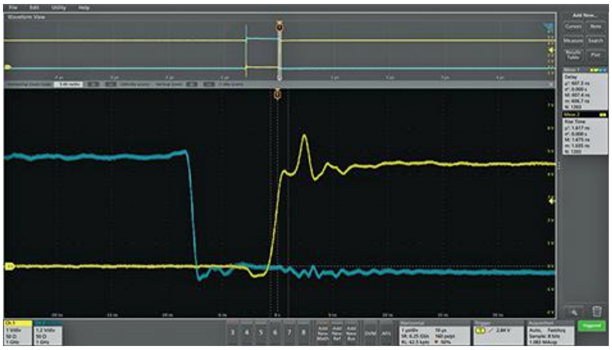

5. The IsoVu technology uses optical communications and power-over-fiber to provide high-voltage isolation for the test probes.

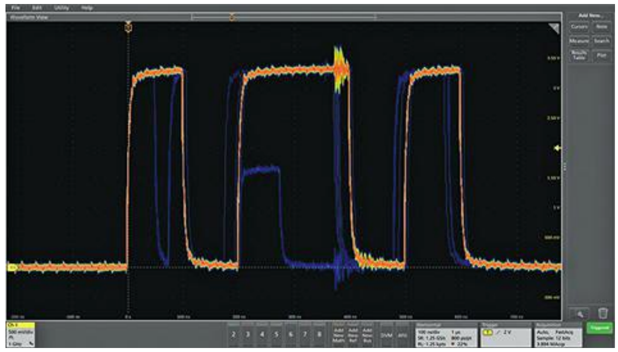

6. The low-noise front end, digital phosphor technology, and large touchscreen display speed the search for transient events and performing common measurement functions such as jitter testing.

The TekVPI probes have status indicators and controls as well as a probe menu button on the comp box. Pushing the button activates a probe menu on the oscilloscope screen, with all relevant settings and controls for the probe. The TekVPI interface enables direct attachment of current probes without requiring a separate power supply.

TekVPI probes can be controlled remotely through a USB or LAN connection to a PC for ATE applications. The 5 Series MSOs provide as much as 80 W power to the front-panel connectors, enough to power all connected probes without need for an additional probe power supply.

The TekVPI interfaces on these oscilloscopes are fortified by the company's IsoVu technology, which uses optical communications and power-over-fiber to achieve complete galvanic isolation for the test probes. This high-isolation technology *(Fig. 5)* helps resolve high-bandwidth differential signals in the presence of large common-mode voltages. For example, for bandwidths to 1 GHz, the probe and oscilloscope combination delivers 120-dB common-mode rejection at 100 MHz and 80-dB common-mode rejection at full 1-GHz bandwidth. The differential dynamic range is greater than 1000 V, with a 60-kV common-mode voltage range.

The 5 Series scopes include a complete set of triggering functions, such as runt, logic, pulse width, window, timeout, rise/fall time, setup-and-hold violation, serial packet, parallel data, and sequence triggers. They feature trigger and decode functions for most common serial standards, such as I2C, USB, CAN, and Ethernet interfaces. Digital phosphor technology reveals the most minute glitches and transient events. In addition, various optional software packages are available to assist with such tasks as jitter analysis *(Fig. 6)*.

The oscilloscopes provide Wave Inspector controls to scan quickly through a record in search of user-defined events. These controls allow an operator to perform searches based on different waveform characteristics, such as edge, pulse width, timeout, runt, window, logic, setup and hold, rise/fall time, and parallel/serial bus packet content.

THE EXTRA MEASUREMENT MILE

If the oscilloscope measurement power wasn't enough, the 5 Series MSOs are either equipped with or available with optional additional measurement functions. For example, a built-in four-digit digital voltmeter (DVM) and trigger frequency counter are activated upon product registration. A 50-MHz function generator and an arbitrary function generator are available as options, providing low-frequency waveforms or noise for testing. The scopes are compatible with the company's ArbExpress PC-based software for quick creation of complex waveforms.

The MSOs also come with an optional solid-state drive (SSD) with 480-GB memory space for data storage and optional Windows 10 operating system (OS) from Microsoft Corp. *(www.microsoft.com)*. Each oscilloscope can operate as a dedicated oscilloscope or in a Windows configuration simply by adding the SSD for Windows-based use; the instrument will boot up from the SSD and run on Windows. Once the drive is removed, the instrument will use its internal configuration. The 5 Series MSO oscilloscopes run an i5 dual-core microprocessor from Intel Corp. *(www.intel.com)* running at 2.7 GHz, aided by 16 GB of DDR3 DRAM and more than 80 GB of internal storage memory.

Each 5 Series MSO with 350- or 500-MHz bandwidth is shipped with one TPP0500B probe per channel. It has a 500-MHz bandwidth and low capacitive loading of 12.7 pF. Higher-frequency oscilloscopes are shipped with one TPP1000 probe per channel, which has a 1-GHz bandwidth and capacitive loading of 3.9 pF. Also included are a 20-pin DisplayPort connector, 29-pin DVI-D connector, and a DB-15 VGA connector to show the oscilloscope display on an external monitor. They also provide two USB 2.0 ports and one USB 3.0 port for external computer, printer, and other device connections. P&A: starting at $12,600. mw

TEKTRONIX INC., P.O. Box 500, 14150 SW Karl Braun Dr., Beaverton, OR 97077; (800) 833-9200, www.tek.com

TEST CABLES *up to 40 GHz!*

Reliability You Can Trust... from $68.95 ea. (qty.1-9)

Why do 10,000 customers trust Mini-Circuits test cables? Because they simply don't fail! Our test cables have been performance qualified to 20,000 flexures* and come backed by our 6-month product guarantee**, so you can be confident you're getting rugged construction, reliability, and repeatable performance you can depend on. Whether you're performing production test, burn-in, over-temperature testing, hi-rel testing – you name it – chances are there's a Mini-Circuits test cable for your application in stock, ready for immediate shipment. Order some for your test setup at minicircuits.com today, and you'll quickly find that consistent long-term performance, less retesting and fewer false rejects really add up to bottom-line savings, test after test!

Model Family	Capabilities	Freq. (GHz)	Connectors†
KBL	Precision measurement, including phase, through 40 GHz	DC-40	2.92mm
CBL-75+	Precision 75Ω measurement for CATV and DOCSIS® 3.1	DC-18	N, F
CBL	All-purpose workhorse cables for highly-reliable, precision 50Ω measurement through 18 GHz	DC-18	SMA, N
APC	Crush resistant armored cable construction for production floors where heavy machinery is used	DC-18	N
ULC	Ultra-flexible construction, highly popular for lab and production test where tight bends are needed	DC-18	SMA
FLC	Flexible construction and wideband coverage for point to point radios, SatCom Systems through K-Band, and more!	DC-26	SMA
NEW! SLC	Super-flexible spaghetti cables with 0.047" diameter and 0.25" bend radius, ideal for enviromental test chambers.	DC-18	SMA/SMP
VNAC	Precision VNA cables for test and measurement equipment through 40 GHz	DC-40	2.92mm

* All models except VNAC-2R1-K+

** Mini-Circuits will repair or replace your test cable at its option if the connector attachment fails within six months of shipment. This guarantee excludes cable or connector interface damage from misuse or abuse.

† Various connector options available upon request.

Contact apps@minicircuits.com to discuss your special requirements.

Mini-Circuits®

www.minicircuits.com P.O. Box 350166, Brooklyn, NY 11235-0003 (718) 934-4500 sales@minicircuits.com

CHRIS BEAN | Application Engineer, AWR Group, NI
www.awrcorp.com

Accelerate PA Design with Source/Load-Pull ACPR and EVM Measurements

Power-amplifier (PA) designers can take advantage of software that allows them to utilize complex load-pull data sets, thereby streamlining the design process.

WITH A RICH set of load-pull data, power-amplifier (PA) designers can thoroughly investigate a device's optimum capability in relation to design goals and performance targets. To fully benefit from this information, designers need an intuitive method to work with complex swept load-pull data sets. These data sets can include multiple fundamental frequencies, nested harmonic load-pull, and/or nested source- and load-pull.

As a result, PA performance becomes easy to understand across multiple operating conditions. In essence, performance can be analyzed in terms of frequency, power, and load or source impedance at the fundamental frequency and/or harmonic frequencies.

Measurements include available output power, gain, efficiency, and intermodulation-distortion (IMD) levels—essentially any performance metric that is able to be measured on a modern load-pull system. The measurements can be readily de-embedded to the current generator reference plane of the device, which is a critical consideration for any designer moving beyond the traditional reduced conduction angle classes of operation.

This article describes how load-pull data files with an independent swept parameter, such as power, can be used directly in the NI AWR Design Environment, specifically Microwave Office circuit design software. It also highlights the design of a Class J PA to show how load-pull data can complement traditional theoretical Class J analysis, thereby streamlining the design flow.

BACKGROUND

Load-pull contours are acquired by sweeping the impedance presented to a device, measuring performance, and plotting the resultant performance data on a Smith chart *(Fig. 1)*. As advanced load-pull measurement systems gain in popularity, increasingly sophisticated capabilities have been added to Microwave Office to help designers deal with ever-more complex load-pull data sets.

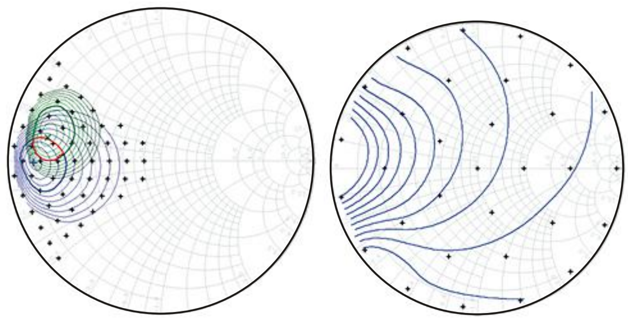

1. Load-pull sweeps the impedance of a device, measures the performance, and plots the resulting performance contours on a Smith chart.

Strategically using these tools ensures a streamlined overall PA design flow, enabling designers to eliminate guesswork and post-fabrication "tweaking" of first-cut prototypes (in the case of PCB designs). The same load-pull capabilities can be applied to simulated compact device models.

DEVICE MODEL AND DESIGN GOALS

The example used for this article is based on Qorvo's T2G6000528-Q3 gallium-nitride-on-silicon-carbide (GaN-on-SiC) high-electron-mobility transistor (HEMT). This device achieves approximately 10 W of output power at 3-dB gain compression (P3dB). It has a drain operating voltage (V_D) of 28 V. The bias point is Class B or very heavy Class AB *(Fig. 2)*.

A Modelithics *(www.modelithics.com)* device model was used, enabling intrinsic IV sensing at the current generator plane of the device. This model allows a designer to "push down" into the model and make IV waveform measure-

2. Shown is the chosen device's Class B behavior with the dynamic load line.

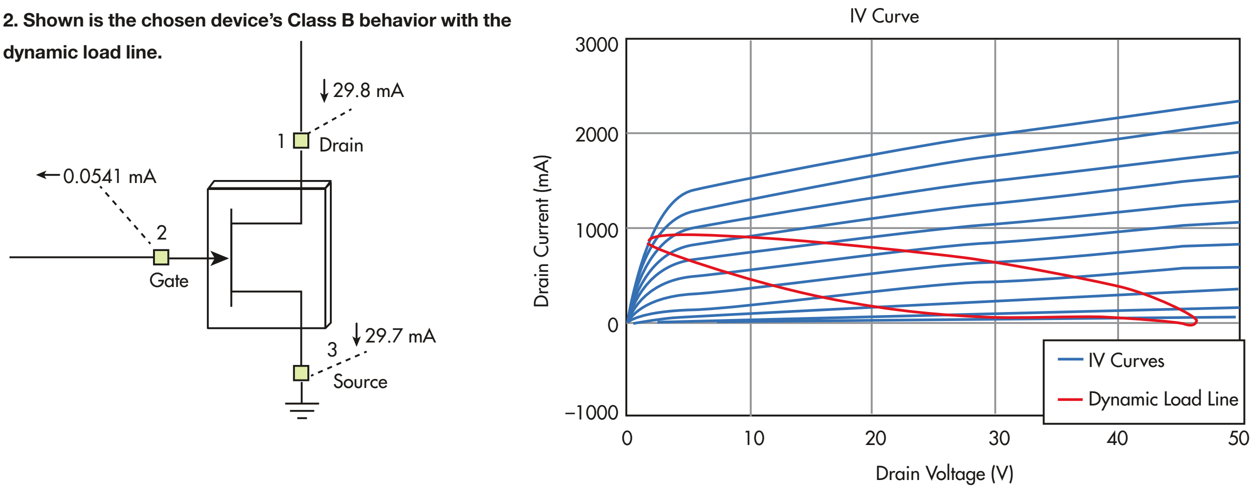

ments—not just at the package leads or transistor feed structure, where a typical, calibrated measurement system reference plane would be defined, but also at the device's actual current generator right at the drain of the transistor *(Fig. 3)*. The gamma probe element enables the user to actually plot the impedances directly at this critical reference plane.

INTRODUCING NESTED SOURCE- AND LOAD-PULL ANALYSIS

Microwave Office software simplifies designing with load-pull data by nesting together source- and load-pull results. Typically, when starting a device design, one needs to establish the appropriate source match before exploring the first-cut load-pull. Depending on the device's level of reverse isolation (S_{12}), a non-50-Ω load impedance will change the source impedance match. Therefore, designers should initially base their source match on the input impedance of the device when terminated with the preferred load impedance, which in turn is impacted by the source impedance.

Determining the optimum source and load impedances is therefore an iterative process. One way to streamline that process is to nest together source pull and load-pull, so that a load-pull data set contains both. For each source point there is a full set of load-pull data, and for each load point there is a full set of source-pull data. As shown on the left of *Figure 4*, the impedance can be selected on the source side. The right side of Figure 4 shows the resulting set of generated contours. The impedance can be changed simply by moving markers, which updates the load-pull contours.

Conversely, on the device output, the load impedance point can be selected and the resulting source-pull contours can be seen *(Fig. 5)*. Again, the source-pull contours are updated by moving the data marker amongst data points on the device's load reference plane. This feature eliminates the need to perform iterative simulations with different source/load terminations in order to define the input and output target impedances—it is all there in one data set.

LOAD-PULL MULTIPLE PERFORMANCE PARAMETERS

Once the initial source match is established, designers can focus on a more rigorous load-pull analysis. Any operating conditions, such as frequency or

3. The device model enabled the designer to make measurements not only at the package plane, but also at the current generator of the device, right on the drain pin of the die plane.

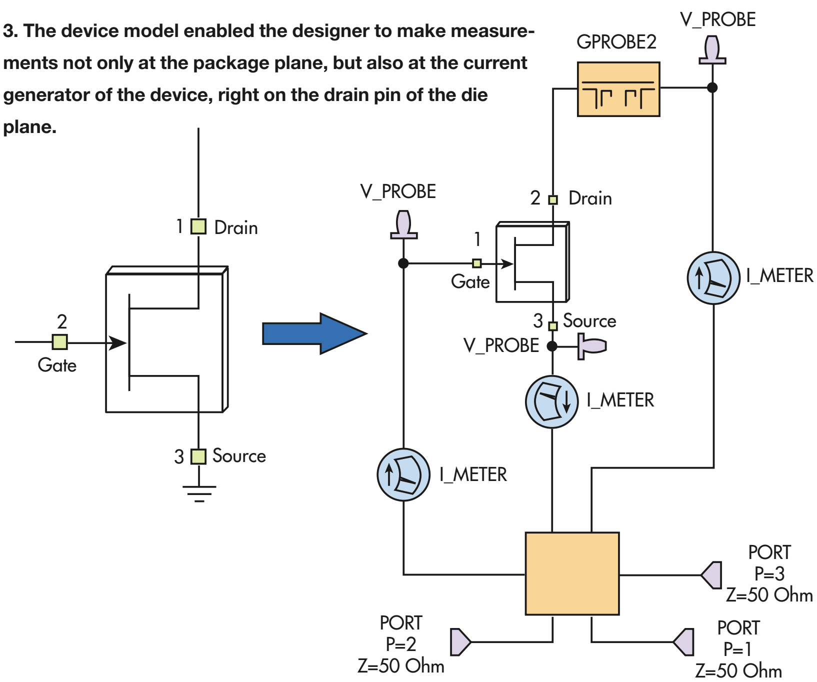

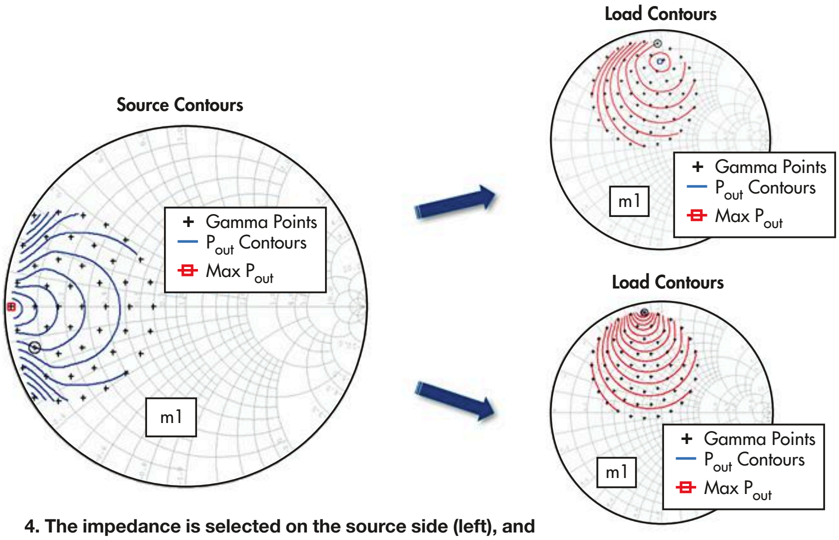

4. The impedance is selected on the source side (left), and the resulting set of contours is shown on the right side. Changing the impedance updates the load-pull contours.

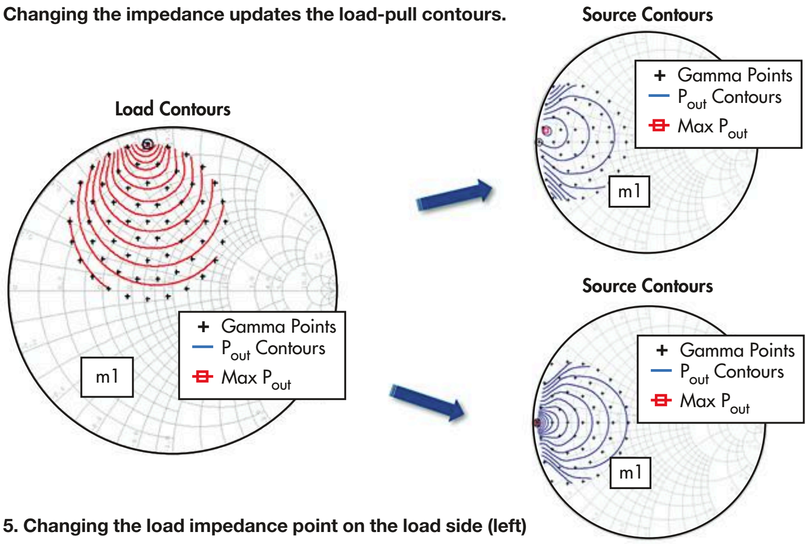

5. Changing the load impedance point on the load side (left) results in the source-pull contours shown on the right.

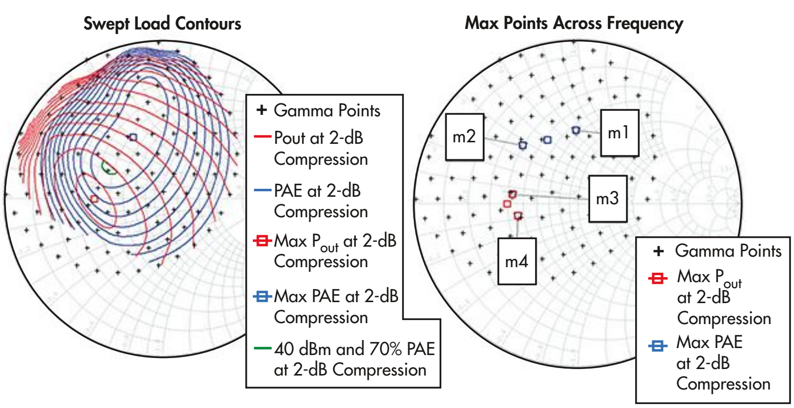

6. The oval shaped contour in the middle of the graph (left) is the overlap contour that meets two performance parameters at the same time. The maximum markers point out the maximum point for any measurement across frequencies.

input power, can be taken into consideration. Rather than plotting strictly in terms of input power, data may be plotted in terms of other performance parameters like specific output power or gain compression points. Furthermore, as many data points as needed can be utilized.

In addition, Microwave Office offers an overlap contour, shown on the left of *Figure 6*. With the overlap contour, two performance parameters are being met at the same time. The graph on the right of Fig. 6 shows the maximum markers that point out the maximum points for any measurement across frequencies.

CLASS J POWER AMPLIFIER OVERVIEW

The *table* provides an overview of amplifier efficiencies. Approaching the shown maximum theoretical efficiencies depends on achieving a perfect short condition at the device's current generator plane for harmonic frequencies. For Class F, the theoretical efficiency is actually 100%, where the voltage and current waveforms are "squared off" and 180 degrees out of phase. Theoretically, achieving this waveform shape would require shorting infinite harmonics, which is not practical. Thus, 88.4% is typically used as the maximum available efficiency achievable through the appropriate load impedances at the second and third harmonics.

Class J was introduced by Dr. Steven Cripps in 2006. It starts with a Class B bias condition and essentially adds the

AN OVERVIEW OF AMPLIFIER EFFICIENCIES

Class	Maximum Efficiency
A	50%
B	78.5%
AB	50 – 78.5%
F	88.4%

7. Class B waveforms are shown on the left, with Class J waveforms shown on the right.

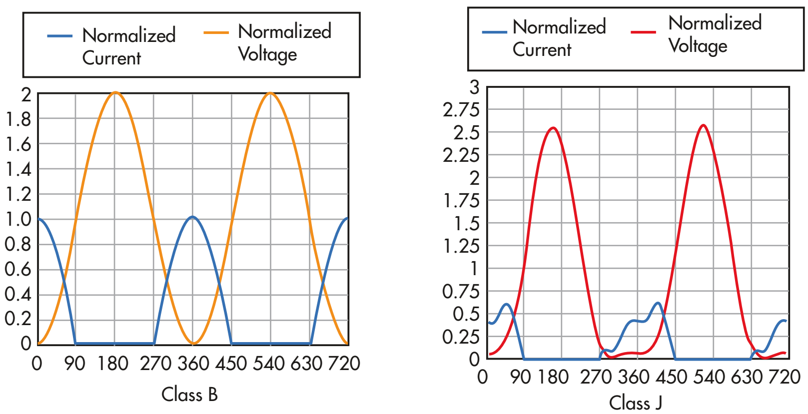

at the drain pin of the actual current generator of the device.

However, the model reference plane may not be at the current generator. If the designer knows the details of the internal matching elements, along with the package or test fixture (as represented by an S-parameter block), that knowledge can be applied in Microwave Office in the form of a de-embedding network. One can then plot the waveforms at the current generator *(Fig. 9)*. Thus, the designer is able to directly determine if it's achieving Class J conditions.

In the absence of either of these capabilities—a model or a de-embedding network—nesting can be used to sweep the fundamental, as well as second- or third-harmonic terminations, to obtain performance contours. This provides a useful design path when de-embedding isn't possible or practical.

reactive termination at both the fundamental and the second-harmonic frequencies. Therefore, the linearity impairment is less than Class E, for instance, which is essentially a switched-mode operation.

What does this mean in terms of the waveform shape? *Figure 7* shows the Class B waveforms on the left and the Class J waveforms on the right.

Class B has a 180-degree conduction cycle. For the Class J waveforms, some harmonic content was added. The current waveform is essentially squared off, minimizing the time when the device has a positive voltage and is conducting. The Class B theoretical efficiency can be reached without requiring short-circuit conditions, which allows for a much more practical approach.

HARMONIC LOAD-PULL

How does this fit in with load-pull? Apart from fundamental load-pull, Microwave Office enables designers to perform load-pull analysis that includes load-pull contours based on termination impedances at harmonic frequencies. This capability allows designers to quickly assess the impact of controlling second- and third-harmonic terminations.

Figure 8 shows a fixed fundamental termination on the load side with the second-harmonic termination essentially being pulled around the entire Smith chart. Power-added-efficiency (PAE) contours can be plotted, which reveals the device's efficiency based on its harmonic terminations and identifies an area of the Smith chart where efficiency is maximized.

DE-EMBEDDING AND WAVEFORMS

De-embedding is important for studying the current and voltage waveforms at the device's current generator plane instead of at the package leads. As noted earlier, the model used in this example enables designers to make measurements

ACPR/EVM LOAD-PULL FOR LINEARITY

In the most recent release (V13) of NI AWR software, load-pull analysis was expanded to communication-system measurements via Visual System Simulator (VSS) co-simulation with Microwave Office. The new capability generates constant performance contours for metrics such as adjacent channel power ratio (ACPR) and error vector magnitude (EVM). This offers insight into amplifier linearity as a function of varying load conditions and how the device will operate under digitally modulated RF waveforms.

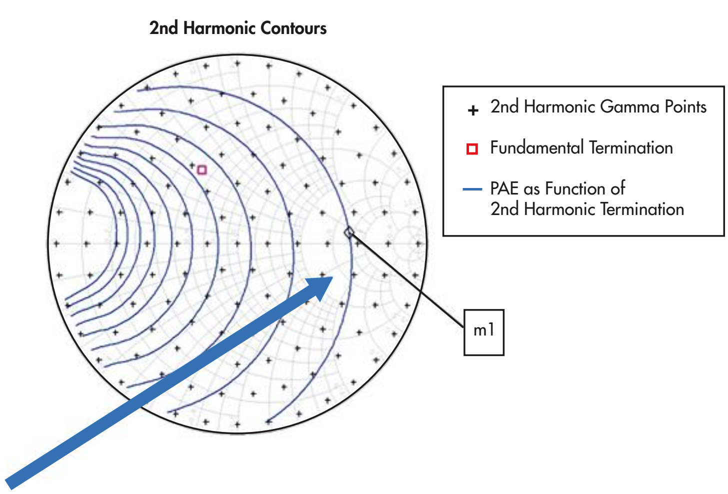

8. With harmonic load-pull, designers can evaluate the impact of controlling the second- and third-harmonic terminations. This capability makes it possible to determine where harmonic impedances can maximize device performance (blue arrow).

UP TO **100 Watt**

AMPLIFIERS

NOW! **100 kHz to 26.5 GHz**

from $995 ea. qty. (1-9)

High-powered performance across wide frequency ranges. Mini-Circuits' class A/AB linear amplifiers have set a standard for wideband high-power performance throughout the RF and microwave industry. Rugged and reliable, they feature over-voltage and over-temperature protections and can withstand opens and shorts at the output! Available with or without heat sinks, they're perfect for demanding test lab environments and for integrating directly into customer assemblies. With standard models covering frequencies from 100 kHz up to 26.5 GHz, chances are we have a solution for your needs in stock. Place your order on minicircuits.com today for delivery as soon as tomorrow! Need a custom model? Give us a call and talk to our engineers about your special requirements!

Model	Frequency (MHz)	Gain (dB)	Pout@ Comp. 1 dB (W)	Pout@ Comp. 3 dB (W)	$ Price* (Qty. 1-9)
ZVM-273HP+	13000-26500	14.5	0.5	0.5	2195
ZVE-3W-83+	2000-8000	35	2	3	1424.95
ZVE-3W-183+	5900-18000	35	2	3	1424.95
ZHL-4W-422+	500-4200	25	3	4	1160
ZHL-5W-422+	500-4200	25	3	5	1670
ZHL-5W-2G+	800-2000	45	5	5	995
ZHL-10W-2G+	800-2000	43	10	12	1395
• ZHL-16W-43+	1800-4000	45	12	16	1595
• ZHL-20W-13+	20-1000	50	13	20	1470
• ZHL-20W-13SW+	20-1000	50	13	20	1595
LZY-22+	0.1-200	43	16	30	1595
ZHL-30W-262+	2300-2550	50	20	32	1995
ZHL-30W-252+	700-2500	50	25	40	2995
LZY-2+	500-1000	47	32	38	2195
LZY-1+	20-512	42	50	50	1995
• ZHL-50W-52+	50-500	50	63	63	1395
• ZHL-100W-52+	50-500	50	63	79	1995
• ZHL-100W-GAN+	20-500	42	79	100	2845
NEW! ZHL-100W-272+	700-2700	48	79	100	7995
ZHL-100W-13+	800-1000	50	79	100	2395
ZHL-100W-352+	3000-3500	50	100	100	3595
ZHL-100W-43+	3500-4000	50	100	100	3595

Listed performance data typical, see minicircuits.com for more details.
• Protected under U.S. Patent 7,348,854
**Price Includes Heatsink*

Mini-Circuits®

www.minicircuits.com P.O. Box 350166, Brooklyn, NY 11235-0003 (718) 934-4500 sales@minicircuits.com

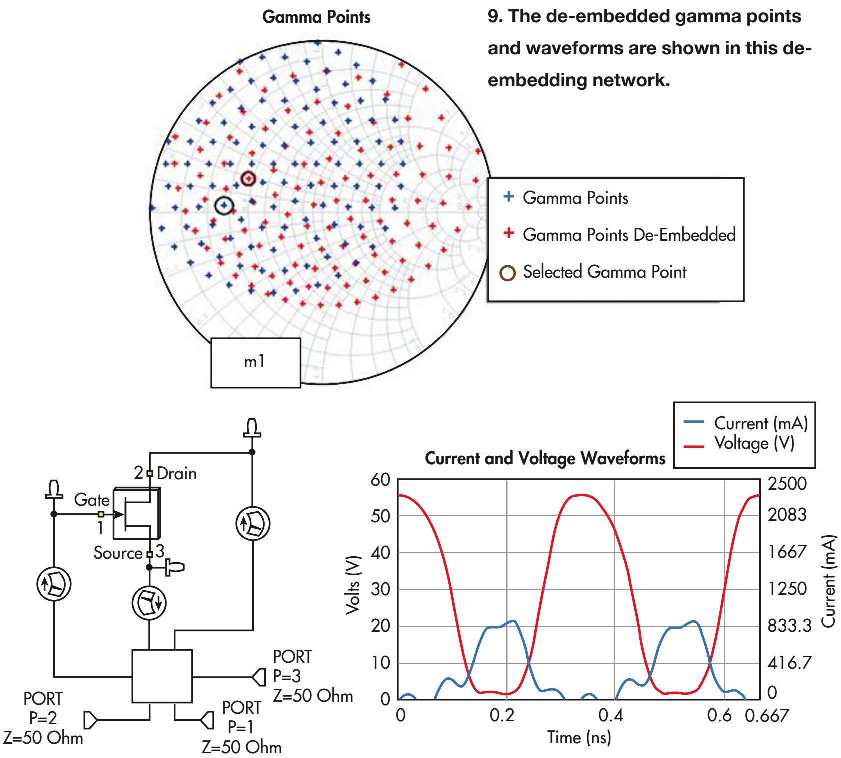

9. The de-embedded gamma points and waveforms are shown in this de-embedding network.

In *Figure 10*, a quadrature-phase-shift-keying (QPSK) signal is applied. More sophisticated signals, such as LTE or 5G (also available in V13) modulated signals, can also be applied to plot communication-standard-specific contours. *Fig. 10* shows plots of ACPR contours for the device.

The new “system-based” load-pull offers the same functionality as using circuit-level load-pull with an expansion of measurements commonly employed in communication systems. As with circuit measurements, these system measurements can be referenced to a specific output power level or any other measurement—it doesn’t have to be just a function of the input power *(Fig. 11)*.

CONCLUSION

Load-pull is an integral part of high-power amplifier design, whether the source data is based on simulated load-pull device models or measured device-under-test (DUT) load-pull files. The unique functionality of nesting source- and load-pull contours in NI AWR Design Environment can significantly shorten the time required to design an amplifier—it streamlines the iterative process of optimizing the impedances presented to the device's input and output terminals.

De-embedding and waveform plotting are critical for observing the matching circuit's impact on waveform shaping (squaring off) to improve amplifier efficiency. When studying the waveform at the device model's current generator is not practical, nested fundamental/harmonic load-pull contours can provide an alternative solution. Lastly, the addition of communication-system measurements to load-pull analysis adds a powerful design aid for engineers studying performance tradeoffs based on system measurements. Such measurements include ACPR and EVM for amplifiers operating with digitally modulated RF signals. mw

11. As with circuit measurements, system-level measurements can be referenced to a specific output power level.

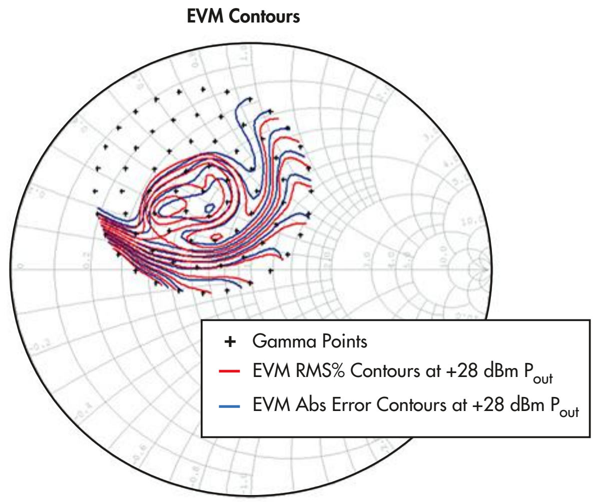

10. System measurements can be contoured to provide further impedance optimization, or to provide insight into the impact of varying load conditions.

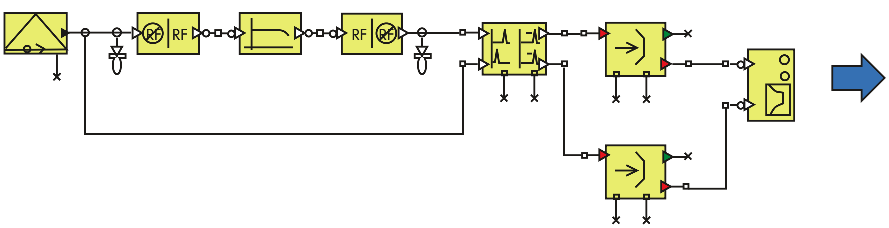

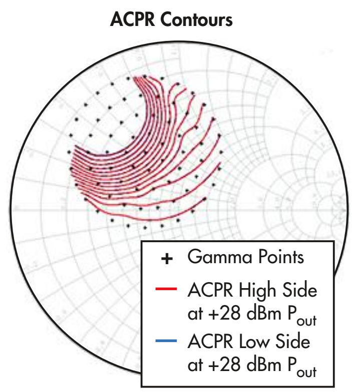

Product Feature

JACK BROWNE | Technical Contributor

PLL Synthesizes 10 MHz to 15 GHz

This compact PLL works with a wide range of reference input signals to generate wideband output signals that are low in harmonics, spurious, and phase noise.

Many systems require clean stable RF/microwave signals with programmable control. The LMX2594 phase-locked loop (PLL) frequency synthesizer from Texas Instruments (*www.ti.com*) provides the performance and flexibility from 10 MHz to 15 GHz that is as well suited to commercial communications as to military radar systems. It has an integrated voltage-controlled oscillator (VCO) and can generate output frequencies over that broad range with minimal spurious content and low phase noise.

The PLL has integer-N and 32-b fractional-N division modes with high phase-detector frequencies (400 MHz in integer-N mode and 300 MHz in fractional-N mode) that yield stable output signals with excellent spectral purity. The N-divider operates without a pre-divider to achieve the excellent spurious performance.

The LMX2594 (*see photo*) packs the VCO, programmable multipliers, dividers, multiplexers, and various control circuits into a 40-pin VQFN package that measures only 6.00 × 6.00 mm and runs on a single +3.3 V dc supply. It can operate with reference input signal frequencies from 5 to 1,400 MHz. The PLL's integrated output driver amplifiers generate as much as +7 dBm output power at the highest frequencies. Output signals are clean, with single-sideband (SSB) phase noise of −110 dBc/Hz offset 100 kHz from a 15-GHz carrier. To meet critical synchronization requirements, the root-mean-square (RMS) jitter is a low 45 fs offset 100 Hz to 100 MHz from a 7.5-GHz carrier.

The on-board VCO is spectrally pure. Its one-octave frequency range of 7.5 to 15.0 GHz allows the frequency divider to handle frequencies below the lower bound but requires the use of frequency calibration to determine the correct VCO frequency band for a desired output frequency. Phase-noise measurements performed at frequencies within the different VCO bands, and at a supply voltage of +3.3 V dc and at room temperature (+25°C), revealed low phase noise for all offsets and carrier frequencies.

For a carrier frequency of 8.0 GHz, the VCO's phase noise is typically −80 dBc/Hz offset 10 kHz from the carrier, −107 dBc/Hz offset 100 kHz from the carrier, and −128 dBc/Hz offset 1 MHz from the carrier. For a 10.3-GHz carrier, the VCO's phase noise is −77 dBc/Hz offset 10 kHz from the carrier, −104 dBc/Hz offset 100 kHz from the carrier, and −126 dBc/Hz offset 1 MHz from the carrier. For a 12.5-GHz carrier, the VCO phase noise is −74 dBc/Hz offset 10 kHz from the carrier, −100 dBc/Hz offset 100 kHz from the carrier, and −123 dBc/Hz offset 1 MHz from the carrier.

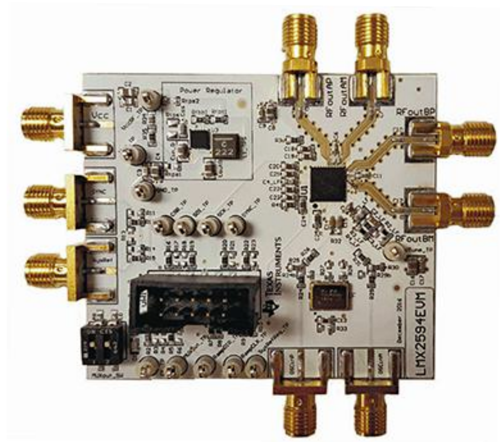

The LMX2594 (shown on an evaluation board) is a PLLfrequency synthesizer supplied in a compact 40-pin VQFN package that measures only 6.00 × 6.00 mm. It generates low-noise output frequencies from 10 MHz to 15 GHz.

Changes in frequency are aided by a fast calibration algorithm that helps to accurately change frequencies in less than 20 μs while recalibrating the VCO as required in the middle of a waveform. The PLL's on-board SYSREF controller makes the LMX2594 a strong candidate for a clock source for high-speed analog-to-digital converters (ADCs) and digital-to-analog converters (DACs). The PLL provides programmable delay adjustments in output signals to allow tuning as fine as 9 ps to account for signal delays caused by differences in coaxial cable lengths or transmission lines on PCBs. mw

TEXAS INSTRUMENTS; P.O. Box 655303, Dallas, TX 75265; www.ti.com

CHRIS DeMARTINO | Technical Editor

The Smith Chart Enters a New Dimension

One team of engineers decided to transform the traditional Smith chart into a three-dimensional tool.

THE SMITH CHART, which is unquestionably one of the most important and fundamental aspects of microwave engineering, has a long history that spans more than 70 years. However, one team of engineers decided to take the classical Smith chart and put a much different spin on it. The result is a 3D Smith chart tool, which the team says is a new vision in microwave analysis and design *(see figure)*.

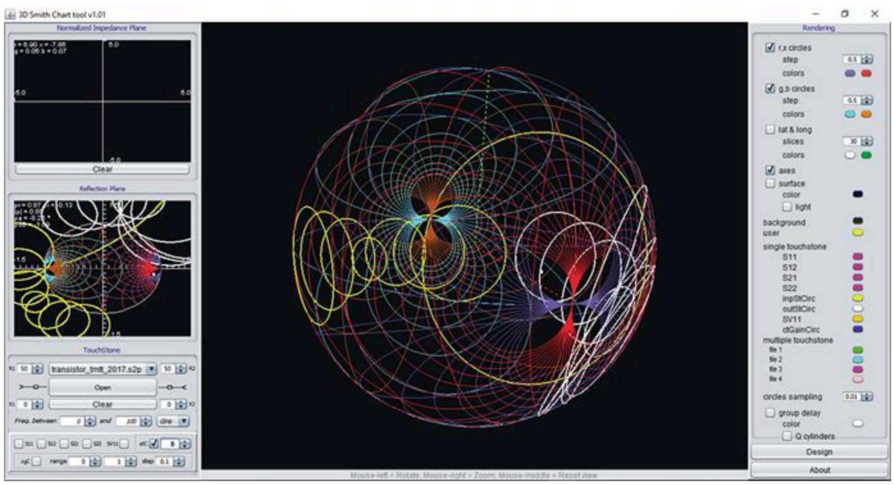

This software tool offers a 3D representation of the Smith chart.

The 3D Smith chart tool is an easy-to-install 3D representation of the classical Smith chart that is intended for high-frequency one- and two-port circuits. It works for all passive and active circuits—even when negative resistance is present. With this tool, users can observe impedance/admittance, as well as stability circles, group delay, quality factor, and unilateral power gain.

The 3D Smith chart differs from the traditional Smith chart in a number of ways. For example, as most already know, the center of the classical Smith chart denotes a perfect match. However, the 3D Smith chart shows a perfect match at the north pole.

In addition, RF/microwave engineers already know that negative resistance (|reflection coefficient| > 1) cannot be shown within the confines of the traditional Smith chart. However, negative resistance is indeed portrayed in the 3D Smith chart. Specifically, the south hemisphere represents negative resistance, with the south pole denoting an infinite reflection coefficient. The north hemisphere of the 3D Smith chart represents positive resistance. Furthermore, the inductive region is designated in the east, while the capacitive region is represented in the west.

Moreover, the program interface includes rendering options, which allow users to select the desired displays. These displays include constant normalized resistance (r), reactance (x), conductance (g), and susceptance (b) circles. Users can also modify colors, as well as the step between circles.

ANALYSIS AND DESIGN

Users can take advantage of both analysis and design modes. With analysis mode, a touchstone file can be loaded to allow one to view a number of parameters on the 3D Smith chart. These parameters include impedance, stability circles, constant gain circles, group delay, quality factor, and unilateral power gain. The S-parameters can also be represented on a 2D Smith chart.

Design mode enables users to obtain normalized matching circuit solutions. One can simply enter the desired normalized impedance parameters and then choose a matching route. The corresponding resistance, inductance, and capacitance values, as well as transmission lines and stubs, can be directly computed.

Those interested in the 3D Smith chart tool can learn more at *www.3dsmithchart.com.* mw

JACK BROWNE | Technical Contributor

Frequency Synthesizer Keeps Noise Levels Low

This fast-switching frequency synthesizer keeps the spurious and phase-noise levels low across a total frequency tuning range as wide as 50 MHz to 21 GHz.

Microwave signal sources must deliver on many different levels. Depending on the application, they may need to switch frequencies quickly, often in fine frequency steps, and always with low phase noise. Such challenges bring out the best in Micro Lambda's Alexander Chenakin, who unveiled his latest creation at the recent 2017 IEEE International Microwave Symposium (IMS) exhibition in Honolulu..

The Luxyn frequency synthesizer features high-speed tuning from 50 MHz to 21 GHz in frequency steps as small as 0.001 Hz in a package that is only 4.0 × 3.6 × 0.9 in. and weighs only 15 oz. It is literally a fit for a wide range of applications, from broadband communications systems to test-and-measurement equipment.

The Luxyn frequency synthesizers are based on a stabilized voltage-controlled oscillator (VCO) with extremely wide tuning range and fast frequency switching speed. The tuning range of a standard Luxyn model MLVS-0520 frequency synthesizer (*see figure*) is 500 MHz to 20 GHz, with lower frequencies available to 50 MHz and higher frequencies available to 21 GHz.

Of course, Micro Lambda is well known for its YIG-oscillator-based frequency synthesizers and the two microwave source technologies have traditionally represented two sets of tradeoffs for high-frequency signal sources. YIG oscillators and synthesizers have long been standards of sorts for low phase noise, although for the penalty of limited tuning speed. Frequency synthesizers such as phase-locked-loop (PLL) sources based on VCOs have been traditionally capable of extremely fast tuning speeds but with limited phase-noise performance compared to YIG-based synthesizers. The Luxyn series of synthesizers combines the best of both source technologies, with fast switching speed and low phase noise—in general, with low noise levels.

The MLVS-0520 frequency synthesizer boasts minimum output power of +15 dBm across the frequency range, consuming 12 W power from a supply of +10 to +16 V dc. With its fast frequency tuning speed of 50 μs, the normal assumption is that it is tuning across its wide frequency range in relatively large frequency steps, but this is not the case for the MLVS-0520. It can tune in steps as fine as 1 mHz without sacrificing the tuning speed.

Luxyn frequency synthesizers feature broadband frequency coverage with low noise levels, fine frequency steps, and fast tuning speed.

The fast frequency synthesizer offers impressively low noise levels, with harmonic levels of typically -12 dBc, subharmonics of typically -50 dBc, and spurious signal levels of typically -60 dBc. It is the phase noise that will grab most system designers' attention, with typical phase noise of -131 dBc/Hz offset 10 kHz from a 5-GHz carrier and -125 dBc/Hz offset 10 kHz from a 10-GHz carrier. The phase noise is typically as low as -154 dBc/Hz offset 10 kHz from a 50-MHz carrier.

The MLVS-0520 is designed to operate with an internal or external reference oscillator, provided that either reference source supplies +5 dBm at 10 MHz. An external reference source is fed to the MLVS-0520 by means of a female SMA input connector, while signals from the frequency synthesizer's internal 10-MHz reference oscillator are available at a female SMA output connector; the RF/microwave output signals from the frequency synthesizer are provided at a third female SMA connector. For remote operation and programming, the MLVS-0520 is also equipped with SPI and USB control connectors. mw

MICRO LAMBDA WIRELESS INC., 46515 Landing Pkwy., Fremont, CA 94538; (510) 770-9221, www.micro-lambda.com

CAUTION
STATIC SENSITIVE
MICRO LAMBDA WIRELESS, INC.
MLMS-2080B
SN:1000
DC:1615
2-8 GHz
PXI
Not actual chassis

JACK BROWNE | Technical Contributor

Analog Signal Generator Vanquishes Phase Noise

This high-performance test signal source is available in various configurations covering as wide as 9 kHz to 20 GHz with generous output power and extremely low phase noise and harmonics.

Evaluating the performance of modern receivers and many high-frequency components requires a test source capable of producing signals with quality exceeding that of the signals employed in the actual applications, whether the receivers or components are for commercial, industrial, or military use. The R&S® SMA100B RF/microwave signal generator from Rohde & Schwarz (*www.rohde-schwarz.com*) provides test signals with impressive purity from 9 kHz through 20 GHz. In addition to high output power across the frequency range, it has low phase noise and low harmonic distortion. It provides the signal purity to meet the measurement needs of device, component, circuit, and system testing for everything from commercial wireless communications to military radar.

The R&S SMA100B RF and microwave signal generator is built in two different physical configurations (*see figure*): with 2 HU or 3 HU rack-mount housings and 5- and 7-in.-diagonal touchscreen displays, respectively. The display screens on both versions provide high, 800 × 480 pixel resolution. The signal generator is available in four models covering all or part of the full frequency range:

- R&S SMAB-B103: 8 kHz to 3 GHz;
- R&S SMAB-B106: 8 kHz to 6 GHz;
- R&S SMAB-B112: 8 kHz to 12.75 GHz;
- R&S SMAB-B120: 8 kHz to 20 GHz.

All four versions have outstanding spectral purity in common, with typical single-sideband (SSB) phase noise of -152 dBc/Hz offset 20 kHz from a 1-GHz carrier and -132 dBc/Hz offset 20 kHz from a 10-GHz carrier. The noise floor (wideband noise) is also very low, at a level of only -162 dBc measured 30 MHz from a 10-GHz carrier. Harmonics do not exceed -63 dBc across the full frequency range, even at the

The R&S SMA100B RF and microwave signal generator is available in two different rack-mount configurations and four frequency ranges, with the widest-bandwidth model covering 8 kHz to 20 GHz.

highest output-power levels, reaching as low as -70 dBc from about 15 to 20 GHz. Nonharmonic noise is -90 dBc at 10 GHz and as low as -100 dBc at the low end of the frequency range.

Judging by the low measured RMS jitter, signals generated with these sources are quite stable and qualified candidates for characterizing the performance of analog-to-digital converters (ADCs) and digital-to-analog converters (DACs). The RMS jitter is almost negligible: a mere 18 fs measured at both 622 MHz and 2.488 GHz. In fact, with an option (B29), the signal generators can provide the flexibility of selectable output waveforms: single-ended sinewaves, differential sine waves, differential square waves, and differential CMOS signals, with standard dc offsets to 3 GHz (or to 6 GHz with another option). The variety of waveforms supports testing of a wide range of analog, digital, and mixed signal devices.

The R&S SMA100B signal generators can perform frequency sweeps as wide as the full bandwidth of each instrument, in linear or logarithmic steps, with dwell times of 3 ms to 100 s between steps. The frequency tuning resolution is 0.01 Hz. The signal generators deliver high test signal output power, with as much as +38 dBm output power through 6 GHz, +30 dBm or more output power at 18 GHz, and +28 dBm output power at 20 GHz. With their precision electronic step attenuators, these signal generators can set output levels as low as -145 dBm in standard models, with resolution of 0.01 dB. The generators require less than 1 ms to settle to a new power level, for efficiency in automatic-test-equipment (ATE) applications.

In addition to the four frequency ranges, the signal generators are available in two different rack-mount versions: with 2 HU or 3 HU housings and 5- and 7-in.-diagonal touchscreen displays, respectively, with 800 × 480 pixel resolution for both screens. For those in need of modulation, there is plenty, with one option providing AM, FM, and phase modulation, and another option adding pulse modulation. The quality of the pulse modulation is noteworthy, since modulation is available with pulse widths of 20 ns or less and rise/fall times of 10 ns or better (and typically 5 ns). The on/off ratios of these pulses is better than 80 dB, and amplitude levels can be tightly controlled in pulses as narrow as 100 ns. The signal generators boast advanced digital automatic-level-control (ALC) circuitry to produce those leveled pulses, and the circuity can even level the tops of pulses from an external modulator.

The R&S SMA100B RF and microwave signal generators are obviously state-of-the-art test instruments with untouchable phase-noise performance and considerable output power across an almost 20-GHz bandwidth. The amount of testing that has gone into these signal generators prior to their release is impressive, with such parameters as level setting repeatability fully characterized across the full operating temperature range. The generators can emulate a wide range of legacy instruments from other vendors for ease of integration into ATE systems, and they are equipped with many user-friendly controls and features to simplify operation, such as context-sensitive help. If there is anything bad to say about these instruments, it is in the amount of options available, which extends not only to the size of the instrument but to the choice of reference clock (including a 1-GHz reference for extremely low phase noise when locking multiple signal generators) and maximum output-power level. The generators come with a three-year warranty. mw

ROHDE & SCHWARZ GMBH & CO. KG; P. O. Box 80 14 69, 81614 Muenchen, Muehldorfstrasse 15, 81671 Munich, Germany; *www.rohde-schwarz.com*

CHRIS DeMARTINO | Technical Editor

Q&A: Philippe Garreau

5G's Impact on the Test Arena

Philippe Garreau, chairman of the Microwave Vision Group (MVG), discusses why over-the-air testing will be needed for 5G.

First, can you tell us about over-the-air (OTA) testing and why it will be needed for 5G?

5G lays the foundation for a connected society in the near future—a world where everything that benefits from being connected will be connected. The internet will move out from computer screens and smartphones and into the physical world, where objects will communicate directly with each other. Examples range from automated factories with production and logistics efficiencies reaching new heights to self-driving cars and services, farming, medical services, consumer electronics, smart homes, smart cities, etc. In short, this is the next digitalization phase of the world. Completely new businesses will be built on this opportunity. It is a movement that will impact all industries, across all markets around the world.

There are three major cornerstones of 5G: increased bandwidth and capacity for mobile data able to handle the ever-increasing amounts of wireless data traffic; ultra-reliability and low latency for mission critical services for real-time critical connections such as in self-driving cars, robotics, automated factories, and medical applications; and reduced overhead for massive-scale Internet of Things (IoT) applications—for example, sensor networks consuming very little bandwidth and power. All this backed up by the cloud through the 5G networks, enabling a multitude of services to be efficiently rolled out. There is quite a broad spectrum of ways 5G standards can be adapted to handle all the application cases of the connected world.

What is critical for enabling all of this to work as expected is the wireless link. Radio performance is the parameter that is most difficult to control, as this performance is heavily device- and installation-dependent. It is of paramount importance to be able to accurately secure the desired wireless performance in the products and services rolled out on the market, in order to fulfill the expectations of the service. The promise of 5G is based on lab results in ideal conditions, while the performance achieved in real life will depend on how well the radio performance actually works. This needs to be tested for each device and application.

From a technical perspective, the architecture in 5G devices will require radio performance parameters, traditionally tested through coaxial cables in RF labs, to be tested OTA, as there won't be any physical connectors available in the devices. The consequence of this is that not only antenna performance needs to be tested OTA. In addition to antenna testing, all other RF system performances and radio resource management parameters need to be tested OTA instead of through a cable. As a result, the amount of OTA test cases will increase significantly. In combination with the obligation to verify the radio and antenna performance in 5G, this puts high demands on the capacity and capabilities of OTA testing in product development, production, and aftermarket support.

How close are we to achieving the OTA test capability that 5G will require?

We identified the needs and challenges posed by 5G at an early stage, and have been preparing a portfolio of test solutions positioned to efficiently handle 5G testing. This includes all stages of a product lifecycle, from early R&D testing through calibration and production testing to what we call scenarios: how a product performs in a real dynamic RF environment.

This said, the 5G is an evolving standard, and most importantly, the amount of applications and use cases are expected to increase over time as 5G is deployed in new industries and markets. This will drive a continuous need for new test solutions, as well as adaptations of existing solutions to be introduced.

One of the bigger challenges in the 5G markets is the test capacity increase needed for 5G product development, as tests will be done OTA instead of through cables. We are already seeing now that companies are starting to transform their labs from purely conducted test labs to OTA-based test labs.

Another challenge on the market is that companies that have never created wireless products before now need to become capable of performing wireless testing in R&D in order to stay competitive. Wireless connectivity will be as natural as internet is today—and this is a big change.

Our first multi-probe system to measure frequencies above 18 GHz, the StarLab 50 GHz, will cover the 18-to-50-GHz frequency band. It will be launched end of June. The feedback we are receiving from potential customers is already highly promising.

How is MVG positioning itself for 5G?

MVG is positioning itself at the forefront of 5G connectivity!

5G is a huge opportunity for MVG to be of added value to its markets, as the needs for OTA testing increase. It is one of our main strategic focus areas right now, and we have recently launched new products optimized for 5G testing.

Our ambition is to be at the leading edge of what the market needs in terms of 5G testing. We are active in 5G standardization committees, as well as other 5G-related industry initiatives such as in the automotive industry. However, we don't just follow. We actively contribute to 5G development by offering the tools and systems needed to achieve best-in-class 5G performance.

The company will benefit from 5G technology, as our technological expertise is a trusted asset to both the telecom and aerospace & defense markets. Technologies traditionally applied in our products mainly used in A&D markets can be used for high-frequency 5G applications, bringing efficiency and fast time-to-market for our customers. In combination with our state-of-the-art multi-probe technology and advanced software applications for data processing and analysis, we are optimizing our technologies for 5G applications.

As 5G is emerging into new industries and applications, we need to be flexible to rapidly respond to what would be beneficial for the markets. We work closely together with customers across the world to align our product roadmap with their product visions and needs, proactively driving our development of competitive test solutions.

We believe that with MVG as a one-stop shop for wireless connectivity testing products and services, we enable our customers to improve their competitiveness. In delivering turnkey systems, our customers can focus on the activities that add the most value to their organizations. The scale of our product portfolio and technologies allows us to flexibly handle changing needs of our customers both today and in the future. mw

Single-Ended Transistors

(Continued from page 34)

LDMOS—one that can dramatically reduce the size and weight of avionics systems. With the right combination of high power levels and over 70% drain efficiency, these devices will usher in new levels of system integration and power performance that was once only possible with bulky combinations of lower-power transistors. On top of that, they will maintain their efficiency while simplifying the overall application solution. mw

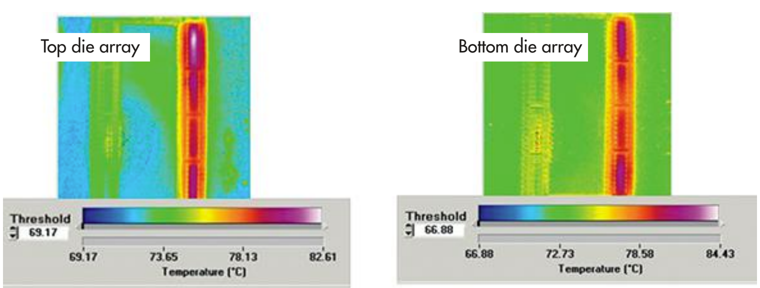

9. Shown here is average thermal imaging with these conditions: V_{DD} = 52 V, pulse width = 32 μs, and pulse period = 1.6 ms (frequency = 960, 1090, 1215 MHz).

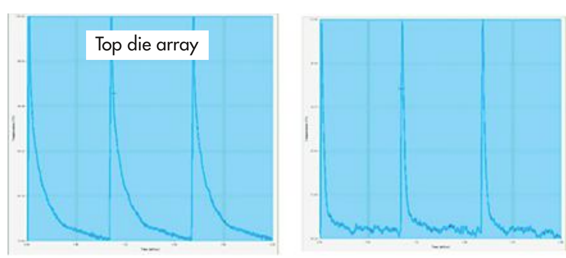

10. Illustrated is transient thermal imaging with these conditions: V_{DD} = 52 V, pulse width = 32 μs, and pulse period = 1.6 ms (frequency = 960, 1090, 1215 MHz).

CHRIS DeMARTINO | Technical Editor

Imagine Life Without Interference

One startup company is aiming to overcome the ever-present issue of interference that plagues wireless communications.

Interference is undoubtedly a major problem with regard to today's wireless communications. That being said, one startup company claims to have developed technology for enabling "life without interference." That company is Austin-based GenXComm (*www.genxcomm.com*), which was founded in 2016 and recently announced the closing of a fully-subscribed round of seed financing.

Earlier this year, GenXComm unveiled its simultaneous self-interference cancellation (S-SIX) technology. This technology is the result of several years of R&D efforts at the University of Texas at Austin. The company is targeting Wi-Fi, backhaul, and 5G markets, with the technology being intended for handsets, tablets, laptops, and more.

With S-SIX technology, the objective is to enable simultaneous transmission and reception of signals—in the same channel. Thus, radios can essentially listen and talk at the same time. In essence, GenXComm believes its technology can enable true full-duplex communications.

S-SIX technology allows channels to be located directly next to one another without any unused spectrum between them. This allows spectrum to be shared more efficiently. Furthermore, the company asserts that significantly lower latencies can be achieved with its technology.

In terms of performance, GenXComm claims that throughput can be increased by as much as 30× in dense environments. "It is very hard to achieve wireless functionality in a dense environment," said Sriram Vishwanath, the company's co-founder and president. "Our technology is scalable in dense environments."

S-SIX technology is intended to satisfy stringent size, weight, and power (SwaP) requirements. The technology is chip-scalable and offers benefits in terms of bandwidth, according to Vishwanath. It also enables physical security.

QUANTIFYING PERFORMANCE

Figure 1 shows a Wi-Fi network model of a dense indoor environment. Such environments could include conferences, concerts, offices, and home apartments. A total of 16 access points are shown in the model.

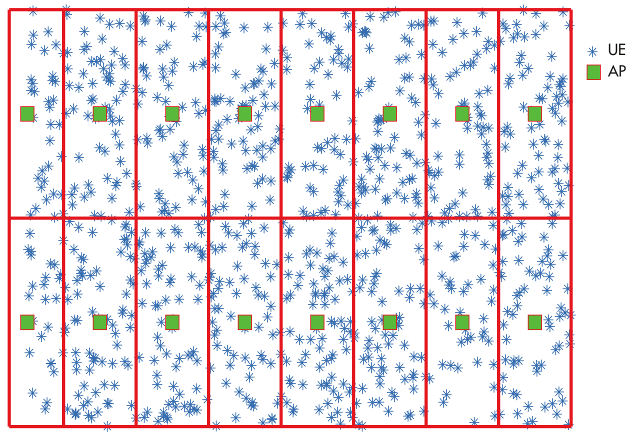

1. This image depicts a Wi-Fi network model of a dense indoor venue.

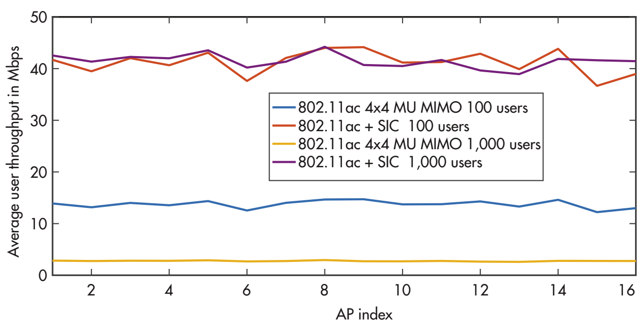

2. This graph shows Wi-Fi throughput in an indoor environment with and without S-SIX technology.

Figure 2 shows the modeled performance of the Wi-Fi network depicted in Fig. 1, both with and without S-SIX technology. The graph illustrates the throughput of networks with 100 and 1,000 users, respectively. In both scenarios, it can be seen that employing S-SIX technology significantly increases throughput. Similar simulations of outdoor networks with thousands of users also demonstrated an improvement in throughput when S-SIX technology is employed.

GenXComm expects a full product launch following its next round of funding. mw

(Continued from page 48)

The change in the LNA's output was observed using a negative-polarity Schottky diode detector.[21] The experimental t_{OFF} and t_{ON} times were 1.5 and 0.04 μs, respectively (*Fig. 9*).

The slow power-down time is due to shunt capacitor C_3 lacking a discharge path. It may be possible to speed up the discharge of C_3 with an external resistor, but this has not been verified. On the other hand, the t_{ON} time compares to the industry's fastest.[22] In conclusion, this MMIC implementation can provide the performances needed for small cell TDD applications with the power-down function included for reduced component count. mw

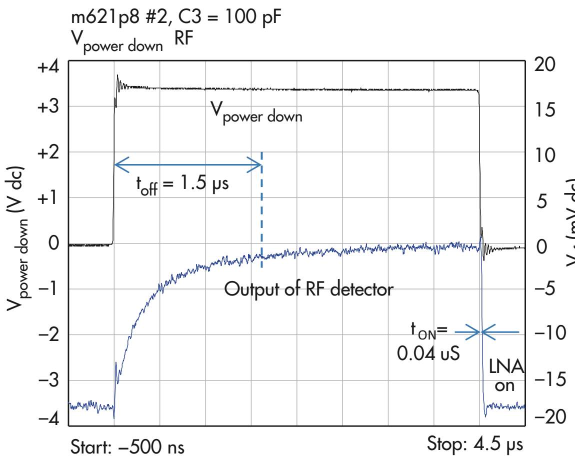

9. The MMIC LNA's power-down and power-up times of 1.5 and 0.04 μs, respectively, are fast enough for TDD application.

ACKNOWLEDGMENTS

The author wishes to thank M.D. Suhaiza and S. Punithevati for assembling the samples, T.W. Lee and Y.Y. Liew for product design and characterization, and S.A. Asrul for supervising this work.

REFERENCES

1. Anonymous, "Small Cells," Wikipedia, *https://en.wikipedia.org/wiki/Small_cell*
2. Anonymous, "About small cells," (n.d.), *http://www.smallcellforum.org//about-small-cells/elevator-pitch/*
3. J.A. Walston and J.R. Miller, eds., "Wideband or video amplifiers," in *Transistor Circuit Design*, McGraw-Hill, New York, 1963, Chap. 19.
4. B.S. Virdee, A.S. Virdee, and B.Y. Banyamin, "Broadband Feedback Amplifiers," in *Broadband Microwave Amplifiers*, Artech House, Norwood, MA, 2004, section 6.5.
5. C. Baringer and C. Hull, "Amplifiers for Wireless Communications," in *RF and Microwave Circuit Design for Wireless Communications*, L. E. Larson, ed., Artech House, Norwood, MA, 1997, p. 360.
6. "Outdoor LTE small cell deployment on lamp posts: A Paris city study," Ranplan Wireless Network Design Ltd., *http://www.ranplan.co.uk.*
7. W. Wu, J.S. Wei, C. Su, R.M. Parkhurst, S.L. Fu, S. Chang, and R.B. Levitsky, "An enhancement-mode pHEMT for single-supply power amplifiers," in *Hewlett-Packard Journal*, February 1998.
8. "Development of E-pHEMT Technology," Avago white paper, *http://avagotech.com*, June 2007.
9. A.S. Virdee and B.S. Virdee, "Computer-aided design of ultrabroadband 100 MHz to 20 GHz amplifiers," *Microwave Journal*, February 2000.
10. I. Piper, "Build an E-pHEMT low-noise amplifier," Microwaves & RF, March 2004.
11. "MGA-62563 current-adjustable low noise amplifier," Avago data sheet, November 2004, *http://www.avagotech.com*.
12. "MGA-62563 high performance GaAs MMIC amplifier," Avago application note 5011, *http://www.avagotech.com.*
13. "BGU8051," Rev. 2, NXP product data sheet, December 2013, *http://www.nxp.com*.
14. Pat Hindle, "2010 GaAs foundry services outlook," *Microwave Journal*, June 2010, pp. 20-28.
15. R. F. Kopf, A. G. Baca, and S. N. G. Chu, "Enhancement- mode power AlGasAs/InGaAs/AlGaAs," *Electrochemical Society Proceedings*, Vol. 2000-1, pp. 110-118.
16. Rogers Corp., "RO4000 series high frequency circuit materials," Rogers data sheet, Publication No. 92-004, April 2006, *http://www.rogerscorp.com*.
17. Keysight Technologies, Advanced Design System (ADS) technical reference (Version 2009), *http://www.keysight.com/find/eesof-technicalreference*.
18. "Library for Keysight ADS," Murata design tools, *http://www.murata.com*.
19. Raymond S. Pengelly, "Improving the Linearity and Efficiency of RF Power Amplifiers," *High Frequency Electronics*, September 2002, p. 26.
20. Agilent Technologies, application note, "Understanding RF/Microwave solid state switches and their applications, May 2010, *http://www.agilent.com*.
21. Agilent Technologies, datasheet 5952-8299, "423B, 8470B, 8472B, 8473B/C low barrier Schottky diode detectors," October 2011, *http://www.agilent.com*.
22. C.L. Lim, "LNA integrates fast shutdown function," *Microwaves & RF*, December 2014.
23. Guerrilla RF, "GRF2104 preliminary data sheet, December 2015, *http://www.guerrilla-rf.com*.

Product SPOTLIGHT

The latest product information presented by Mini-Circuits®
www.minicircuits.com

Cavity Bandpass Filter Cleans 2.2 to 2.4 GHz

Mini-Circuits' model ZVBP-2300A+ is a cavity bandpass filter with low-loss passband from 2.2 to 2.4 GHz and wide lower and upper stopbands. The 50-Ω filter has typical passband insertion loss of 0.5 dB and typical rejection of 40 dB in the lower stopband from DC to 2 GHz and the upper stopband from 2650 to 8050 MHz. It provides sharp transitions between passband and the two stopbands and handles as much as 15 W input power. It is an effective solution for suppressing noise and interference from fixed and mobile communications systems at 2.4 GHz. The RoHS-compliant filter measures 3.10 × 1.25 × 0.77 in. (78.81 × 31.75 × 19.50 mm) with female SMA input and output connectors and an operating temperature range of -40 to +85°C.

Ultra-Thin, 6-Way 0-deg. Power Splitter/ Combiner Channels 0.6 to 6.0 GHz

Mini-Circuits' model ZN6PD1-63SMP+ is a DC-pass six-way, 0-deg. power splitter/combiner with a frequency range of 0.6 to 6.0 GHz. It offers low insertion loss of typically 1.0 dB through 3 GHz and 1.25 dB through 6 GHz and high isolation between ports of typically 20 dB across the full frequency range. The 50-Ω, RoHS-compliant splitter/combiner handles as much as 20 W input power as a splitter and 1.5 W per port as a combiner and can pass as much as 100 mA current though each of its six splitter ports (600 mA total). It is supplied in a compact, low-profile housing measuring just 9.50 × 4.25 × 0.43 in. (241.30 × 107.95 × 10.92 mm) with SMP snap-on connectors. It has an operating temperature range of -55 to +100°C and is well suited for signal-processing applications in communications systems.

Armored Test Cables Send Signals to 18 GHz

Mini-Circuits' model APC-4FT-SMNM+ armored coaxial test cables are built with rugged, crush-resistant construction and are supplied in 4-ft. lengths for applications from DC to 18 GHz. The tripled-shielded cable assemblies achieve shielding effectiveness (SE) of better than 100 dB. They are characterized by low insertion loss: typically 0.8 dB from DC to 2.5 GHz, 2.0 dB or less from 2.5 to 12.0 GHz, and 2.55 dB from 12 to 18 GHz. Return loss is typically 30 dB from DC to 6 GHz, 27 dB from 6 to 12 GHz, and 22 dB from 12 to 18 GHz. The flexible, RoHS-compliant cables are qualified to 20,000 bend cycles (with a 6-month guarantee) with excellent amplitude and phase stability with flexure. The cables are terminated in stainless-steel male SMA and male Type N connectors to eliminate the need for coaxial adapters. They handle operating temperatures from -55 to +105°C.

10-Way Splitter/Combiner Covers 2250 to 2800 MHz

Mini-Circuits' model ZC10PD-26W+ is a 10-way, 0-deg. power splitter/combiner with frequency range of 2250 to 2800 MHz. It handles as much as 10 W input power as a splitter and as much as 0.8 W input power per port as a combiner. Insertion loss, above the theoretical 10-way division loss, is typically 0.7 dB from 2300 to 2600 MHz and typically 0.9 dB from 2250 to 2800 MHz. Isolation between ports is typically 22 dB from 2300 to 2600 MHz and typically 21 dB from 2250 to 2800 MHz. The 50-Ω splitter/combiner has full-band amplitude balance among signal paths of typically 0.6 dB or better and full-band phase balance among signal paths of typically 10 deg. or better. The VSWR is 1.45:1 or better at all ports across the full frequency range. The power splitter/combiner measures 6.13 x 3.00 x 0.53 in. (155.70 x 76.20 x 13.46 mm) in a low-profile housing with SMA female connectors. It has an operating temperature range of -55 to +100°C.

USB/Ethernet SP6T Switch Box Provides Long Lifetime from DC to 12 GHz

Mini-Circuits' model RC-1SP6T-A12 is a single-pole, six-throw (SP6T) switch matrix that can be remotely controlled by a computer with USB or Ethernet connection. The 50-Ω electromechanical switch matrix operates from DC to 12 GHz with long operating lifetimes: at least 10 million switching cycles when hot switching 100-mW signals and typically 1 million switching cycles when hot switching 1-W signals. The switching time is typically 25 ms. The absorptive, fail-safe switch matrix is well suited for ATE applications, with insertion loss of typically 0.25 dB or less from DC to 12 GHz, and isolation of typically 100 dB from DC to 1 GHz and 90 dB or more from DC to 12 GHz. The VSWR is 1.20:1 or better across the full frequency range. The switch matrix is supplied with SMA female connectors and handles as much as 20 W through-path power. It can be controlled with Windows®, Mac®, or Linux® environments using free software and DLLs downloadable from the Mini-Circuits' web site.

Directional Coupler Channels 850 to 2500 MHz

Mini-Circuits' model ZADC-15-252+ is a low-loss directional coupler that handles as much as 8 W power from 850 to 2500 MHz. It can also pass as much as 0.5 A DC current from input to output. Coupling is 14.5±1.5 dB and directivity is typically 16 dB across the full frequency range. The full-band insertion loss is typically 0.7 dB while the full-band return loss is typically 20 dB or better at input, output, and coupled ports. The RoHS-compliant directional coupler, which is available with either Type N or SMA connectors, has an operating temperature range of -55 to +100°C. It measures 2.0 × 2.0 × 0.75 in. (50.80 × 50.80 × 19.05 mm).

Programmable Attenuator Controls 0 to 60 dB to 13 GHz

THE RUDAT-13G-60 programmable attenuator features an attenuation range of 0 to 60 dB, adjustable in 0.5-dB steps from 10 MHz to 13 GHz. It achieves typical attenuation accuracy of ±0.5 dB. The RoHS-compliant, single-channel attenuator has high linearity, with typical input third-order intercept point (IP3) of +41 dBm through 13 GHz. It includes USB, RS-232, and SPI (via a D-sub connector) interfaces for easy control from a user's PC, with software support available by means of free download from the Mini-Circuits website. The 50-Ω programmable attenuator measures just 2.0 × 3.0 × 0.6 in. and is well suited for use in automated test systems, radar testing, and receiver sensitivity testing.

MINI-CIRCUITS, P.O. Box 350166, Brooklyn, NY 11235-003; (718) 934-4500, *www.minicircuits.com*

GaN Amp Assembly Powers Four Bands

THE SSPA 0.1-3.5-500 is a GaN-based power amplifier assembly that operates across VHF, UHF, L-band, and S-band frequencies. Suitable for communications or electronic-warfare (EW) applications, it provides separate TNC female input connectors for each of the four bands and combines all four into a single output connector. The amplifier assembly measures 6.0 × 9.0 × 3.0 in. and incorporates reverse polarity protection, open- and short-circuit protection,and over- and under-voltage protection. It provides +53 dBm output power with at last 25-dB gain at VHF; +50 dBm output power with at least 21.8-dB gain at UHF; +49 dBm output power with at least 24.2-dB gain at L-band; and +49-dBm output power with at least 21.5-dB gain at S-band. The bands can be switched on and off in 100 µs or less. The amplifier assembly, with 2.0:1 input and output VSWR, is designed for operating temperatures from –40 to +85°C.

AETHERCOMM, INC., 3205 Lionshead Ave., Carlsbad, CA 92010; (760) 208-6002, e-mail: sales@aethercomm.com, *www.aethercomm.com*

SMPM Cable Assemblies Extend DC to 20 GHz

SMPM COAXIAL CABLE assemblies are available in fixed lengths from 3 to 48 in. (10 to 200 cm) for applications to 20 GHz. The cable assemblies are suitable for high-reliability applications, including in military and aerospace systems. The 50-Ω cable assemblies feature low-loss SMPM plug connectors that function with both radial and axial misalignments, enabling them to perform well when exposed to high levels of shock and vibration.

AMPHENOL RF, 4 Old Newtown Rd., Danbury, CT 06810; (203) 743-9272, *www.amphenolrf.com*

Manually Tuned Filter Screens 4 to 6 GHz

MODEL 5CTB-4000/6000-5-N/N is a manually controlled tunable bandpass filter covering 4,000 to 6,000 MHz. Based on a multiple-section Chebyshev filter architecture, the filter provides a passband with 3-dB bandwidth that is within 5% of the tuned center frequency. The filter exhibits low passband insertion loss of 1 dB or less, and delivers 50-dB out-of-band rejection for frequencies that are 3.5 times lower or higher than the tuned center frequency. The tuned dial accuracy is ±1%. Although not specified for maximum input power, lower-frequency models in the series are rated for input power levels as high as 50 W CW.

K & L MICROWAVE, 2250 Northwood Dr., Salisbury, MD 21801; (410) 749-2424, *www.klmicrowave.com*

Gain Block Boosts 415 to 2,018 MHz

THE RFCA8830 high-linearity gain block from Qorvo is now available from stocking distributor RFMW, Ltd. With 18.7 to 19.4 dB gain from 415 to 2,018 MHz, it supports the DOCSIS 3.1 data-over-cable specification. The RoHS-compliant gain block has noise figure of less than 2 dB and composite-second-order (CSO) performance of better than –75 dBc. The composite-triple-beat (CTB) performance is –77 dB. The gain block is supplied in a SOIC-8 package and provides +24 dBm output power at 1-dB compression (P1dB). The gain block, which is suitable for use with optical receivers, laser drivers, and balanced antenna systems, draws 277 mA at +4.5 to +5.5 V dc.

RFMW, LTD. (QORVO STOCKING DISTRIBUTOR), 188 Martinvale Ave., San Jose, CA 95119; (408) 414-1450, e-mail: info@rfmw.com, *www.rfmw.com*

Combiner/Divider Spans 3 to 5 GHz

THE 802-2-4.000-M01 power divider/combiner maintains 0.3 dB maximum insertion loss above the theoretical 3.01-dB division loss from 3 to 5 GHz with an average power rating of 20 W. The 50-Ω combiner/divider exhibits input VSWR of 1.30:1 and output VSWR of 1.25:1. It provides at least 20 dB isolation between ports, with amplitude balance within 0.2 dB and phase balance within 4 deg. The RoHS-compliant component is equipped with passivated stainless-steel female SMA connectors and is usable at temperatures from –55 to +85°C.

MECA ELECTRONICS, INC., 459 E. Main St., Denville, NJ 07834; (866) 444-6322, e-mail: sales@e-MECA.com, *www.e-MECA.com*

Amplifier Drives Unlicensed LTE-A Band

THE SKY66288-11 high-efficiency power amplifier (PA) is designed for use in the unlicensed frequency spectrum of LTE-A small cells from 5,150 to 5,925 MHz. It provides 4 W output power with 25% power-added efficiency (PAE). It achieves 34.5 dB small-signal gain with +28-dBm output power. The PA, which runs on a single +5-V dc supply, can be used as a driver amplifier in micro and macro wireless base stations and in multiple-input, multiple-output (MIMO) antenna array applications. It is impedance matched to 50 Ω at input and output ports and is supplied in a 16-pin, 5 × 5 × 1.3 mm package.

SKYWORKS SOLUTIONS, INC., 20 Sylvan Rd., Woburn, MA 01801; (781) 376-3000, *www.skyworksinc.com*

Filter Keeps Out Wi-Fi Interference

THE WIFI2412-1 WI-FI cavity bandpass filter (BPF) has a 22-MHz passband centered at 2412 MHz (2401 to 2423 MHz). The maximum passband insertion loss is 3 dB and typically only 2 dB, while the out-of-band rejection of unwanted interference is at least 60 dB. The cavity BPF, which handles 50 W power, features passband return loss of 15 dB or better and maximum passband ripple of 1.2 dB. It has input and output impedance of 50 Ω and is designed for operating temperatures from –40 to +85°C. It is supplied with Type N female connectors and measures 108 × 56 × 26 mm.

ANATECH ELECTRONICS, INC., 70 Outwater Ln., Garfield, NJ 07026; (973) 772-4242, e-mail: sales@anatechelectronics.com, *www.anatechelectronics.com*

GaN PA is Efficient Through 6 GHz

THE HMC8205BF10 is a gallium-nitride (GaN) broadband power amplifier (PA) with +45.8 dBm (35 W) output power and 38% power-added efficiency across an instantaneous bandwidth of 300 MHz to 6 GHz. It is internally matched to 50 Ω and dc blocking capacitors for the RF input and output ports are integrated into the packaged PA. Suitable for both continuous-wave (CW) and pulsed applications, the amplifier is supplied in a 10-lead ceramic leaded chip carrier (LDCC).

ANALOG DEVICES INC., 804 Woburn St., Wilmington, Mass 01887; (781) 329-4700, *www.analog.com*

Oscilloscopes Add Waveform Generator Option

R&S RTO2000 and R&S RTE series high-speed oscilloscopes are now available with a 100-MHz-bandwidth arbitrary waveform generator and pattern generator option that provides two analog signal channels and eight digital signal channels that are operated by an oscilloscope's controls. The oscilloscopes are available with two or four channels and analysis bandwidths from 600 MHz to 6 GHz. The integrated test source, with data rates to 40 MSample/s, simplifies measurement setups by eliminating the need for an external signal generator.

ROHDE & SCHWARZ USA, INC., 6821 Benjamin Franklin Dr., Columbia, MD 21046; (410) 910-7800, (888) 837-8772, *www.rohde-schwarz.com*

Attenuator is Continuously Variable from 2 to 4 GHz

THE P4804-10 continuously variable provides a 10-dB attenuation range from 2 to 4 GHz. The panel-mount attenuator is ideal for applications where front-panel adjustments must be made. It achieves 0.1-dB or better resettability and handles 5 W average power and peaks as high as 5 kW. The maximum insertion loss is just 0.5 dB and maximum VSWR is 1.80:1. The attenuator is supplied with SMA female connectors and is designed for operating temperatures from –55 to +85°C.

ARRA, INC., 15 Harold Ct., Bay Shore, NY 11706-2296; (516) 231-8400, *www.arra.com*

4.3-10 Connectors Extend to 6 GHz

A FAMILY OF 18 4.3-10 connectors and adapters exhibits VSWR as low as 1.08:1 from DC to 6 GHz. A good fit for cellular base stations and distributed antenna systems (DAS), the 4.3-10 connectors and adapters feature low coupling torque and outstanding passive intermodulation (PIM) performance of typically –166 dBc. The connectors and adapters have silver-plated center contacts and corrosion-resistant finish on the body and outer conductors. The components have an IEC 61169-54 compliant interface and 30% smaller footprint than 7/16 DIN connectors.

PASTERNACK, 17792 Fitch, Irvine, CA 92614; (949) 261-1920, *www.pasternack.com*

Rack-Mount Amplifier Boosts 6 to 18 GHz

THE SSPA 6.0-18.0-50- RM is a high-power, rack-mountable amplifier with better than 20 W output power from 6 to 18 GHz based on nominal input power of +5 to +6 dBm. Power gain ranges from 44.3 dB at 6 GHz to 35.5 dB at 18 GHz. The maximum input and output VSWR is 2.0:1. The amplifier occupies 4U space in a standard 19-in. rack and operates from a 120 V ac supply. Temperature control is provided by two fans. The amplifier includes SMA female input and output connectors.

AETHERCOMM, INC., 3205 Lionshead Ave., Carlsbad, CA 92010; (760) 208-6002, *www.aethercomm.com*

This index is provided as an additional service by the publisher, who assumes no responsibility for errors or omissions.

Subscription Assistance and Information:
(ISSN 0745-2993)
Microwaves & RF is published monthly. Microwaves & RF is sent free to individuals actively engaged in high-frequency electronics engineering. In addition, paid subscriptions are available. Subscription rates for U.S. are $95 for 1 year ($120 in Canada, $150 for International). Published by Penton Media, Inc., 9800 Metcalf Ave., Overland Park, KS 66212-2216. Periodicals Postage Paid at Kansas City, MO and additional mailing offices. POSTMASTER: Send change of address to Microwaves & RF PO Box 2100, Skokie, IL 60076-7800. For paid subscription information, please contact Microwaves & RF at PO Box 2100, Skokie IL 60076-7800. Canada Post Publications Mail agreement No. 40612608. Canada return address: IMEX Global Solutions PO Box 25542, London ON N6C 6B2.